INTRASEASONAL RAINFALL VARIABILITY AND CLIMATE CHANGE ADAPTATION IN EAST AFRICA

By

Obed Matundura Ogega
Reg. No.: N85/38113/2017

A Research Thesis Submitted in Fulfilment of the Requirements for the Degree of Doctor of Philosophy in Environmental Studies (Climate Change and Sustainability) in the School of Environmental Studies of Kenyatta University

NOVEMBER 2021

DECLARATION

This thesis is my original work and has not been presented in any other university or for any other award. No part of this thesis may be reproduced without prior permission of the author or Kenyatta University.

Signature……. ……... Date……

Obed Matundura Ogega, N85/38113/2017

Department of Environmental Sciences and Education

SUPERVISORS

We confirm that the work reported in this thesis was carried out by the candidate with our approval as the University Supervisors

Signature: ……. Date: ……

Dr James Koske

Department of Environmental Sciences and Education

Kenyatta University

Signature ……. Date: ……

Prof. James B. Kung'u

Department of Environmental Sciences and Education

Kenyatta University

DEDICATION

To the great people of Nyamakorobo village, Kisii County, for triggering in me a desire to understand and conserve the environment for prosperity; my lovely family for support and an enabling environment for my academic exploits; and my colleagues and friends for igniting, fuelling, and advancing my pursuit for excellence.

ACKNOWLEDGEMENT

I am grateful to the Almighty God for this important milestone. He has indeed been Ebenezer. To Him be all the glory. I also appreciate my parents for giving me a chance at education. They went beyond their means to ensure that we had a good education. A special appreciation of my lovely family for encouraging, and giving me an enabling environment, to undertake my studies. I did not have difficulties making my field works, conferences, summer schools, and writing retreats. I hope my sons will forgive me for occasionally locking them out of my study room or missing out on days when I needed to be away from home. Now that I have completed my Ph.D. studies, I promise to spend more time with them. To my lovely siblings, who often doubled up as my research assistants, I appreciate you.

Many thanks to colleagues, friends, and institutions that contributed to the delivery of my research work: my supervisors, Dr. James Koske and Prof. James Kung'u; my collaborators and mentors Dr. Benjamin Gyampoh (Kwame Nkrumah University of Science and Technology), Dr. Malcom Mistry (Ca' Foscari University of Venice), Dr. Enrico Scoccimarro (Fondazione CMCC Centro euro-Mediterraneo sui Cambiamenti Climatici), and Dr. Hussen Endris (IGAD Climate Prediction and Applications Centre). A special mention of colleagues and friends from Kenyatta University's School of Environmental Studies, the African Academy of Sciences, the University of Nairobi's Institute for Climate Change and Adaptation (ICCA) and Department of Meteorology, JPI Climate's European Research Area for Climate Services (ERA4CS), and Coastal Oceans Research and Development – Indian Ocean (CORDIO) East Africa. Your invaluable guidance, mentorship, and support is highly appreciated.

Finally, the contribution of various climate modelling groups participating in CORDEX and the developers of CHIRPS, CRU, MAP, TAMSAT, and any other datasets used in the thesis are acknowledged for availing their data that made this work possible.

TABLE OF CONTENTS

LIST OF FIGURES

LIST OF TABLES

LIST OF ACRONYMS AND ABBREVIATIONS

AfDB	Africa Development Bank
ANN	Annual
BI	Burundi
CanESM2	Canadian Earth System Model
CCCma	Canadian Centre for Climate Modelling and Analysis
CDO	Climate Data Operators
CERFACS	Centre Européen de Recherche et de Formation Avancée en Calcul Scientifique (European Centre for Research and Advanced Training in Scientific Computing)
CES	Cessation
CHIRPS	Daily Climate Hazards Group InfraRed Precipitation with Station data
CLMcom	Climate Limited-area Modelling Community
CNRM	Centre National de Recherches Météorologiques
CORDEX	Coordinated Regional Climate Downscaling Experiment
COSMO-CLM	Consortium for Small-Scale Modelling - Climate Model
CRCM	Canadian Regional Climate Model
CSIRO	Commonwealth Scientific and Industrial Research Organisation
CWD	Consecutive wet days
DMI	Danish Meteorological Institute
EA	East Africa
EAC	East African Community
EC-EARTH	European community Earth-System Model
ECMWF	European Centre for Medium-Range Weather Forecasts
ENSO	Niño/Southern Oscillation
ESM	Earth System Model
ETCCDI	Expert Team on Climate Change Detection and Indices
FGD	Focus group discussion
GCM	Global Climate Model

GDP	Gross Domestic Product
GFCS	Global Framework for Climate Services
GFDL	Geophysical Fluid Dynamics Laboratory
ICHEC	Irish Centre for High End Computing
ICTP	Abdus Salam International Centre for Theoretical Physics
IOD	Indian Ocean Dipole
IPCC	Intergovernmental Panel on Climate Change
IPSL	Institut Pierre-Simon Laplace
ITCZ	Intertropical convergence zone
IVS	Inter-annual variability score
IWMI	International Water Management Institute
JAS	July-August-September
KE	Kenya
KNMI	Royal Netherlands Meteorological Institute, De Bilt, The Netherlands
MAM	March, April, and May
MIROC	Model for Interdisciplinary Research on Climate
MJO	Madden–Julian oscillation
MOHC	Met Office Hadley Centre
MPI	Max Planck Institute for Meteorology
NCAR	National Center for Atmospheric Research
NCC	Norwegian Climate Centre
NCL	NCAR Command Language
NOAA	National Oceanic and Atmospheric Administration
NorESM	Norwegian Earth System Model
OECD	Organisation for Economic Co-operation and Development
ON	October-November
OND	October, November and December
ONS	Onset
Open GrADS	Open Grid Analysis and Display System

QBO	Quasi-biennial oscillation
QCCCE	Queensland Climate Change Centre of Excellence
RA	Rwanda
RCA	Rossby Centre regional atmospheric model
RCM	Regional Climate Models
RCP	Representative Concentration Pathway
RCP	Representative Concentration Pathway
RMS	Root-mean-square
SDG(s)	Sustainable Development Goal(s)
SDII	Simple daily precipitation intensity index
SMHI	Sveriges meteorologiska och hydrologiska institute (Swedish Meteorological and Hydrological Institute)
SOI	Southern Oscillation Index
SST	Sea-Surface Temperature
TAMSAT	Tropical Applications of Meteorology using SATellite and ground-based observations
TZ	Tanzania
UG	Uganda
UQAM	Universite du Quebec a Montreal
WCRP	World Climate Research Program

ABSTRACT

The study assessed historical intraseasonal rainfall variability, generated future intraseasonal rainfall scenarios, and made recommendations to build on climate service foundations for a sustainable climate change adaptation in East Africa. First, an assessment of the performance of regional climate models (RCMs), participating in the Coordinated Regional Climate Downscaling Experiment (CORDEX), in simulating East Africa's spatio-temporal precipitation characteristics was done. Using a set of eight descriptors of East Africa's precipitation, the RCM assessment was done to determine the best model runs for evaluating East Africa's historical and future precipitation characteristics. The descriptors are the consecutive dry days (CDD), consecutive wet days (CWD), simple precipitation intensity index (SDII), mean daily annual (ANN), seasonal (March to May, MAM and October to December, OND) precipitation, and representatives of heavy precipitation (90p) and very intense precipitation (99p) events. Specifically, (i) nine reanalysis data (ERAINT)-driven and (ii) 24 model runs from five general circulation model (GCM)-driven CORDEX-Africa RCMs were analysed. Relatively better performing RCM runs were then used to assess projected precipitation changes (for the period 2071-2099 relative to 1977-2005) over the study domain under the representative concentration pathway (RCP) 8.5 scenario. Results showed the performance of RCMs to be descriptor- and scope- specific. Overall, RCA4 (r1i1p1) forced by CNRM-CERFACS-CNRM-CM5 and MPI-M-MPI-ESM-LR, REMO2009 (r1i1p1) forced by MPI-M-MPI-ESM-LR, and RCA4 (r2i1p1) forced by MPI-M-MPI-ESM-LR emerged as the top four RCM runs. Further, an ensemble mean of the top four model runs outperformed an ensemble mean of 24 model simulations and ensemble means for all runs in an RCM. An analysis of projections showed a reduction(increase) in mean daily precipitation for MAM(OND), an increase(decrease) in CDD(CWD) events, and a general increase in SDII and the width of the right tail of the precipitation distribution (99p-90p). An increase in SDII and 99p-90p implies a possibility of heavy and extreme precipitation incidences by the end of the 21st century. Examples of how the climate information generated from the analysis could be used in various sectors were made. First, an assessment of historical and future rainfall variability over Kilifi County, a typical coastal community whose primary source of livelihood is rain-fed smallholder farming, was done. Using climate information and data from the social survey on the farmers' perceptions of climate variability, adaptive capacity, and adaptation activities, an innovative climate change adaptation model was co-developed with smallholder farmers to help build the farmers' adaptive capacity in Kilifi and beyond. Secondly, the study assessed the potential impacts of global warming scenarios of 1.5 ^{o}C and 2 ^{o}C on malaria transmission in East Africa. Under the two warming scenarios, results showed an imminent increase in seasons and geographical extents of malaria transmission in East Africa. The study recommended intensification of efforts to sustain the gains made towards malaria elimination. Lastly, a status review (in terms of climate, population, and land-use change over Nairobi metropolis) was done, and recommendations made to help safeguard the future of Nairobi National Park. Overall, the thesis findings provide essential information to support the region's climate change adaptation and mitigation efforts for sustainability.

CHAPTER 1: INTRODUCTION

This chapter gives some background information on the current study (1.1), a description of the problem being addressed (1.2), a list of research questions (1.3), and objectives (1.4) that guide the study. It also lays out the hypotheses under investigation (1.5), why the current research is necessary (1.6), a conceptual framework (1.7) followed, and definitions of Key Terms (1.8).

1.1 Background

By the year 2017, human-induced global warming, defined as an increase in combined surface air and sea surface temperature averaged over the globe and over 30 years, had reached about 1^{o}C above pre-industrial levels (Hoegh-Guldberg et al., 2018). The impacts of a warming globe are disproportionately affecting various regions of the world with people living in low- and middle-income countries being the most affected (Handmer et al., 2012). Small islands, coastal regions, and high mountain range areas are among the world's most affected regions (Albert et al., 2018) given their relatively higher exposure to climate hazards.

Rainfall in East Africa is quite variable in time and space (Kiros et al., 2017; Ogega, 2017; Opiyo et al., 2014). While the region tends to experience more deficit than surplus precipitation events, major heavy rainfall events have been recorded over time (e.g. Kilavi et al., 2018) which, often, lead to massive losses in life and property (Davis et al., 2009; Heron et al., 2012). The region experiences a complex blends of stressors brought about by environmental, political, socio-economic, and structural factors in the region (e.g. Gbegbelegbe et al., 2018). Hence, an occurrence of extreme climate events (in the form of prolonged droughts, extensive floods, and heatwaves) is likely to adversely affect the region's socio-economic stability.

East Africa's economy is mainly supported by agriculture, tourism, and related sectors, which are predominantly rainfed (Alessandro et al., 2015). Here, agriculture accounts for approximately 36% of the East African Community (EAC) 's gross domestic product (GDP; AfDB, 2018). About 80% of EAC's population draws its livelihood from

agriculture (EAC, 2018). For instance, agriculture accounts for more than a quarter of Kenya's GDP, 65% of exports, 70% of rural jobs, and 60% of foreign exchange (Alessandro et al., 2015; FAO, 2018). Yet, about 95% of farmed land in sub-Saharan Africa is rain-fed (Rockström et al., 2010; IWMI, 2018).

Health is one of the sectors affected by global warming. For instance, a special report on global warming of 1.5 ^{o}C (hereinafter SR1.5) published by the Intergovernmental Panel on Climate Change (IPCC; Hoegh-Guldberg et al. 2018) identified weather and climate as one of the primary drivers of the intensity, spatial, and temporal extent of malaria transmission (Ren et al., 2016; Semakula et al., 2017). The climatic factors including temperature, rainfall, and humidity influence the abundance and survival of mosquitoes and, hence, malaria transmission (Metelmann et al., 2019; Nsoesie et al., 2016). Due to a non-linear relationship between weather and climate and the spatial and temporal occurrence of malaria, mapping patterns of change in risk is likely to be more difficult with additional warming (Ren et al., 2016).

While efforts are underway towards malaria elimination, malaria remains a significant disease burden in East Africa (Bashir et al., 2019; WHO, 2020). In 2018, approximately 228 million malaria cases and about 405,000 deaths were reported globally (WHO, 2020) with about 93% of the malaria cases and 94% of the malaria-related deaths occurring in sub-Saharan Africa. In East Africa, Uganda has the highest number of malaria cases, accounting for 5% of global totals in 2018. Further, the geographical distribution and prevalence of mosquito vectors for Chikungunya, Dengue fever, and Zika virus is projected to change in a warmer climate (Colón-González et al., 2013; Mweya et al., 2016; Tjaden et al., 2017). Hence, a significant investment is required to enhance monitoring of changes in environmental factors as well as provide timely adaptive and mitigative measures to minimize the risks.

Overall, the impacts of a warming global climate system (IPCC, 2014) are likely to affect the region's socio-economic well-being adversely. With the structure of East Africa's economy not expected to abruptly shift from being climate-dependent, concerted efforts from all actors are required to develop effective climate services to enhance the adaptive

capacity of East Africans for sustainable socio-economic development in the face of the climate crisis.

The Global Framework for Climate Services (GFCS) defines climate services as those that provide individuals and organizations with information that facilitates climate-smart decision making (Hewitt et al., 2012). These services must be produced, translated, and delivered promptly (National Research Council, 2001) to make them useful to intended beneficiaries. There is an increasing discourse on the need for more location and sector-specific climate services, but lack of adequate and effective policy mainstreaming at national and sub-national levels often leads to sporadic individual and uncoordinated initiatives that yield minimal results (Hassanali, 2017; Naab et al., 2019; Ojwang et al., 2017).

Therefore, the current study sought to contribute to ongoing efforts to enhance the understanding of current precipitation patterns over East Africa and how these patterns may change in the future under various global warming scenarios. Specifically, the study assessed the performance of 24 model runs from CORDEX RCMs in simulating East Africa's spatial and temporal precipitation variability. An analysis of potential future changes in East Africa's heavy and extreme precipitation events was done and suggestions made on how to enhance the delivery and use of effective climate services for sustainability in East Africa's agriculture, health, and tourism sectors in a warming climate.

1.2 Problem Statement

East Africa's economy is mainly supported by agriculture, tourism, and related sectors. Here, agriculture accounts for approximately 36% of the East African Community (EAC)'s gross domestic product (GDP; AfDB, 2018), and approximately 80% of EAC's population draws its livelihood from agriculture (EAC, 2018). However, the agriculture and allied sectors almost entirely depend on rainfall (e.g. Alessandro et al., 2015). The dependency of the main economic drivers on rainfall puts the entire economy of East Africa vulnerable to climate variability and change.

Indeed, East Africa experiences high rainfall variability in the form of heavy and extreme (wet and dry) rainfall events (e.g. Lyon & Dewitt, 2012; Tierney et al., 2015). A generally decreasing rainfall over time has also been recorded (Nicholson, 1996; Segele et al., 2009), although this trend may change in the future in what has been termed as the "East African Climate Paradox" (Wainwright et al., 2019). While efforts have been made towards enhancing the understanding of East Africa's rainfall variability, most works tend to focus on seasonal to annual and decadal scales (e.g. Endris et al., 2013; Omondi et al., 2012; Souverijns et al., 2016). Consequently, rainfall variability at sub-seasonal to seasonal scales, which has a significant impact on the region (e.g. Fiwa et al., 2014; Silungwe et al., 2019), remains least-understood. Hence, the current study sought to enhance the understanding of East Africa's past and future intraseasonal rainfall variability to inform better climate change adaptation efforts for socio-economic development and sustainability.

1.3 Research Questions

The study was guided by the following research questions:

1. What are the historical intraseasonal rainfall characteristics over East Africa?
2. How adequate are regional climate models in generating future rainfall change scenarios for East Africa?
3. How is intraseasonal rainfall likely to change by the year 2100 under global warming?
4. How can knowledge of intraseasonal rainfall variability be used to inform the detection and mitigation of immediate and expected climate risks in the agriculture, tourism, and health sectors?

1.4 Objectives

This study's main objective was to assess historical intraseasonal rainfall variability, generate future intraseasonal rainfall scenarios, and build on climate service foundations for sustainable climate change adaptation in East Africa.

Specifically, the study sought to:

1. evaluate the performance of CORDEX RCMs in simulating observed

a) spatial and temporal intraseasonal rainfall characteristics and
b) heavy precipitation events over East Africa

2. investigate whether observed rainfall characteristics change in the future under global warming
3. build on foundations for the use of climate services for sustainability in the agriculture, health, and tourism sectors

1.5 Hypothesis

East Africa will experience a significant change in intraseasonal rainfall characteristics by the end of the 21st century under global warming.

1.6 Significance of the Study

The current study sought to enhance the understanding of past and historical intraseasonal rainfall change and variability over East Africa and give examples of how this information can be used to inform effective climate change adaptation. While the economy of East Africa is mainly driven by agriculture and allied sectors (AfDB, 2018; EAC, 2018; Alessandro et al., 2015; FAO, 2018), most agricultural activities in the region are smallholder and predominantly rainfed (Alessandro et al., 2015; FAO, 2018). Yet, rainfall over East Africa is quite variable in time and space (e.g. Cook & Vizy, 2013; Nicholson, 2017; Tierney et al., 2015).

A good understanding of historical intraseasonal rainfall variability in terms of onset and cessation dates, intensity, frequency, and duration will significantly benefit the region (e.g. Fishman, 2016; Guan et al., 2015; Silungwe et al., 2019). Even with various studies made, East Africa's precipitation variability at the sub-seasonal to seasonal scales is yet to be fully understood (e.g. Cattani et al., 2018; Endris et al., 2019; Wainwright et al., 2019). This study identified the best performing models in simulating East Africa's rainfall characteristics, facilitating the assessment of future climate projections for the region. An analysis of past rainfall characteristics and an outlook of projected changes in the area was also made. This information will be useful for future rainfall studies in the region in addition to informing the formulation and implementation of robust climate

change adaptation strategies for East Africa. In so doing, the potential negative impacts of a changing climate on agriculture, health, and allied sectors will be minimized. The region will also be better positioned to harness the potential benefits of the positive impacts of a changing climate and, ultimately, livelihoods improved.

1.7 Conceptual Framework

A conceptual framework is a presentation (in a narrative form, or both) of how the researcher intends to tackle a particular task. It links concepts, empirical research, and essential theories that the researcher intends to address (Collins & Stockton, 2018; Grant & Osanloo, 2014; Miles & Huberman, 1994). Given its logical arrangement, the conceptual framework gives a picture of how the research ideas flow and relate to one another (Grant & Osanloo, 2014). Here, the research methodology agrees with variables (independent, dependent, or otherwise), relationships, and contexts (Miles & Huberman, 1994; Ravich & Carl, 2016).

The current study modelled its conceptual framework (Figure 1.1) around the Global Framework for Climate Services. GFCS aim at enabling the development and use of climate services to help decision-making in response to climate-related risks (Hewitt et al., 2012). Implementation of the GFCS is grouped into five components: observations and monitoring; research, modelling, prediction; and capacity development. The components tackle five priority areas: agriculture and food security, disaster risk reduction, water, energy, and health. This current study adapted three components and three priority areas shown in Figure 1.1.

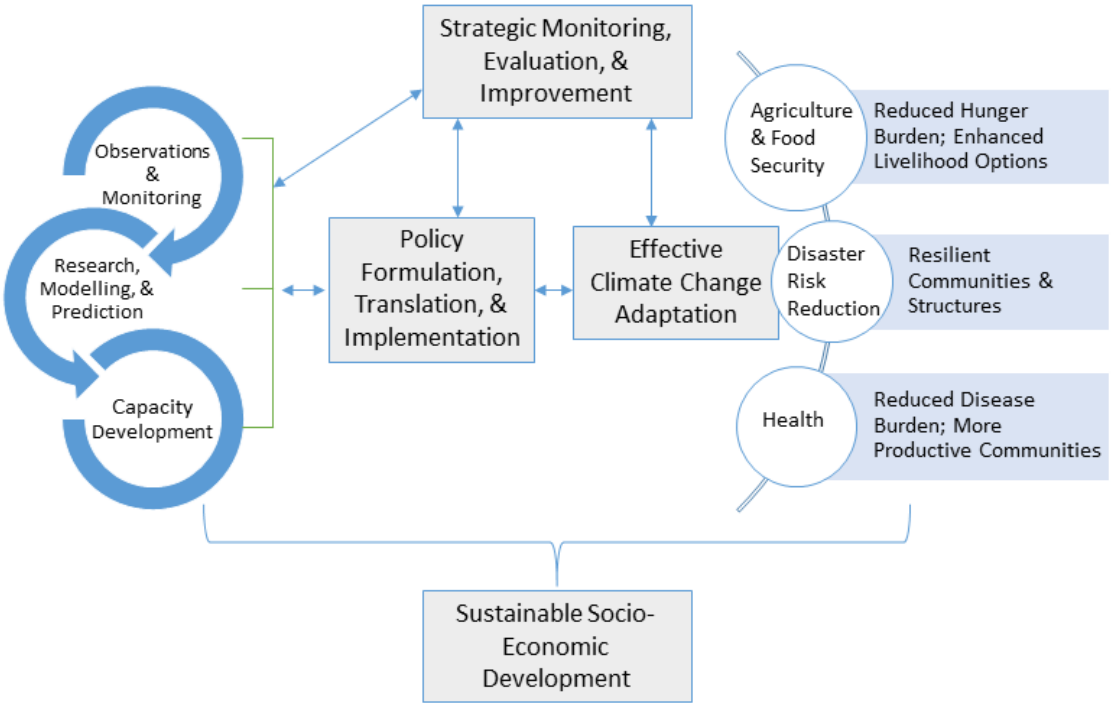

Figure 1.1. The conceptual framework for the study (adapted from GFCS, Hewitt et al., 2012)

The main goal of the current study was to facilitate effective climate change adaptation in East Africa (the main dependent variable in the conceptual framework). For effective climate change adaptation to take place, a robust policy formulation, interpretation, and implementation process is paramount. Here, climate information (from observations and models) provides the scientific evidence into the policy space to facilitate the design and adoption of effective policies that will deliver effective climate change adaptation. The outcomes of these processes is disaster risk reduction, improved agriculture and food security, and improved health and well-being. Through strategic knowledge co-production and sharing, climate information informs development activities, ultimately leading to sustainable socio-economic development.

1.8 Definition of Key Terms

The **climate** of a given area is defined as average weather conditions ranging from months to years. The World Meteorological Organization (WMO[1]) recommends 30 years as the classical period for averaging climate variables including temperature, precipitation, and wind. These variables belong to a cluster referred to as a climate system which comprises of, mainly, the atmosphere, the cryosphere, the hydrosphere, the biosphere, and the land surface. Interactions among the climate system components coupled with external factors, such as solar variations and human activities, make the climate system quite dynamic and difficult to predict (WMO, 2020).

Climate change: defined by the United Nations Framework Convention on Climate Change (UN, 1992) as "a change of climate which is attributed directly or indirectly to human activity that alters the composition of the global atmosphere and which is in addition to natural climate variability observed over comparable time periods". Climate change occurs when the mean and variability characteristics change and persist over an extended period, say 30 years (IPCC, 2018). On the other hand, climate variability refers to changes lasting a few months or years; but less than 30 years (WMO, 2020).

Climate variability: refers to variations in the mean state and other statistics of the climate on all temporal and spatial scales, beyond individual weather events. It often refers to deviations of climatic statistics over a given period (e.g. a month, season, or year) when compared to long-term statistics for the same calendar period. The variability may be caused by either natural internal processes within the climate system or by changes in natural or anthropogenic external factors (WMO, 2020). Most of the changes in the climate system are natural. However, human activities aggravate the variability and change, hence causing disruptions to human and natural systems, resulting in the occurrence of enhanced extreme weather conditions (Mysiak et al., 2016). For instance,

[1] https://public.wmo.int/en

the Intergovernmental Panel on Climate Change (IPCC) 's 5th Assessment Report (AR5) concluded that at least 50% of the observed increase in global average surface temperature for the period 1951 to 2010 was "extremely likely" to have been caused by the rise in anthropogenic forcing (Bindoff et al., 2014; Jones et al., 2013). Anthropogenic activities, such as the consumption of fossil fuels, increase the concentration of greenhouse gases (GHG)[2] in the atmosphere hence contributing to global warming[3] and climate change (e.g. Akdag & Yıldırım, 2020; Alola et al., 2019).

The process of adjustment to expected or actual climate and its effects to minimize the damage or exploit the potential benefits is referred to as **climate adaptation** (IPCC, 2018; Tàbara et al., 2019). The effectiveness of climate change adaptation depends on the ability of systems, humans, institutions, and other organisms to adjust to potential damage, to respond to consequences, or to benefit from arising opportunities; the adaptive capacity (MEA, 2005; IPCC, 2018).

Climate change mitigation refers to human interventions aimed at minimizing the sources or strengthening sinks of greenhouse gases in the environment (IPCC, 2001). To effectively address climate-related challenges, adaptive and mitigative measures must be designed and implemented together (e.g. Kongsager, 2018). Indeed, some measures, such as planting trees, can be both mitigative and adaptive. Indeed, some measures, such as planting trees, can be both mitigative and adaptive.

Climate services: The Global Framework for Climate Services (GFCS[4]) defines climate services as those that provide individuals and organizations with information that facilitates climate-smart decision making (Hewitt et al., 2012) and these services must be produced, translated, and delivered in a timely manner (National Research Council, 2001) to make them useful to intended beneficiaries.

---

[2] https://bit.ly/2zTfMbC

[3] https://go.nasa.gov/3g3lf0d

[4] https://gfcs.wmo.int/what-are-climate-services

Future: the current study refers to the period 2071-2099 as the "future"

Global warming: The Intergovernmental Panel on Climate Change (IPCC) defines global warming as an increase in combined surface air and sea surface temperatures averaged over the globe and over a 30-year period (Allen et al., 2016). The warming is, often, expressed relative to an approximation of pre-industrial temperatures such as the period 1850-1900 used in the IPCC's 5th Assessment Report (AR5).

Intraseasonal climate variability refers to inconsistent behaviour of climate variables within seasons.

Pre-industrial period refers to an approximation of period when emissions from industries was minimal compared to the world today. For instance, the IPCC AR5 uses the period 1850-1900 as the pre-industrial period.

Baseline: the current study refers to the period 1977-2005 as the baseline.

CHAPTER 2: LITERATURE REVIEW

This section sought to review existing literature on rainfall variability over East Africa. It is divided into four parts namely historical rainfall variability over East Africa (1), systems that influence East Africa's rainfall (2), East Africa's future rainfall projections (2.3), and building on foundations for climate services (2.4).

2.1 Historical Rainfall Variability over East Africa

Rainfall in East Africa is quite variable in both time and space (Muthoni et al., 2019; Nicholson et al., 2018; Wenhaji Ndomeni et al., 2018). The region experiences devastating prolonged droughts (Gebremeskel Haile et al., 2019; Nicholson, 2014) and perennial floods (e.g. Li et al., 2016; Masih et al., 2014; Uhe et al., 2018) that often disrupt livelihoods and lead to loss of life. Additionally, variability within seasons at annual, interannual, and decadal scales is quite pronounced (e.g. Omondi et al., 2012; Wainwright et al., 2019; Yang et al., 2014). This high variability calls for continuous research to enhance the understanding of East Africa's past and future rainfall characteristics to inform effective climate change adaptation and sustainable development.

A study by Nicholson (2017) inferred that, among other things, (1) the concept of two "rainy seasons" in East Africa emanating from the biannual crossing of the Intertropical Convergence Zone (ITCZ) at the equator is insufficient; (2) The March-May (MAM) rains should not be regarded as a single season given that its character, causal factors, and teleconnections are significantly different for each month in the MAM; (3) Factors associated with the October-December (OND) are nonstationary; and (4) Droughts in East Africa are prolonging and intensifying even across seasons, and there is minimal knowledge about their causes. These conclusions have significant implications on the region's socio-economic development which is heavily dependent on environmental factors.

At the intraseasonal scale, the focus of this thesis, variability is difficult to predict due to the atmosphere's chaotic nature (Luo & Wood, 2006) and influences from the land and ocean conditions (Hudson et al., 2011). Yet, intraseasonal forecasts are of great

importance for the agricultural and other economic sectors that depend on rainfall. The intraseasonal predictions close the gap between weather and seasonal forecasts, ranging from 10 to 60 days (Hudson et al., 2011).

Some studies have been done towards understanding intraseasonal rainfall variability over East Africa. Gitau (2010) looked at seasonal rainfall total, mean rainfall intensity, and daily rainfall frequency aspects of the region's rainfall variability. His study showed that locations with decreasing trends in the mean duration of wet spells, number of wet days, and mean rainfall intensity experienced during the long rainy season did not have an organized pattern. His analysis showed an increase in cases with prolonged dry spells within the rainfall seasons. However, his study did not adequately establish distinct trends in intraseasonal rainfall variability over East Africa.

Kuya (2016) analysed temperature and precipitation extremes over East Africa using observational data and the RCA downscaled 8 GCM data. The analysis showed an increase in extreme precipitation events over East Africa for both historical and future precipitation. The study identified the influence of modes of variability, namely ENSO, IOD, SOI, and QBO but missed to show a direct relationship between the modes of variability and the intraseasonal precipitation variability. Kuya (2016) recommended further research to assess the timing of extreme weather events over East Africa. More recently, Cattani et al. (2018) set out to analyse the temporal and spatial variability and trends of rainfall over East Africa at seasonal and annual scales. Their results show that the OND season has more trend signals for extreme weather events than the MAM season. However, the study did not show the correlation between the observational intraseasonal precipitation variability and the modes of variability over East Africa.

2.2 Systems that Influence Rainfall over East Africa

East Africa's climate is controlled by various systems including the subtropical high-pressure zones, the ITCZ, and trade winds. Others include the El Niño Southern Oscillation (ENSO), the Indian Ocean Dipole (IOD), the Maiden-Julien Oscillation (MJO), and subtropical high-pressure zones (Figure 2.1). The region is also punctuated with large lakes, mountains, and other topographic features that affect the region's

weather and climate. All these factors, most of which are interconnected, result in intricate climatic features that change quickly and over short spatial extents – making EA one of the most climatically complex regions in Africa (e.g. Omondi et al., 2012; Nicholson, 1996; Souverijns et al., 2016).

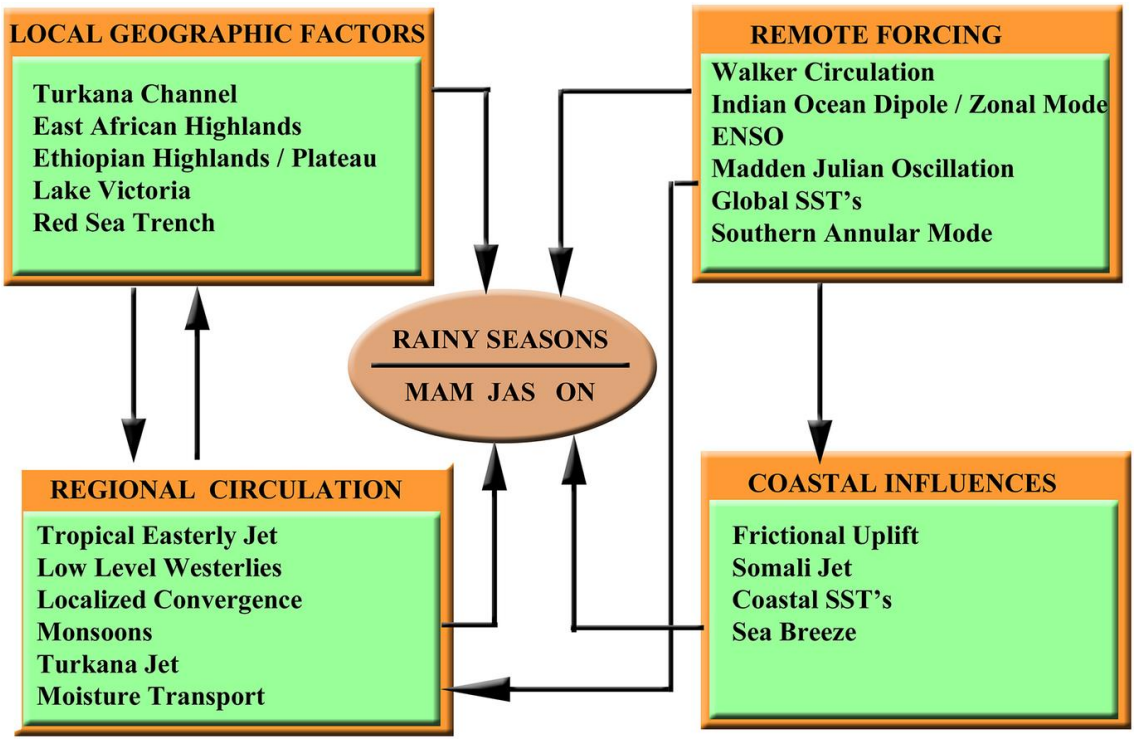

Figure 2.1. An illustration of factors (and their interrelationships) influencing the three rainy seasons (MAM, JAS, and ON) of eastern Africa. The figure is reproduced from Nicholson (2017) under the terms of the Creative Commons Attribution 4.0 International license (CC-BY 4.0)

At the interannual time scale, the OND season over East Africa shows high year-to-year variability and a strong spatial coherence of rainfall anomalies in most of the region with strong links to large-scale circulation anomalies in the tropical oceans (e.g. Hastenrath et al., 2004; Philippon et al., 2002; Saji et al., 1999). The MAM rains show inconsistent spatial variability and weak linkage to global sea-surface temperatures (SSTs; Camberlin et al., 2009). Seasonal rainfall over East Africa shows inhomogeneity within the seasons. For instance, a time series analysis for the MAM season shows differing year-to-year variability of each month in the MAM season (e.g. Indeje et al., 2000; Nicholson, 2017; Nicholson & Kim, 1997). Spatial rainfall anomaly patterns have been similar between

March and April but quite different for May (e.g. Philippon et al., 2002). Further, the MAM rainfall over East Africa usually shows a strong/weak linkage to local systems/remote forcing. However, events post the year 2000 (e.g. the 2000, 2008, 2009, 2011, and 2017 droughts) tend to show a strong linkage to Indo-Pacific SSTs (e.g. Lyon & Dewitt, 2012; Vigaud et al., 2017). These analyses show that intraseasonal rainfall variability over E. Arica, especially for the MAM season, remains least understood (e.g. Boyard-Micheau et al., 2013; Wainwright et al., 2019).

2.2.1 The ITCZ and East Africa's Topography

The ITCZ (Figure 2.2) is a permanent low-pressure area in the equatorial trough where surface trade winds meet forming a zone of enhanced cloudiness, convection, and precipitation. It is laden with moisture and heat hence making it an essential contribution to the earth's energy and water budget (Waliser & Jiang, 2015). The ITCZ follows the sun's seasonal positioning on earth, moving northwards during the northern hemisphere summer and southwards during the southern hemisphere summer (Schulman, 1973). The ITCZ's asymmetric spread has been attributed to unequal receipt of solar insolation across the tropics and sea-level temperature variations (Folland et al., 2001).

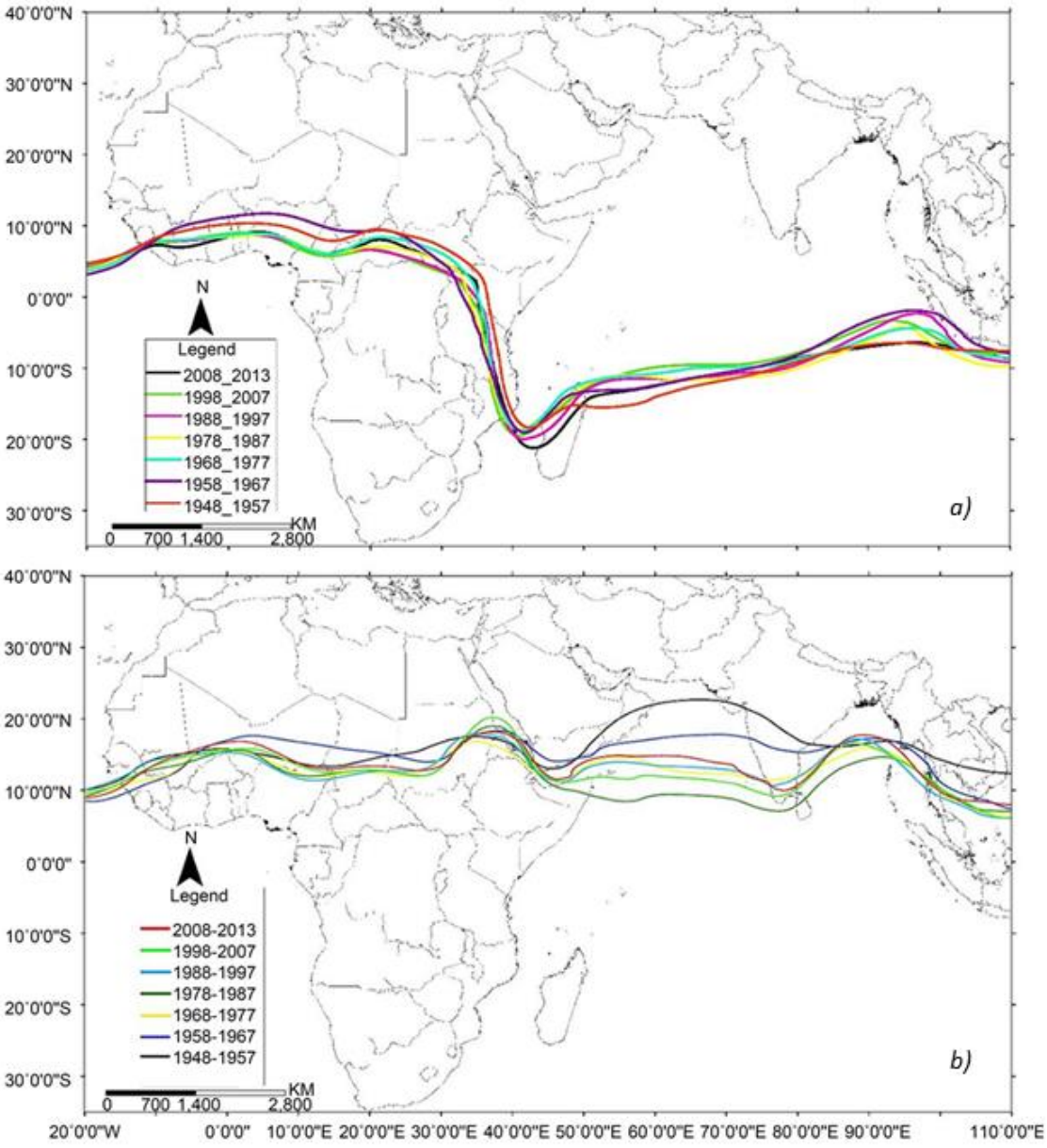

Figure 2.2: Time-averaged position of the ITCZ in the months of March (a) and November (b). The figure is reproduced from Lashkari et al. (2017) as provided for in the Creative Commons Attribution 4.0 International license (CC-BY 4.0)

For a long time, the ITCZ was thought to be one of MAM rainfall's primary drivers over equatorial EA. However, this notion is changing with recent studies suggesting that the ITCZ's influence should be limited to coastal equatorial East Africa, where the trade winds are influential (Nicholson et al., 2018). Instead, factors such as saturation mean static energy, mean static energy ,and vertically integrated moisture from the Indian

Ocean are thought to be among key drivers of MAM rainfall (Yang et al., 2015). Others include the role of topography (Hession & Moore, 2011; Jackson et al., 2009) and large-scale systems such as the Madden-Julian oscillation (Berhane & Zaitchik, 2014) and vertical cells over the Indian Ocean (e.g. Hastenrath et al., 2011; Nicholson et al., 2018). Camberlin et al. (2014) established that while mean elevation seemed to have little effect on the amount of rainfall received, it strongly contributed to the frequency of rainfall occurrence. Further, topography influences low-level flows. For instance, East Africa's highlands channel the flow of currents into a strong southerly current that transitions to south-westerly current after crossing the equator and becoming the source of the Somali Jet and southwest monsoon flow (Slingo et al., 2005). Currents over Turkana also form into an intense low-level jet (Kinuthia, 1992). Therefore, more work is required to enhance the understanding of systems that influence East Africa's rainfall (Nicholson, 2018).

2.2.2 El Niño Southern Oscillation (ENSO)

By definition, the El Niño Southern Oscillation arises from ocean-atmosphere coupled feedbacks (Bjerknes, 1966) in the equatorial Pacific Ocean. ENSO alternates irregularly between its cold phase, La Niña, and its warm phase, El Niño, peaking during boreal winter at a frequency of 2 to 7 years. The central-to-eastern tropical Pacific Ocean warms during an El Niño event and cools during a La Niña event, causing different large-scale disruptions in atmospheric and ocean circulations worldwide. Simultaneously, the atmospheric sea-level pressure is higher/lower at the eastern/western tropical Pacific Ocean. As a result, the oceanic thermocline shifts eastwards to about 30m in the far east Pacific and up to 200m in the west Pacific (Kiladis et al., 1989; Schneider et al., 2014). Therefore, ENSO is the year-to-year shift from the seasonally evolving climatological state where anomalous warming of the eastern equatorial Pacific during an El Niño is associated with weaker than normal Walker Circulation, punctuated with weaker than normal Trade Winds, a thermocline tilt, and an east-west atmospheric pressure gradient (Figure 2.3). Interaction of these elements results in a positive Bjerknes-coupled feedback loop (Bjerknes, 1966) continues until the end of a calendar year when damping happens.

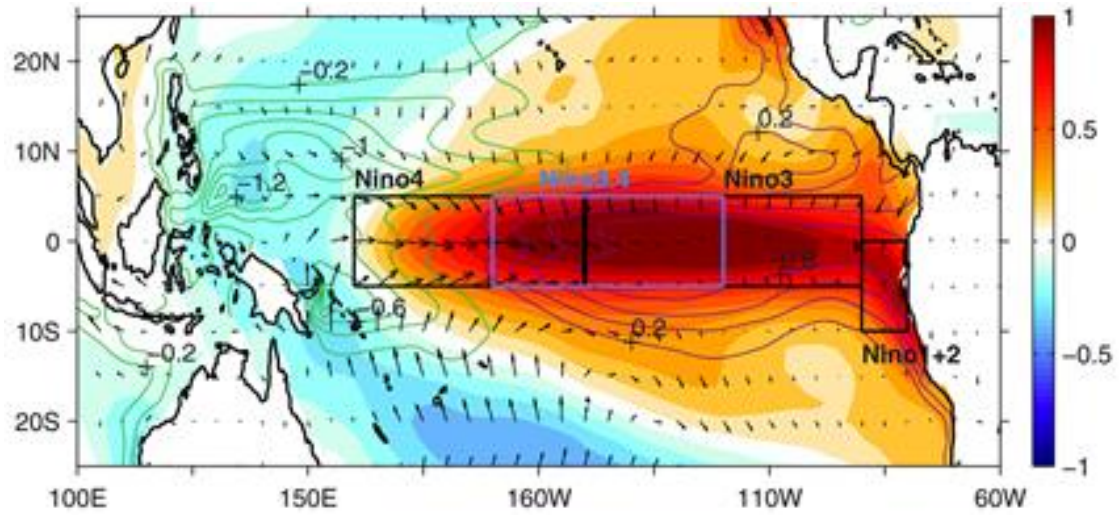

Figure 2.3: A plot of general ENSO properties showing anomalous patterns in SST (colour shading), T300 (contours), and surface wind velocities (vectors), shown as regressions onto the Niño3.4 index. The figure is reproduced from Santoso et al. (2017) under the terms of the Creative Commons Attribution 4.0 International license (CC-BY 4.0)

The large-scale changes augment the likelihood of extreme weather events worldwide, including extreme rainfall (e.g. Power & Callaghan, 2016) and cyclones (e.g. Jin et al., 2014). ENSO's impacts tend to be more pronounced for extreme El Niño events, such as the 1982/1983 and 1997/1998 (e.g. McPhaden et al., 1998) events, compared to La Niña events. Although peculiar compared to other El Niño events, the 1982/1983 and 1997/1998 El Niño events caused significant environmental disruptions worldwide (e.g. McPhaden et al., 1998).

Work has been done towards understanding ENSO and its potential future behaviour (e.g. Camberlin, 1997; Indeje et al., 2000; Osima et al., 2018; Stevenson et al., 2012). However, significant variability between El Niño - La Niña events makes it difficult to decipher whether ENSO can even be termed as a true oscillatory phenomenon and not a series of feedback-amplified stochastic anomalies (e.g. Gebbie et al., 2007; Jin et al., 2006). Nonetheless, the impacts of ENSO events continue to be felt across the globe. Physical changes in the Pacific Ocean, such as a change in heat content, are likely to affect ENSO's future dynamics. Therefore, continuous study and monitoring of ENSO is paramount in efforts to mitigate climate risks.

Over East Africa, the OND rainfall variability has been linked to ENSO as a primary driver (e.g. Camberlin, 1997; Endris et al., 2016). The future of ENSO under a warming climate, however, remains uncertain. Some studies (e.g. Zelle et al., 2005) suggest that there may not be significant changes in ENSO's frequency, duration, amplitude, and spatial characteristics. Others (e.g. Collins et al., 2010) suggest difficulty in determining the exact implication of a changing climate on processes that lead to El Niño and La Niña events. Some projections (e.g. Cai et al., 2015) show an increase in La Niña events under a warming climate. Hence, further research is required to enhance the understanding of ENSO's dynamics and their impact on East Africa's rainfall variability.

2.2.3 The Indian Ocean Dipole (IOD)

The IOD refers to the difference in SST anomalies between the tropical western Indian Ocean and the tropical south-eastern Indian Ocean (e.g. Hastenrath & Polzin, 2003; Mpelasoka et al., 2018; Owiti et al., 2008; Saji et al., 1999). It occurs in seasonal phases with onset in May, a peak in October, and cessation in December. A negative/positive phase is associated with cooler/warmer SST in the tropical western Indian Ocean and warmer/cooler SST in the tropical south-eastern Indian Ocean. Over East Africa, IOD's positive/negative phase tends to enhance/diminish OND rainfall (Owiti et al., 2008).

The future of the IOD over East Africa under a warming climate is not clear. Some studies (e.g. Cai et al., 2013; Zheng et al., 2013) suggest that a warming climate is likely to change the equatorial Indian Ocean's mean state, with the western part of the Indian Ocean warming faster than the eastern region. With expected changes in general atmospheric circulations (such as an expansion of the Hadley cell, mid-latitude jets, and convergence zone shifts), significant changes in the links between IOD and its teleconnections may occur (e.g. Lau et al., 2008; Stevenson et al., 2012). As a result, East Africa may experience more rainfall variability in the future. This calls for more studies to monitor the changing systems and enhance the understanding of future climate risks for the region.

2.3 Rainfall Change Projections for East Africa

Various studies analysing climate projections over East Africa indicate an increasing rainfall by 2100 (e.g. Buontempo et al., 2015; Niang et al., 2014; Ogega, 2017; Shongwe et al., 2011). These projections directly contrast to historical climate trends hence creating what has been referred to as East Africa's climate paradox whose causes remain unclear (e.g. Gebrechorkos, 2019; Rowell et al., 2015). Precipitation changes experienced over the tropics in the annual mean have been linked to thermo-dynamical increases in precipitation (e.g. Chadwick et al., 2013). By applying a classification of circulation characteristics on historical and future regional climate models (RCMs), Souverijns et al. (2016) deduced that under a high greenhouse gas emission scenario, changes in the occurrence of typical circulation types is attributed to 23% of the total change in precipitation over East Africa by the year 2100. The rest (77%) of the changes are not attributable to East Africa's synoptic features (such as topography, local feedback, and moisture distribution).

Normally, East Africa is classified as a region with the minimal average change in terms of drought severity. Projections indicate that Africa may be the continent most affected by the impacts of climate change (Niang et al., 2014). Other projections show a possibility of more frequent and intense droughts in some parts of East Africa (e.g. Gizaw & Gan, 2017). Further, drought projections for East Africa indicate considerable uncertainties. While general precipitation projections for East Africa indicate a general increase in average rainfall by the end of the 21st century, the range of precipitation change is given to be -2 to 20%. Seasonal precipitation changes are said to range from -42 to 78% for the January to March period and from -10 to 70% in the OND season (Dabernig et al., 2017).

2.4 Building on Foundations for Climate Services in East Africa

There is an increasing discourse on the need for more location and sector-specific climate services. However, a lack of effective policy mainstreaming at national and sub-national levels often leads to sporadic individual and uncoordinated initiatives that yield minimal results (e.g. Hassanali, 2017; Naab et al., 2019; Ojwang et al., 2017). The following subsections focus on the health and agriculture sectors as examples where climate services are needed.

2.2.4 Climate Services in the Agriculture Sector

The importance of weather and climate to agriculture in Africa is well documented (e.g. Knox et al., 2012; Ziervogel et al., 2014). Identification of types of weather and information services useful for agriculture in Africa, the quality and relevance of available weather and climate services, and how farmers can use the information for enhanced productivity and livelihood has been done (e.g. Cooper et al., 2008; Landman & Beraki, 2012; Tall et al., 2018). For instance, a review by Vaughan et al. (2019) highlights the need to improve the design, delivery, and impact of agricultural weather and climate services in Africa. The review established a need for activities that could enhance the evidence of access, use, and effects of weather and climate services. It also calls for activities that can advance the use and usability of evidence for practical use in policy formulation and implementation.

2.2.5 Climate Services in the Health Sector

Climatic factors (including precipitation, temperature, and humidity) contribute to Malaria transmission by influencing the abundance and survival of mosquitoes (e.g. Metelmann et al., 2019; Nsoesie et al., 2016). The SR1.5 identifies a knowledge gap in the impacts of global and regional climate change at 1.5 ^{o}C on, *inter alia*, public health and infectious diseases, particularly for developing nations. Some work has been done towards understanding the potential impact of global warming in East Africa (e.g. Gudoshava et al., 2020; Osima et al., 2018). However, no conclusive literature exists on the potential impacts of 1.5 ^{o}C and 2 ^{o}C global warming levels (hereinafter GWL1.5 and GWL2.0) in East Africa.

2.2.6 Climate Services in the Tourism Sector

Unplanned land-use change in areas adjacent to conservation areas has been linked to changes in biodiversity and ecological functions inside the conservation areas (Ahmad et al., 2011; Vitousek, 1997). Seno & Shaw (2002) and Kiboro and Kiboro (2015) established that the rapidly increasing human population and the consequential land-use changes, including settlement, directly impact wildlife conservation areas' well-being.

Rampant land sub-divisions around protected conservation areas result in the shrinking of wildlife migration corridors (Kiboro and Kiboro 2015).

A review of literature indicates that while some animal species are likely to benefit from a warming climate, some species are likely to be negatively affected by a warming climate (Descamps et al., 2017). This calls for robust monitoring of trophic relationships between and within ecosystems to detect demographic, population, and ecosystem changes to inform appropriate conservation priorities against a changing climate's backdrop. Ogutu et al. (2016) and Said et al. (2016) showed that migration corridors for Nairobi National Park (NNP) have shrunk over time. The shrinking of the migration corridors is attributed to landscape fragmentation caused by settlements, transport infrastructure, and agricultural activities among others (Said et al., 2016).

Climate model projections suggest an increasing rainfall for East Africa for the period ending 2100 (e.g. Endris et al., 2013; Ogega, 2017). However, minimal literature is available on the link between climate change and urban growth and the prosperity of NNP. This study analyses the interplay of a changing climate, urban growth dynamics and the park's future survival prospects.

2.5 Research Gaps

In summary, many studies done over East Africa tend to concentrate on annual cycles, inter-annual variability, and their drivers. There is minimal knowledge of the historical characteristics of intraseasonal rainfall variability in the region and its potential drivers. Further, there is a need to explore the potential of regional and global climate models in generating projections for East Africa's future intraseasonal rainfall projections to inform better planning for East Africa's rainfall-dependent sectors' economy. The current study sought to enhance the understanding of intraseasonal rainfall variability over East Africa and make recommendations to stakeholders for improved climate change adaptation.

CHAPTER 3: METHODOLOGY

This section gives details on the data, materials, and methods used in the study. Specifically, the section is subdivided into study area (3), study design, (3.2) sampling procedure (3.3), data collection procedure (3.4), and data analysis (3.5).

3.1 Study Area

The study focused on the equatorial part of East Africa (hereafter CORDEX EA) that receives a bi-modal rainfall in a year (area marked EA in Figure 3.1). The bi-modal rainfall seasons are March-May (MAM) and October-December (OND, locally referred to as the "long rainy season" and the "short rainy season," respectively) (Favre et al., 2011). A slight study area extension was done to cover the five countries represented in the CORDEX-EA region, namely Kenya, Tanzania, Uganda, Rwanda, and Burundi (Figure 3.1).

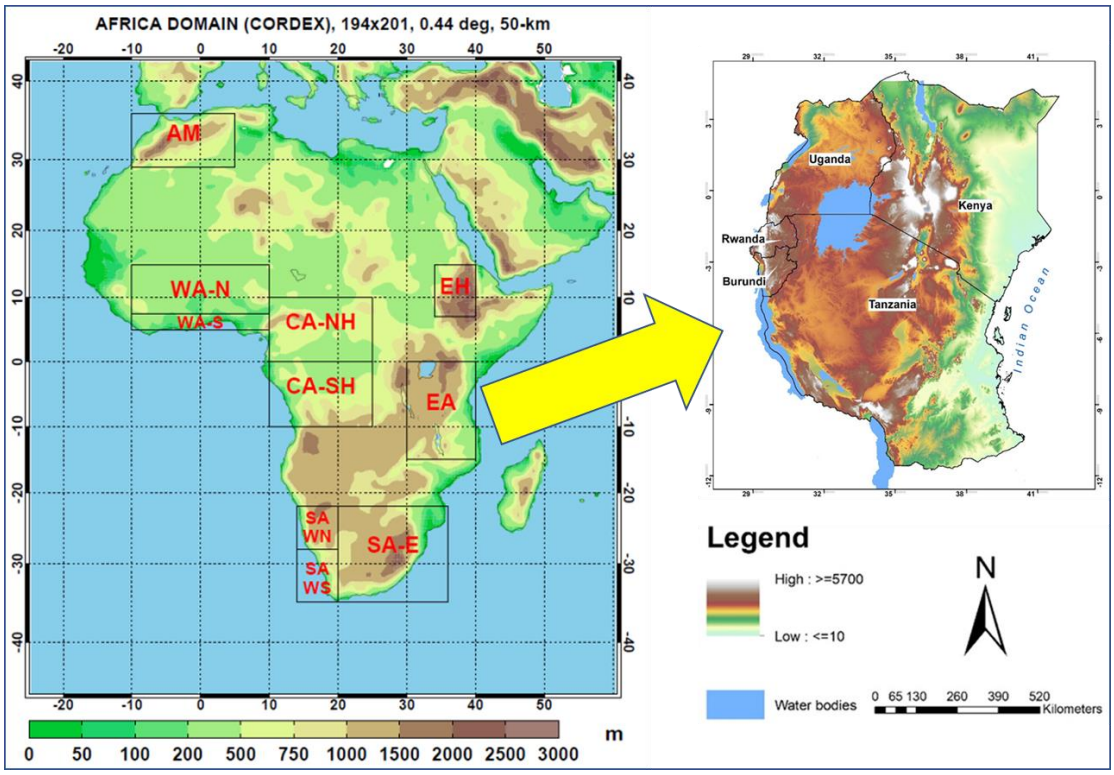

Figure 3.1. Map of the study area (adapted from Kim et al., 2014)

East Africa is one of the world's most complex climatological regions to study. Here, large-scale tropical controls, including many major convergence zones, superimpose

regional features associated with topography, lakes, and maritime influence (Nicholson, 1996). For this reason, the region's climatic characteristics are significantly intricate and often change quickly over small spatial extents.

Just like many other parts of Africa, nearly half of the population in East Africa lives below the USD 1.25/day poverty line (AfDB, 2018). The region struggles with poor infrastructure, limited market competitiveness, inadequate agricultural productivity, abject poverty conditions, and increasing inequalities and unemployment, among other socio-economic challenges (AfDB, 2018). The agriculture sector has historically driven East Africa's economy as the primary source of livelihood. For instance, agriculture contributed about 41% of the region's GDP in 2017 (AfDB, 2018). Therefore, a good understanding of East Africa's rainfall patterns, which are of great importance to the region's agricultural productivity, is paramount for its socio-economic development and sustainability.

3.1.1 Climate Services for Sustainability in Agriculture

Kilifi County (Figure 3.2) receives a mean annual rainfall ranging from 300 mm at the hinterland to about 1300 mm at the coastal strip. Evaporation in the county ranges from 1800 mm along the coastal strip to 2200 mm in the Nyika plateau in the hinterland. Temperatures range from 21^{o}C to 30^{o}C at the coastal belt and from 30^{o}C and 34^{o}C at the hinterland (Kilifi County, 2013).

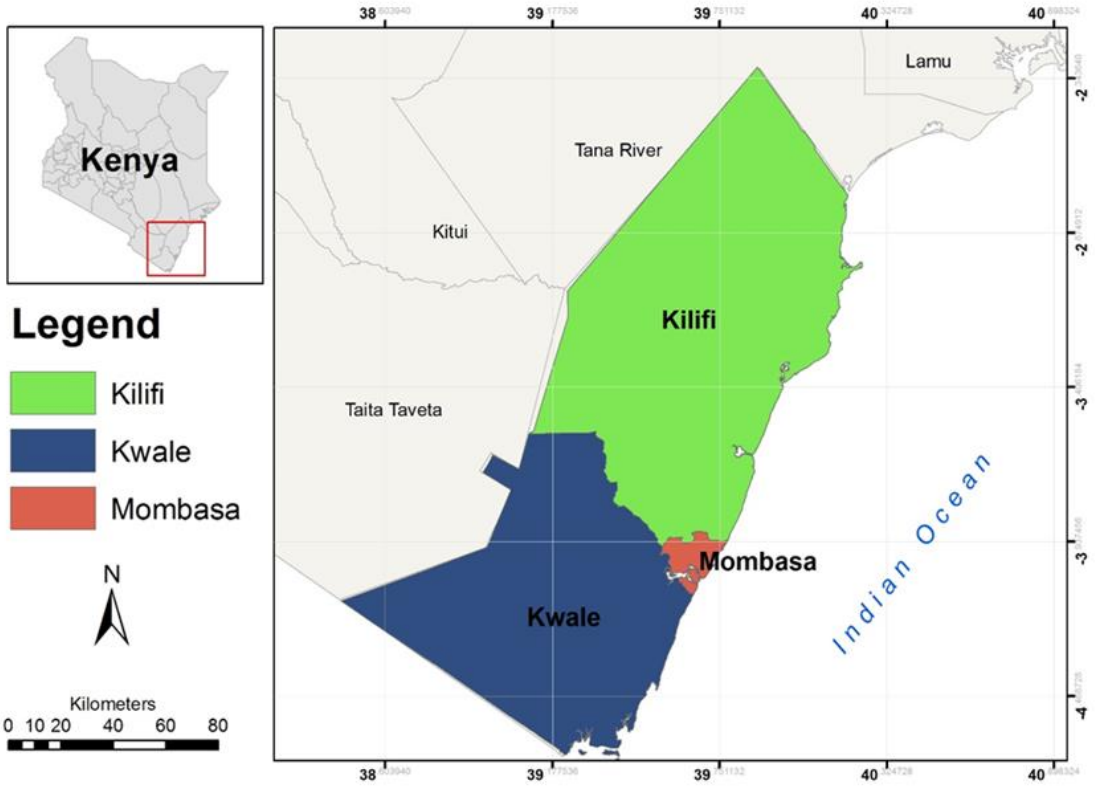

Figure 3.2: Map showing Kilifi County where the social survey was conducted (source: author)

3.1.2 Climate Services for Sustainability in Tourism

Nairobi National Park (NNP, Figure 3.3) is located between 36.5 and 37^{o} East and 1.5 and 1.1^{o} South, at a general elevation of 1,795 meters above sea level. NNP has a subtropical highland climate with December - March being the warmest season (with a mean maximum temperature of 24 ^{o}C) and June/July being the coldest season with temperatures dropping to about 9 ^{o}C. It receives a bi-modal rainfall with a mean rainfall of 899 mm for MAM season, 638 mm for OND, and annual mean precipitation of 786.5 mm (Nairobi City County, 2018).

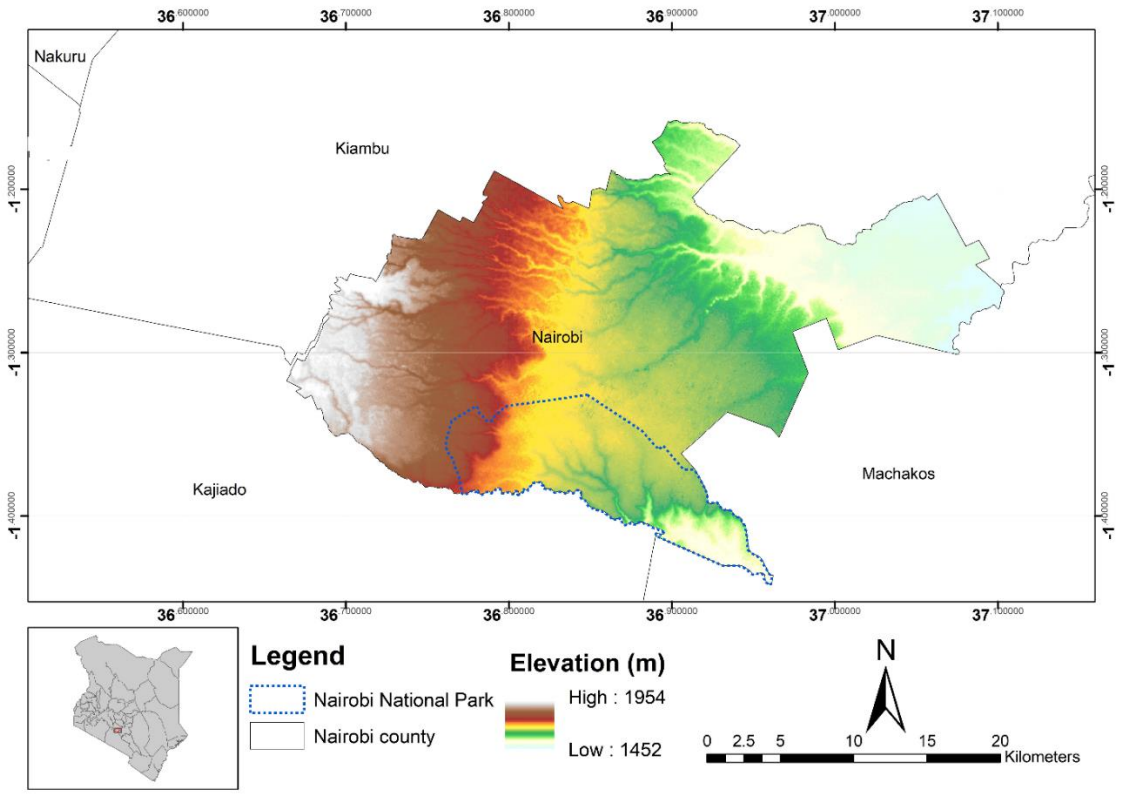

Figure 3.3: Map of Nairobi County showing the location of Nairobi National Park (source: author)

In 1947, the Nairobi National Park was gazetted as a protected area (Owino et al., 2011), covering 117 square kilometres in present-day Nairobi and Machakos Counties. The Park provides habitat to animals such as the black rhino, lions, wildebeest, zebra, eland, and giraffes (Nkedianye, 2004). While NNP was established at the city's edges, urbanization has gradually increased human settlement pressure on the park (Owino et al. 2011). For instance, there was a significant growth of the population from 1963 to 1979 due to the lifting of restrictions on migration previously enforced by the colonial government (Olima, 2011). By 1973, the city boundaries were extended to cover 695 square kilometres under the Nairobi Metropolitan Growth Strategy (Mwaniki et al., 2015). However, the park's edges do not protect the entire wildlife ecosystem (Owino et al. 2011). Herbivores migrate out of the park during the dry season across the Mbagathi River (which forms the southern border of the park) into the Athi-Kapiti plains and come back into the park during the rainy season (Deshmukh, 1985). This southern border is the

only unfenced section of the park (Nkedianye 2004), forming a continuous ecological unit (Owino et al. 2011).

Kajiado County, located at the southern border of the NNP, provides migratory corridors connecting to the Athi-Kapiti plains and the Kitengela wildlife dispersal areas. However, increased land sub-divisions in originally communally owned land continues to diminish the park's wildlife dispersal areas (e.g. Ngotho and Kangu 2016). In the 1989 census, for instance, Kajiado district was flagged as one of the regions of Kenya recording an increase of more than 20% in immigration (CBS, 1996), with 9.7% of the total population documented as immigrants between the year 1998 and 1999 alone (CBS, 2002).

Due to its relatively small spatial extent (about 117 km^2), NNP is not self-sustaining, requiring migration corridors to cater to its wildlife (Rodriguez et al., 2012). However, the migration corridors in Ngong, Kitengela, and Athi Kapiti plains have experienced massive human activity including settlements, pastoralism, and agriculture. These activities make it difficult for wildlife to migrate to and from NNP. For instance, wildlife migrating to the Lenchani and Enkirgirri ecosystems to the South of NNP must pass through privately-owned farms and settlement areas. The limitation of wildlife dispersal areas exacerbates human-wildlife conflicts, often destroying property and even the loss of life for humans and wildlife (Kutatoi and Waweru, 2018).

3.2 Research Design

The current study adopted a causal research design to demonstrate the relationship between independent and dependent variables (Oppewal, 2010). By definition, causal research can adequately explore and demonstrate these relationships hence making it the best approach in the current study.

The causal research design fits the present study given that changes in weather and climate parameters have an impact on various sectors of the economy. Specifically, the current study computed changes in East Africa’s future rainfall patterns and used the information (in form of climate services) to show how the changes would affect the

agriculture, health, and tourism sectors. Statistical research methods were used to analyse the cause-and-effect connection between various variables in the study.

3.3 Sample Size and Sampling Procedure

3.3.1 Choice of East Africa for climate studies

Climate research is guided by the World Climate Research Programme (WCRP[5]) to facilitate the analysis and prediction of variability in the Earth system. The collaborative research provides information for a range of practical applications of direct relevance, benefit, and value. The Coordinated Regional Climate Downscaling Experiment (CORDEX[6]) is one of the initiatives of the WCRP aimed at advancing and coordinating the science and application of regional climate downscaling through global partnerships. The African part of CORDEX has been grouped into 21 sub-regions based on the similarity of their average climatic conditions (e.g. Kim et al., 2014; Nikulin et al., 2012). The current study focused on the CORDEX EA sub-region in response to regional and global climate research priorities. Specifically, the study is in line with Kenya's Vision 2030[7] by contributing to knowledge useful for ending drought emergencies flagship projects[8]. Regionally, the work aligns with Africa's Agenda 2063[9], especially on "A prosperous Africa based on inclusive growth and sustainable development" (First Aspiration). The study contributes information relevant for the realization of Agenda 2063's 7th Goal (under Aspiration 1) on "Environmentally sustainable and climate-

[5] https://www.wcrp-climate.org/
[6] http://www.cordex.org/
[7] http://vision2030.go.ke/
[8] https://vision2030.go.ke/enablers-and-macros/
[9] https://au.int/en/agenda2063/goals

resilient communities." The work also contributes to Africa's climate research priority areas[10] and the Sustainable Development Goals (SDGs[11]), specifically SDG 13.

3.3.2 Smallholder farmers in Kilifi County

To facilitate the understanding of climate change and variability on farming in East Africa, smallholder farmers in Kilifi County were selected owing to their unique situation of being peri-urban smallholder farmers. Kilifi County falls within the arid and semi-arid land area that are particularly vulnerable to climate variability and change. Additionally, the current study benefited from the availability of social survey data obtained from Ogega (2017).

3.3.3 Nairobi National Park

To showcase the impacts of climate change and variability on tourism, the Nairobi National Park (NNP) was selected due to its unique nature as the world's only national park within a city. NNP is also faced with pressure from urbanization which has often resulted in park encroachment and human-wildlife conflict (Karimi, 2016).

3.3.4 Choice of Malaria transmission

On health, malaria was chosen due to its significant contribution to East Africa's disease burden (Frings et al., 2018; Homan et al., 2016). Additionally, Malaria transmission and occurrence is significantly influenced by weather and climate parameters especially precipitation and temperature. Hence, an analysis of how the projected rainfall changes in East Africa would affect Malaria transmission in the region would be useful for the match towards Malaria elimination in East Africa.

3.4 Data Collection

[10] https://www.uneca.org/cr4d/pages/about-cr4d
[11] https://www.undp.org/content/undp/en/home/sustainable-development-goals.html

3.4.1 Climate Model Data

Total daily precipitation and temperature data from the CORDEX-Africa Regional Climate Models (RCMs) at 0.44-degree (~ 50 km at the equator) gridded resolution were used. Specifically, two datasets were used: (i) RCMs forced by the European Centre for Medium-Range Weather Forecasts (ECMWF) Interim Re-Analysis (hereinafter ERAINT; Dee et al., 2011; Table 1) and (ii) RCMs forced by GCMs (Table 2) as detailed in Nikulin et al. (2012). When driven by re-analysis fields, the RCM simulations are forced to the temporal evolution of large-scale weather hence making them closest to observations data. Usually, there are no historical simulations that have assimilations of observational data implying, therefore, that RCM simulations forced by GCMs are independent of day-to-day weather observations (e.g. Eden et al., 2012, 2014). Thus, the current study used data for RCMs forced by ERAINT (Table 1), and RCMs forced by GCMs (Table 2) to facilitate comparison. The data were downloaded from *https://bit.ly/3dsLafw*.

Table 1: A list of ERAINT-forced RCMs used in the current study

Institute	RCM ID	Herein-after	References
Abdus Salam International Centre for Theoretical Physics, Italy	ICTP-RegCM4-3	ICTP	Gao & Giorgi, 2017; Pal et al., 2007
Royal Netherlands Meteorological Institute, De Bilt, The Netherlands	KNMI-RACMO22T_v1	KNMI	KNMI (2017)
Sveriges Meteorologiska och Hydrologiska Institut (SMHI), Sweden	SMHI-RCA4_v1	RCA	SMHI (2017)
Université du Québec à Montréal (UQAM), Canada	UQAM-CRCM5.v1	UQAM	Winger (2017)
Climate Limited-area Modelling Community (CLM-Community)	CCLM4-8-17. v1	CLMcom	Panitz et al. (2015)
Helmholtz-Zentrum Geesthacht, Climate Service Center, Max Planck Institute for Meteorology	REMO2009.v1	MPI	GERICS (2017)
Danish Meteorological Institute	HIRHAM5.v1	DMI	Christensen et al. (2017)

Met Office Hadley Centre	HadGEM3-RA.v1	MOHC-RA	MOHC (2017)
	HadRM3P.v1	MOHC	MOHC (2017a)

Table 2: GCM-forced RCMs used in the current study (detailed in Nikulin et al., 2012)

Institute	RCM	Herein-after	Ensemble	Driving Model
Climate Limited-Area Modelling (CLM) Community	CLMcom COSMOCLM (CCLM4)	CCLM4	r1i1p1	MOHC-HadGEM2-ES
				MPI-M-MPI-ESM-LR
				CNRM-CERFACS-CNRM-CM5
			r12i1p1	ICHEC-EC-EARTH
Max Planck Institute (MPI), Germany	MPI-CSC-REMO2009	MPI-REMO2009	r12i1p1	ICHEC-EC-EARTH
			r1i1p1	MPI-M-MPI-ESM-LR
Sveriges Meteorologiska och Hydrologiska Institut (SMHI), Sweden	SMHI Rossby Center Regional Atmospheric Model (RCA4)	RCA4	r1i1p1	CSIRO-QCCCE-CSIRO-Mk3-6-0
				MIROC-MIROC5
				MOHC-HadGEM2-ES
				NCC-NorESM1-M
				MPI-M-MPI-ESM-LR
				IPSL-IPSL-CM5A-MR
				NOAA-GFDL-GFDL-ESM2M
				CCCma-CanESM2
				CNRM-CERFACS-CNRM-CM5
				ICHEC-EC-EARTH
			r12i1p1	ICHEC-EC-EARTH
				MPI-M-MPI-ESM-LR
			r3i1p1	MPI-M-MPI-ESM-LR
				ICHEC-EC-EARTH
Koninklijk Nederlands Meteorologisch Instituut	KNMI Regional Atmospheric Climate Model, version	RACMO22T	r1i1p1	MOHC-HadGEM2-ES
				ICHEC-EC-EARTH

(KNMI), Netherlands	2.2 (RACMO2.2T)			
Danish Meteorological Institute (DMI)	DMI-HIRHAM5	HIRHAM5	r3i1p1	ICHEC-EC-EARTH
			r1i1p1	NCC-NorESM1-M

3.4.2 Observational Climate Data

The Climate Hazards Group InfraRed Precipitation with Station data (CHIRPS) version 2.0 is one of the two reference datasets used in the current study. CHIRPS data incorporates satellite imagery (at 0.05^{o} and 0.25^{o} resolution) with in-situ station data resulting in a gridded precipitation time series - available from 1981 to near-present (Funk et al., 2015). The other reference dataset utilized is the Tropical Applications of Meteorology using SATellite and ground-based observations, version 3 (TAMSAT3, Maidment et al., 2017). Both datasets have been validated for EA and found to be suitable for use as reference datasets (Dinku et al., 2018).

Three other data products considered are the daily global historical climatology network (GHCN – Daily, Menne et al., 2012); the global precipitation climatology project (GPCP, Huffman et al., 2009); and the Multi-Source Weighted-Ensemble Precipitation (MSWEP, Beck et al., 2019). While GHCN-Daily had significant data gaps for the study area, GPCP data ranges from 1996 to near present, thus falling outside the study period (1981 to near present). A data request to the creators of MSWEP, a global gridded precipitation dataset at 0.1^{o} resolution generated by optimally merging various satellite, re-analysis estimates, and gauge data, went unanswered. Hence, CHIRPS and TAMSAT3 were used as reference data. Mean temperature data were obtained from the Climatic Research Unit time-series (CRU) dataset. CRU data are developed on 0.5 by 0.5-degree resolution grids using a database of monthly mean temperatures from over 4,000 weather stations from around the world (Harris et al., 2020).

3.4.2 Social Survey Data

Social survey data on smallholder farmers' perceptions of climate change in Kilifi County (hereafter Kilifi) and their current adaptation measures were obtained from a previous study done by Ogega (2017). Here, primary qualitative data were generated from a social survey conducted to get information on smallholder farmers' perceptions of climate

change and their current adaptation measures. Additionally, semi-structured questionnaires, focus group discussions, and key-informant interviews were used for the survey. Kilifi County's average household size was six persons, while the population was approximately 1.11 million (Kilifi County, 2013) at the time of the study. A sample size of 1500 people (translating to about 250 households) was computed using the pre-determined margin of error (Smith, 2010) sample size estimation method given by

$$ME = z\sqrt{\frac{p(1-p)}{n}}; \qquad \text{..... Equation 1}$$

where *ME* is the desired margin of error, *z* the z-score, *p* is a prior judgment of the correct value of *p*, and *n* is the sample size.

The focus group discussions (FGDs) were comprised of a two representatives of smallholder farmers, a representative of the local government (Department of Agriculture in Kilifi), a community-based organization working with the smallholder farmers in Kilifi, a local journalist working on agricultural activities in Kilifi County, and a representative of the County Meteorological Office. The unifying factor for all the FGD members is that they were all working at the same area (Kilifi County) and towards a common goal of enhancing the adaptive capacity of smallholder farmers in Kilifi County.

3.4.3 Clinical Malaria Cases Data

Clinical malaria cases data for East Africa were obtained from the Malaria Atlas Project (MAP; Hay & Snow, 2006; Weiss et al., 2019). MAP receives, curates, and shares various malariometric data in the form of nationally representative cross-sectional surveys of parasite rate, malaria cases reported by surveillance systems, and satellite imagery capturing global environmental conditions that influence malaria transmission. The MAP data have been validated (e.g. Nakakana et al., 2020) and used widely worldwide (e.g. Battle et al., 2019; Weiss et al., 2019).

3.4.3 Population Data for Nairobi Metropolis

A desk review of literature on the Nairobi National Park, the Nairobi metropolis, and related concepts provided rich insights into its historical urban development. Population

size, density, and distribution were the core components of urban growth data reviewed and analysed. Population data were collected from the Kenya Population Census documents from 1969 to 2019 when the last national count was done. The 1960s were selected as the baseline period because this was the decade of Kenya attaining her independence. The analysis of population trends focused on three counties within the Nairobi metropolis: Nairobi, Kajiado, and Machakos counties. Besides, the study focused on sub-counties within the immediate vicinity of the unfenced section of the park.

3.4.4 Land Use Change Data

Analysis of land cover and land-use change was done using remotely sensed data obtained from the Landsat 8 (Roy et al., 2014) satellite provided by the US National Aeronautics and Space Agency (NASA). Landsat 8 acquires global moderate-resolution measurements of the Earth's terrestrial and polar regions in the near-infrared, thermal infrared, visible, and short-wave ranges. The satellite images (for 1988 and 2019, corresponding to the national population census) were accessed from the Earth Explorer archive. The images are of the same season and spatial resolution of 30 meters in pixel size

3.5 Data Analysis

Processing (conversion to a standard calendar, units, grid, and resolution) and statistical computations (e.g. means, anomalies, standard deviation, summations, and data de-trending) of climate (temperature and precipitation) data were done in version 1.9.8 of the Climate Data Operators (CDO). CDO is a command-line suite for manipulating and analysing climate data. Additional computations were done in the R Project for Statistical Computing (hereinafter R; version 3.6.3). Spatial data visualization was done in Grid Analysis and Display System (GrADS, version 2.2.1.oga.1), while line plots were made in R using the *ggplot2* (version 3.3.0) package. Due to data grid and resolution differences, computations were done in native grids and resolutions (as in Diaconescu et al., 2015) before bilinearly interpolating the processed files (as in Zhou et al., 2017) to facilitate comparison between model simulations and reference data.

3.5.1 Performance of CORDEX RCMs in Simulating East Africa's Precipitation Characteristics

The performance of RCMs was measured against a set of eight descriptors (Table 3), representative of both moderate and extreme precipitation events (precipitation-based indices and annual precipitation statistics). The consecutive dry days (CDD), consecutive wet days (CWD), and simple precipitation intensity index (SDII) are climate indices (Peterson et al., 2001) considered to be highly sensitive to global warming and climate change and are widely used in extreme precipitation identification and monitoring (e.g. Jiang et al., 2015; Osima et al., 2018; Sillmann et al., 2013; Zhou et al., 2014). Two criteria were used in the analysis: the performance of models in simulating spatial rainfall characteristics over East Africa. The other criterion was the performance of RCMs in simulating temporal characteristics of rainfall over East Africa.

Table 3: Climate indices and precipitation statistics used as descriptors of a rainy season in the study

Descriptor	Acronym	Description	Unit
Simple precipitation intensity index	SDII	Mean precipitation amount on a wet day. Let RR_{ij} be the daily precipitation amount on wet day w ($RR \geq 1$ mm) in period *j*. If *W* represents the number of wet days in *j* then the simple precipitation intensity index $SDII_j = sum\ (RR_{wj}) / W$	mm/ day
Consecutive dry days	CDD	Maximum length of dry spell ($RR < 1$ mm) Let RR_{ij} be the daily precipitation amount on day *i* in period *j*. Count the largest number of consecutive days where $RR_{ij} < 1$ mm.	days
Consecutive wet days	CWD	Maximum length of wet spell, maximum number of consecutive days with $RR \geq 1$mm: Let RR_{ij} be the daily precipitation amount on day *i* in period *j*. Count the largest number of consecutive days where: $RR_{ij} \geq 1$mm	days
Mean daily precipitation for MAM season	MAM	For every adjacent sequence *t_1, ..., t_n* of timesteps of the same year it is: $o(t, x) = mean\{i(t', x), t_1 < t' \leq t_n\};$ computed for March-May of every year in the series	mm/ day

Mean daily precipitation for OND season	OND	For every adjacent sequence *t_1*, ..., *t_n* of timesteps of the same year it is: $o(t, x) = mean\{i(t', x), t_1 < t' \leq t_n\}$; computed for October-December of every year in the series	mm/ day
Mean daily precipitation in a year	ANN	For every adjacent sequence *t_1*, ..., *t_n* of timesteps of the same year it is: $o(t, x) = mean\{i(t', x), t_1 < t' \leq t_n\}$; computed for every year in the series	mm/ day
Representative of heavy precipitation events	90p	For every adjacent sequence *t_1*, ..., *t_n* of timesteps of the same year it is: $o(t, x) = p^{th}$ percentile $\{i(t', x), t_1 < t' \leq t_n\}$; here computed for the 90^{th} percentile. For this study, 90p represents the threshold for identifying heavy precipitation events	days
Representative of very intense precipitation events	99p	For every adjacent sequence *t_1*, ..., *t_n* of timesteps of the same year it is: $o(t, x) = p^{th}$ percentile$\{i(t', x), t_1 < t' \leq t_n\}$; here computed for the 99^{th} percentile. For this study, 99p represents very intense precipitation events.	days

First, the performance of RCMs in simulating the region's rainfall characteristics was done using RCMs forced by re-analysis data (ERAINT) for the period 1990-2008, corresponding to data availability for all RCMs (Table 1). Secondly, performance assessment was done on RCMs forced by GCMs. Here, 24 model runs (Table 2), their ensemble mean, and ensemble means for model runs by each RCM were analysed. The assessment was done for the period 1983 to 2005 corresponding to data availability for reference data (CHIRPS and TAMSAT3, which are available from 1981 and 1983 to near present, respectively) and the historical simulations of the CORDEX-Africa RCMs (available from around 1950 to 2005).

3.5.1.1 Spatial Correlation Analysis

Taylor diagrams (Taylor, 2001) were plotted to show the overall skill of RCMs (forced by ERAINT) in simulating spatial patterns of precipitation relative to observations. A Taylor diagram is used to characterize the statistical relationship between two items: the reference item and the test item. The distance between the origin and the test item is the standard deviation, while the distance between the test and the reference items is the root-mean-square (RMS). The cosine of the polar angle equals the correlation. As calculated

by the root-mean-square (RMS), a model with no error would be considered a "perfect" model.

In the current study, Taylor diagrams were plotted using de-trended data to minimize the influence of data stationarity and the non-zero mean (e.g. Reid, 2017; Wu et al., 2007). Given that RCMs forced by GCMs are not time-synchronous (Eden et al., 2014), Taylor diagrams were plotted only for RCMs forced by ERAINT.

3.5.1.2 Inter-annual Variability Skill Score

Inter-annual variability skill scores (IVS; Chen *et al.,* 2011) were computed to show the performance of RCMs in simulating inter-annual precipitation characteristics for East Africa. The IVS is given by:

$$IVS = \left(\frac{STD_m}{STD_o} - \frac{STD_o}{STD_m}\right)^2 \quad \text{..... Equation 1}$$

where STD_o and STD_m represent the standard deviation for observations and models, respectively. An IVS value of 0 implies that STD_o is equal to STD_m and the closer an IVS value is to 0 the better the skill in simulating the inter-annual variability (Chen et al., 2011).

3.5.1.3 Comprehensive Rating Metrics (MR)

An overall rating of the RCMs' performance in simulating both spatial and temporal rainfall characteristics was done. Here, a comprehensive rating index (MR, Jiang et al., 2015) was used as follows:

$$MR = 1 - \frac{1}{nm}\Sigma_{i=1}^{n} rank_i \quad \text{..... Equation 2}$$

where *n* is the number of indices under consideration and *m* the number of RCMs.

In the MR ranking, models are ranked from position 1 to position *m* - where *m* is the number of models being ranked. The model with an *MR* value closest to 1 gives the best simulation compared to other models under consideration (Jiang et al., 2015). In the current study, MR values were computed for both IVS and spatial correlation coefficients

(PCC) and presented in scatter plots. The best performing models (for both criteria) are located on the 1st quadrant (Q1) while the least performing ones are on the 3rd quadrant.

3.5.2 Future Rainfall Change Projections for East Africa

Using the top-performing models identified in subsection 1.4 and their ensemble mean, an analysis of future changes in the eight rainfall descriptors was done using climate projections following the RCP 8.5 (Moss et al., 2010) forcing. The RCP 8.5 (also referred to as 'worst-case scenario') assumes net radiation (at the top of the atmosphere) of 8 W/m^2 by the end of the current century (the year 2100). The period 1977 to 2005 was used as a reference period (hereafter, Baseline), representing the last part of the 'historical' CORDEX simulation. The analysis of future changes in East African rainfall was done for the period 2071 to 2099 (hereafter, Future).

Specifically, significant (at 95% confidence interval) differences in the Future and the Baseline climatology were computed and plotted for each of the eight descriptors. Box plots were also done for all the eight descriptors to show spatial variability in future changes. Additionally, the right tail distribution of precipitation events, represented as the difference between 99th and 90th percentiles (99p–90p), was used to assess past and future heavy precipitation events over east Africa. Here, the 99p represents the threshold for very intense precipitation, while the 90p represents the threshold for heavy precipitation events. The 90th and 99th percentiles (hereafter 90p and 99p, respectively) were computed by aggregating daily precipitation values of the period under study over each grid point (as in Scoccimarro et al., 2013).

3.5.3 Building Foundations for Climate Services for Sustainability

This section worked on examples to show how the knowledge generated from the meteorological part of the current study (objectives 1 and 2) can be used in various sectors of the economy. Specifically, applications on the agriculture, tourism, and health sectors were done as detailed in the following subsections.

3.5.3.1 Climate Services for Sustainability in Agriculture: A Case of Smallholder Farmers in Kilifi County

This part of the study used data from a social survey done in Kilifi County from October 2015 to February 2016 to establish the smallholder farmers' perceptions of climate change. The survey, done by the author of this thesis (Ogega, 2017), also sought to determine the farmers' reactive and proactive responses to the changing climate. Semi-structured questionnaires were administered to 350 households representing all the 35 Wards of Kilifi County. Additionally, key-informant persons drawn from the farming community and the county administration were interviewed in parallel with the household survey. Findings from the questionnaire and key-informant interview data were shared with stakeholders in focus group discussions (FGDs) for feedback, validation, and dissemination.

Historical rainfall data analysis for the period 1981 to 2018 was done using CHIRPS – Daily, v.2.0 data. An ensemble mean of the top models identified in subsection 3.5.1 was used to assess Kilifi's climate projections under RCP 8.5. Specifically, an analysis of CDD, CWD, SDII, MAM, and OND, as described in Table 3, was done. Year-to-year area-averaged standardized rainfall anomalies for Kilifi County were plotted (using CHIRPS data) to show historical seasonal precipitation patterns over Kilifi County. The use of standardized anomalies frees data from the influences of dispersion (Dabernig et al., 2017). Values within -1 and 1 imply a normal range while those between -2 and -1 and 1 and 2 represent below and above normal, respectively. Values below -2 and above 2 imply the extreme occurrence of the parameter under consideration (in the current study, precipitation). Future precipitation change projections for Kilifi County were computed by subtracting the climatological means between the Baseline (period 1977 to 2005) and the Future (period 2071 to 2099). Plots for the significant (at 95% confidence level) for Kilifi were made.

Through FGDs - whose membership was comprised of representatives of farmers, local administration, academia, civil society organizations, and the media - potential solutions to issues raised in the social survey were exhaustively discussed. Among the key issues emerging from the social survey was the need for a robust and well-coordinated climate

change adaptation approach as a pathway to sustainable farming activities in Kilifi County. The focus-group discussions and knowledge from the literature resulted in an innovative climate change adaptation approach for smallholder farmers in Kilifi County. The approach uses climate services as a critical input for effective climate change adaptation and sustainability.

3.5.3.2 Climate Services for Sustainability in Health

As an example of how climate services can be used in the health sector, an assessment of the potential impact of global warming scenarios (1.5 ^{o}C and 2.0 ^{o}C) on Malaria transmission in East Africa was done. Climatic factors (e.g. temperature and precipitation) play an important role in malaria vector abundance and distribution (Arab et al., 2014; Mohammadkhani et al., 2016). In the current study, a review of the literature was done to identify precipitation and temperature thresholds within which malaria vectors thrive. The review results were used to analyse historical (2000-2017) trends in precipitation, temperature, and clinical malaria cases. Specifically, standardized anomalies (as in Dabernig et al., 2016) were computed to determine normal, above/below normal, and extreme events. Linearly de-trended temperature and precipitation data were correlated with reported clinical malaria cases in the study domain to assess climatic factors' potential influence on Malaria cases.

With reference to the pre-industrial period (1861-1890), years 2022 and 2037 have been identified as mid-years for 30-year windows when 1.5 ^{o}C and 2.0 ^{o}C global warming level (GWL)s, respectively, are first expected (Nikulin et al., 2018). Therefore, with the period 1977-2005 as the control (CTL), differences between periods 2008-2037 and 2023-2052 (corresponding to 1.5 ^{o}C and 2.0 ^{o}C GWLs, respectively) were calculated for temperature and precipitation over the study domain. A comparison of temperature and precipitation values in the control (CTL), 1.5 ^{o}C, and 1.5 ^{o}C GWLs (relative to established thresholds within which malaria vectors thrive) was used to determine the potential impact of 1.5 ^{o}C and 2.0 ^{o}C GWLs on malaria transmission in East Africa.

3.5.3.3 Climate Services for Sustainability in Tourism: The Future of Nairobi National Park in a Changing Climate and Urban Growth

Gridded temperature (CRU TS) and precipitation (CHIRPS) data were used to compute historical (1981 to 2018) annual and inter-annual variability over Nairobi. Here, standardized anomalies were used to show extents of variability above or below the normal range. An analysis of future temperature and precipitation changes over Nairobi was done by computing differences (at 95% confidence level) between the Baseline (1977 to 2005) and the Future (2071 to 2099), under RCP 8.5.

A review of open-source satellite imagery from Landsat (Landsat 4 Thematic Mapper and Landsat 8, Roy et al., 2014) was done to identify spots of spatial change with an impact on the borders and surrounding NNP. Urban development elements with an effect on the park were also mapped to illustrate anticipated urbanization trends into the future. Specifically, atmospheric correction and radiometric calibration were performed separately on the satellite bands to enhance the image quality and accuracy (as in Liang et al. 2002). Image pre-processing was done using QGIS Semi-Automatic Classification plugin and exported for stacking using the ArcGIS 10.6 software. Band stacking and mapping were done to generate urban sprawl images. This was done by combining near infra-red, red, and green bands. The study used bands 4, 3, and 2 for the Landsat Enhanced Thematic Mapper (ETM) and 5, 3, and 2 bands for Landsat 8.

CHAPTER 4: RESULTS AND DISCUSSION

This section gives a presentation and discussion of the results from the analysis. Subsection 4 presents the climatology of East Africa while 4.2 presents the performance of CORDEX RCMs in simulating East Africa's rainfall variability. Subsection 4.3 presents projections of rainfall variability over East Africa while 4.4 presents examples of climate services for effective climate change adaptation in agriculture, tourism, and health in East Africa.

4.1 The Climatology of East Africa

An analysis of the annual climatology of East Africa (Figure 4.1) showed the highest mean rainfall concentration over most of Uganda, western Kenya, and parts of southern Tanzania compared to the rest of the study domain. Areas over northern Kenya recorded the least precipitation with mean daily precipitation values below 2 mm/day. The MAM season recorded the highest amount of rain followed by OND and JJA, respectively. The JJA season showed a relatively dry rainfall regime over most of the study domain except for most of Uganda and western Kenya. The three seasons correspond to the main planting seasons in East Africa (e.g. Ogutu et al., 2018; Vrieling et al., 2013), although the seasons' suitability is area-specific.

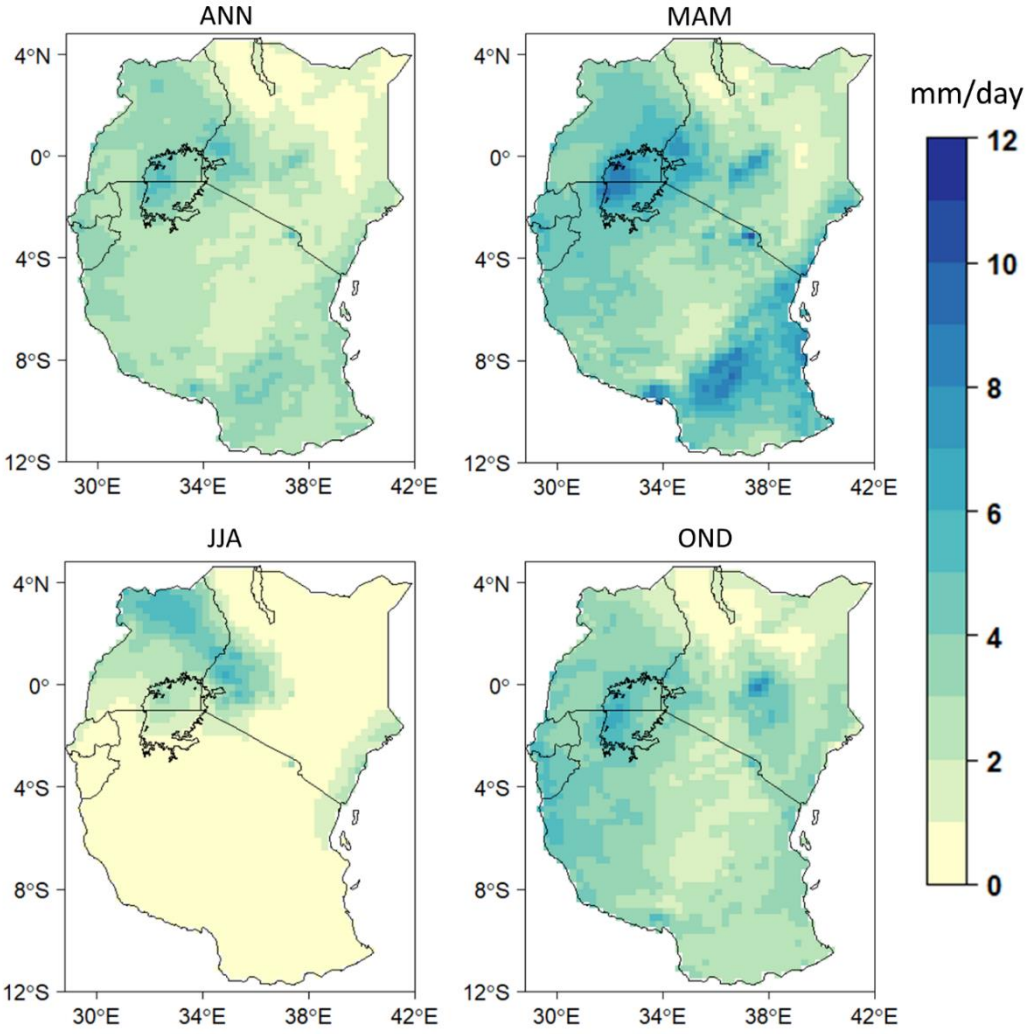

Figure 4.1. Seasonal rainfall climatology over East Africa for the period 1981-2019. All units are in mm/day

Many areas over north-eastern Kenya and central and south-western Tanzania recorded more than 150 consecutive dry days (CDD) compared to the rest of the study domain (Figure 4.2). Uganda recorded the least CDDs with areas around Lake Victoria receiving less than 50 CDDs in a year. Areas around Lake Victoria and southern Tanzania recorded the highest consecutive wet days (CWD). The least episodes of CWDs (of less than 5, especially in the northern part of the country) were recorded over Kenya compared to her neighbours in the region. In terms of intensity (SDII), the eastern part of the study domain recorded more intense rainfall than the western part. The highest intensity was recorded in central Kenya (around 1 ^{o}S 38 ^{o}E) and southern Tanzania (around 9 ^{o}S 37 ^{o}E).

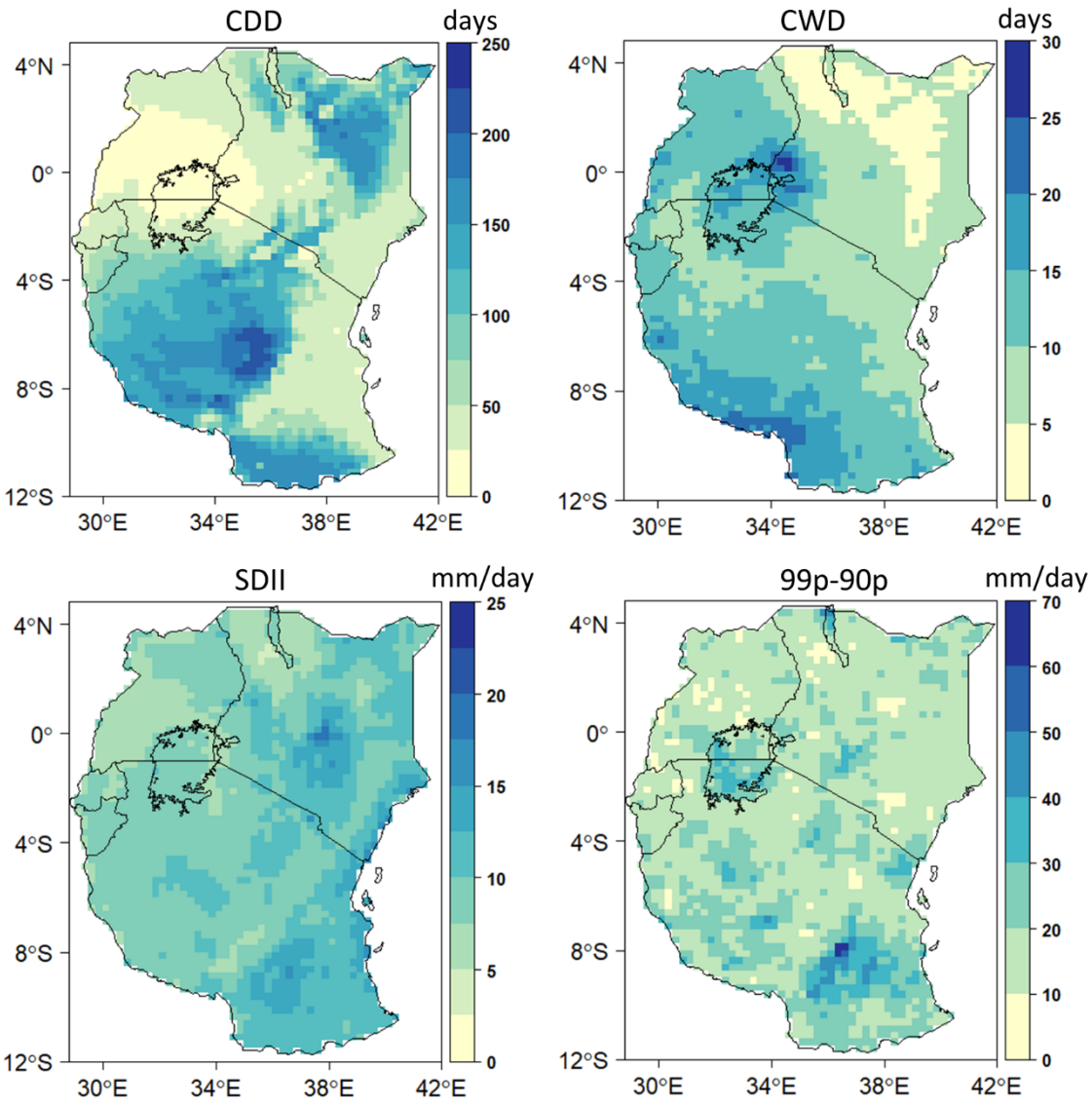

Figure 4.2: Mean annual precipitation indices over East Africa for the period 1981-2019. Units are in days (CDD and CWD), mm/day (SDII), and mm/year (99p-90p)

An analysis of the width of the right tail precipitation distribution over the study domain (Figure 4.2, 99p-90p) showed a sporadic spread of heavy precipitation events with most areas recording less than 20 mm/day. However, a few areas over Lake Victoria and southern Tanzania recorded heavy precipitation episodes exceeding 50 mm/day.

A plot of annual precipitation cycles for select parts of the region (Figure 4.3) showed two peaks (March and November) in precipitation. The two peaks correspond to mid-months of the MAM and OND main rainy seasons in East Africa. However, this analysis

showed an earlier onset for MAM and OND seasons where MAM rains seemed to begin in February and the OND rains beginning in September. January and February recorded significant precipitation hence alluding to a merger between OND and MAM seasons in several areas of the region. Increasing rainy season lengths could be pointing out to what has been termed as the 'East African climate paradox' (e.g. Wainwright et al., 2019). Here, climate projections show an increasing rainfall in the future period contrary to observed long-rains decline spanning the early 1980s to the late 2000s.

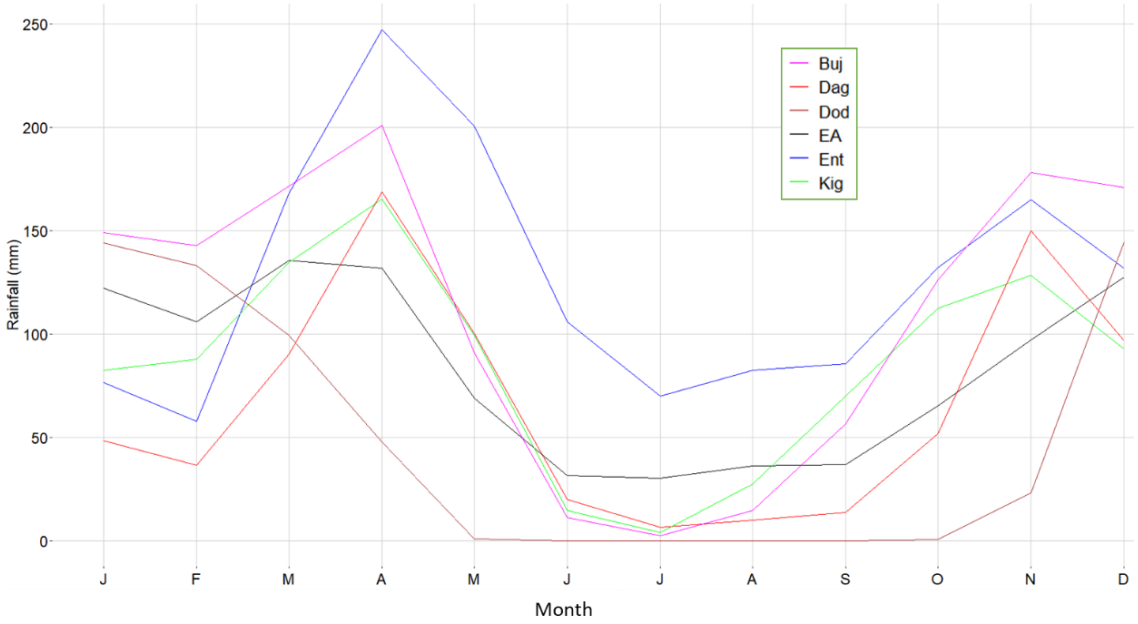

Figure 4.3: Annual precipitation variability for Bujumbura (Buj), Dagoretti (Dag), Dodoma (Dod), Entebbe (Ent), Kigali (Kig), and an average for East Africa (EA). All units are in mm/year

A plot of year-to-year precipitation totals (Figure 4.4) shows high spatial and temporal variability. Except for Entebbe, the other stations analysed show a marginal increase in rainfall totals from 2010 to 2019. Entebbe, on the other hand, receives more rainfall than the other stations considered in this analysis.

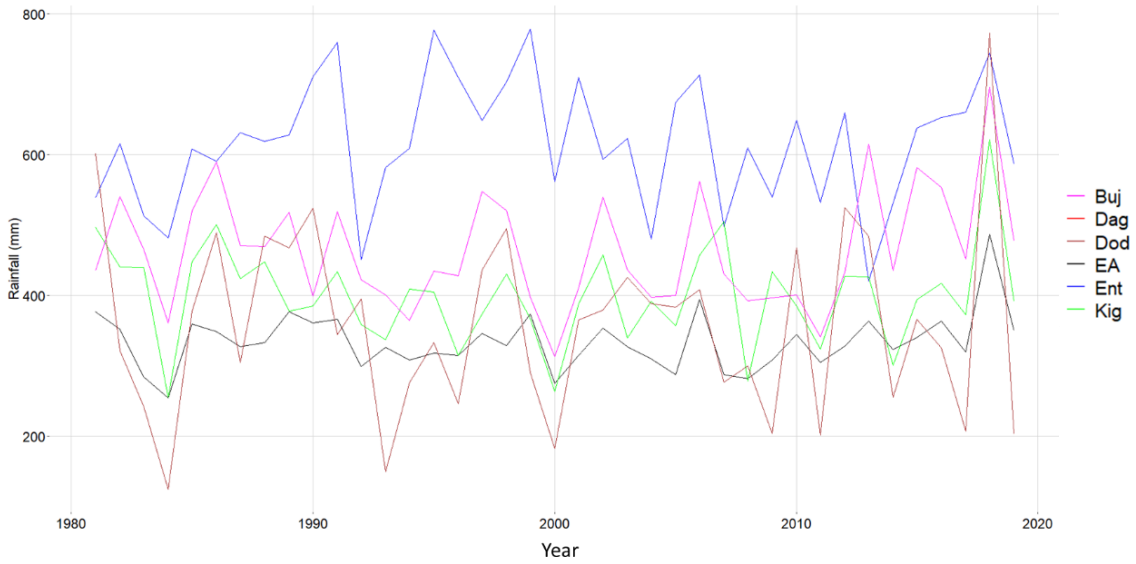

Figure 4.4: As in Figure 4.3 but for inter-annual precipitation cycles

Overall, rainfall in East Africa showed a high variability in both time and space as inferenced by similar studies (e.g. Endris et al., 2013; Nicholson, 2014; Wenhaji Ndomeni et al., 2018). With the current trends in climate change and variability in the region (Ogega et al., 2020; Osima et al., 2018), concerted efforts should be made to enhance the understanding of rainfall variability for socio-economic sustainability.

4.2 Performance of CORDEX RCMs in Simulating East Africa's Rainfall Characteristics

This subsection analyses the performance of CORDEX RCMs in reproducing annual (ANN) and seasonal (MAM and OND) rainfall characteristics over East Africa. The MAM and OND seasons were selected for being the corresponding rainfall seasons to the main planning seasons in East Africa.

4.2.1 Simulation of Spatial Rainfall Patterns over East Africa

First, spatial plots of differences between models (ensemble mean) and observations in mean annual (ANN) and seasonal (MAM and OND) rainfall values over the study domain were made (Figure 4.5). Comparatively, no discernible differences were observed between values obtained with either CHIRPS or TAMSAT3 as the reference dataset. Generally, the RCMS could represent the spatial precipitation characteristics over the

study domain with good skill. The RCMs seemed to over-estimate precipitation over Lake Victoria and some areas over central and western Tanzania. The RCMs also showed a marginal under-estimation of precipitation over northern Uganda.

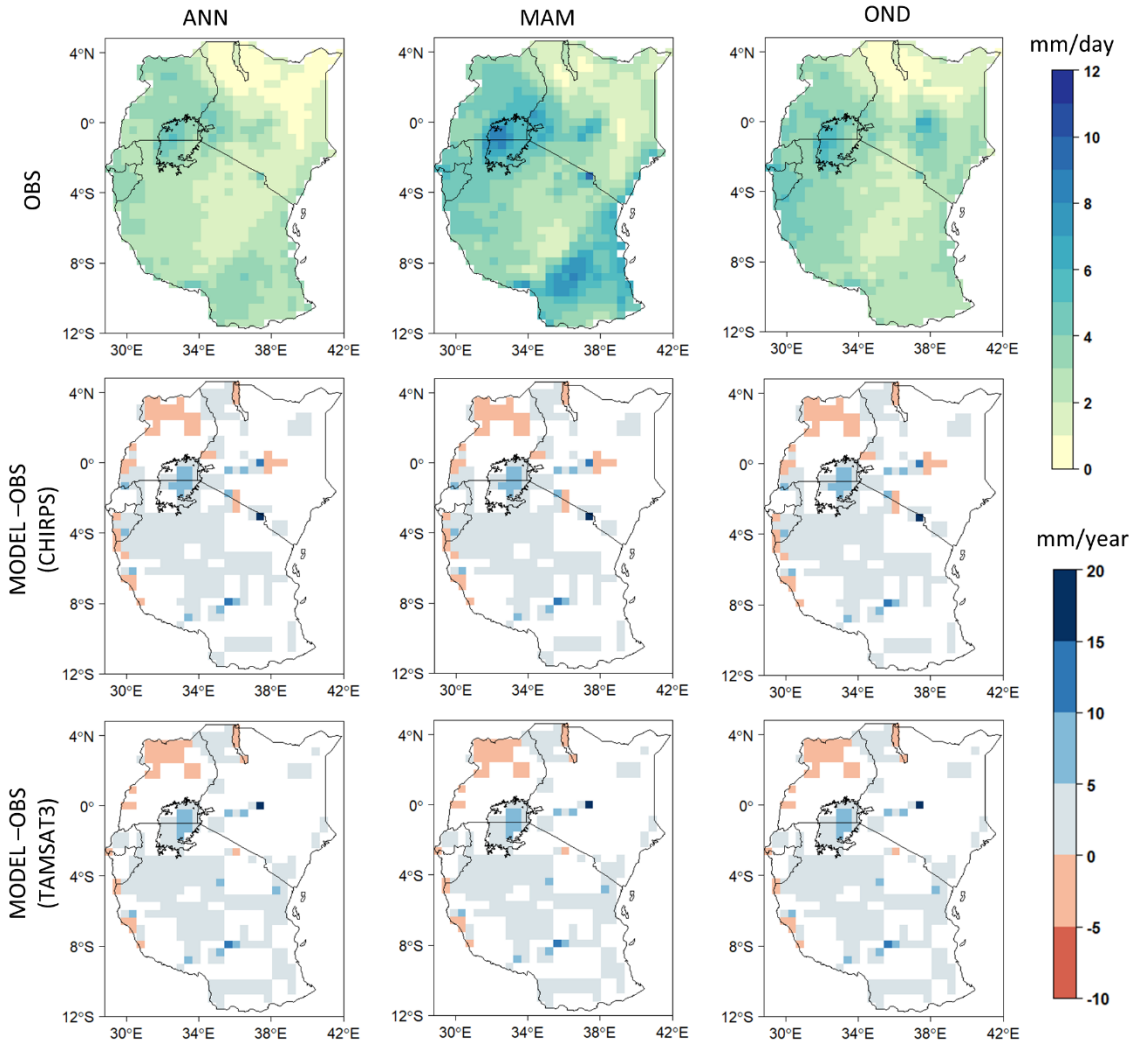

Figure 4.5. Climatology (top panel, using CHIRPS) and differences in mean MAM, OND, and ANN precipitation values between GCM-driven RCMs (ensemble mean) and observations (CHIRPS and TAMSAT3) for the period 1983-2005. The mid and bottom panels show significant values at 95% confidence level while areas with no significant differences are shown in white. Units are in mm/day (top panel) and mm/year (mid and bottom panels)

An analysis of the width of the right-tail distribution of precipitation (99p-90p) over the study domain (Figure 4.6, first column) showed a general model agreement with observations over most of the study domain except in many areas over Uganda where

models seemed to under-estimate the 99p-90p statistic. Additionally, the models seemed to over-estimate the 99p-90p statistic over a few areas over Lake Victoria and western Kenya. There were no discernible differences between values obtained using CHIRPS and TAMSAT3 as reference datasets.

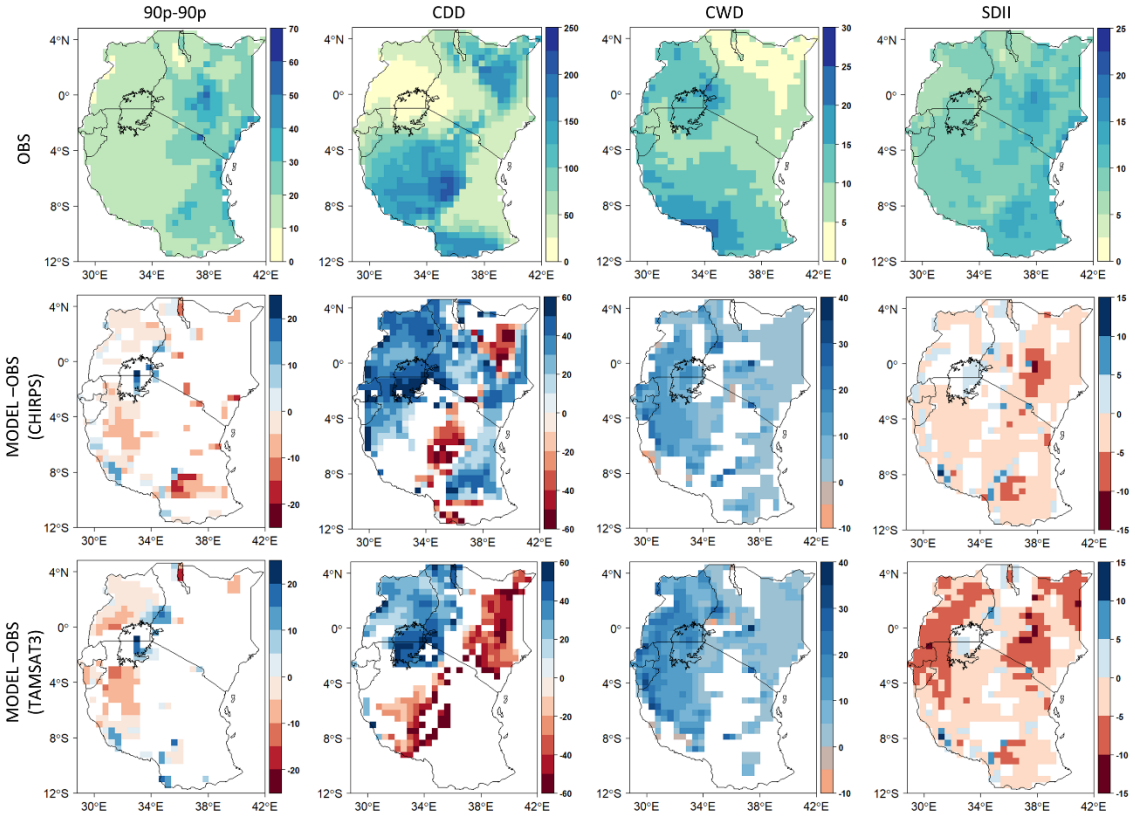

Figure 4.6. Same as Figure 4.5 but for 99p-90p, CDD, CWD, and SDII. All units are in mm/day (99p-90p and SDII), days (CDD and CWD)

The RCMs generally under-estimated the SDII index (Figure 4.6, fourth column) over most of the study domain. The biggest differences were recorded over central Kenya, and TAMSAT3 showed the more under-estimation than CHIRPS. The RCMs generally over-approximated the CWD index (Figure 4.6, second column) with values exceeding 50 days over parts of Lake Victoria. Additionally, the models under-estimated the CWD index over sections of the domain with values of up to 50 days recorded over north-eastern Kenya and central Tanzania. The CDD index (Figure 4.6, third column) was generally over-estimated by the models but with values not exceeding 20 days over most of the domain.

Using model simulations forced by ERAINT, Taylor diagrams were plotted to show the performance of the simulations in reproducing spatial precipitation patterns relative to observations. Here, the multi-model ensemble mean was the median top performer compared to individual model simulations, for all the eight precipitation descriptors analysed. For ANN, MAM, and OND (Figure 4.7), OND recorded the highest correlation (ranging from 0.75 to 0.98) between RCMs and observations. Here, CLMcom and MOHC and CLMcom and UQAM showed the highest correlation with reference to CHIRPS and TAMSAT3, respectively. With both CHIRPS and TAMSAT3 as reference datasets, the multi-model ensemble mean for all RCMs was among those with the highest correlation coefficients for both ANN and MAM. The CLMcom model featured among the models with the highest correlation coefficients for ANN, MAM, and OND with TAMSAT3 as the reference dataset. The MAM season recorded the least correlation coefficients with the highest being 0.55 with CHIRPS as the reference dataset.

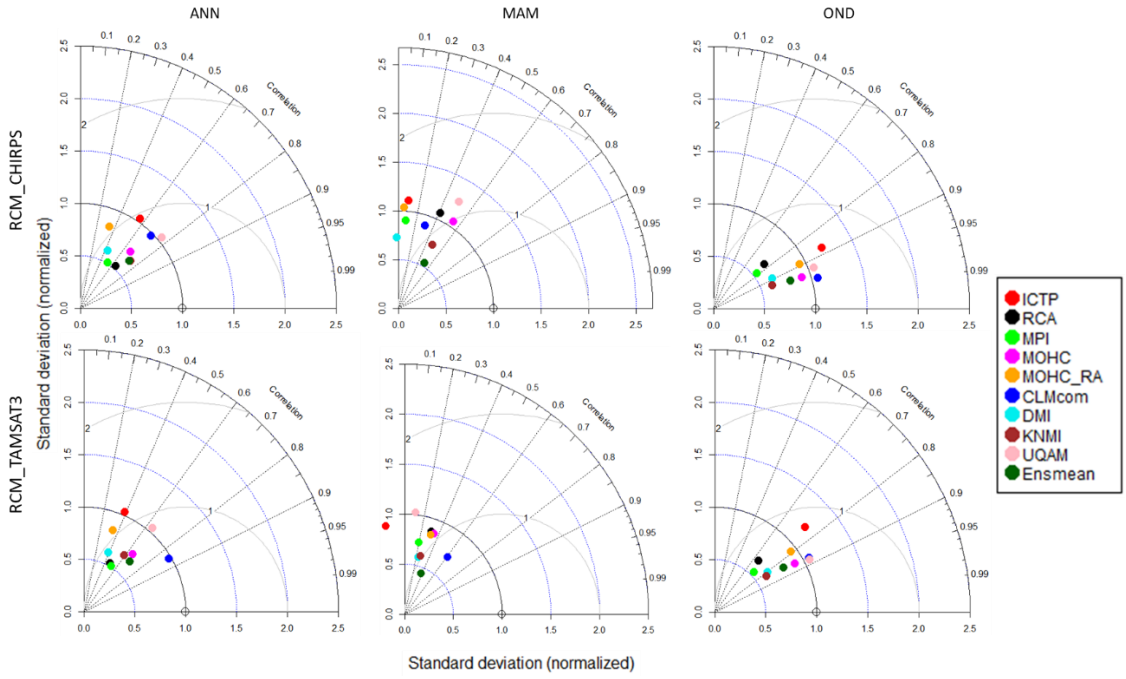

Figure 4.7: Taylor Diagrams showing spatial correlation (for the period 1990-2008) between models and observations for ANN, MAM, and OND

Relatively lower correlation coefficients were recorded for CDD, CWD, and SDII (*Figure 4.8*). The highest correlation coefficient was about 0.76 recorded for CWD and SDII. CDD recorded the lowest coefficients, somewhat, compared to CWD and SDII.

The multi-model ensemble mean (Ensmean) outperformed individual models in reproducing CDD for both TAMSAT3 and CHIRPS. The top performers for CWD and SDII were MOHC- HadRM3P and RCA and UQAM and Ensmean, respectively, with reference to CHIRPS. In comparison with TAMSAT3 data, KNMI and MOHC-HadRM3P gave the best simulation for CWD while SDII was best simulated by CLMcom and MOHC- HadRM3P.

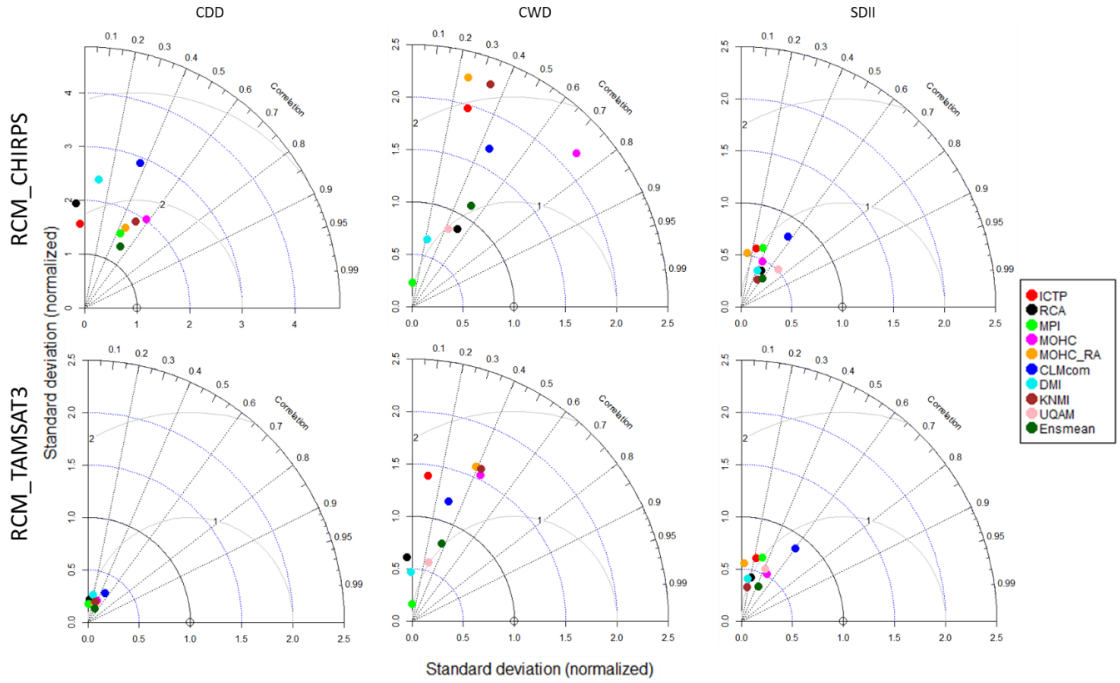

Figure 4.8: As in Figure 4.7 but for CDD, CWD, and SDII

As shown in Figure 4.9, the RCMs gave a better reproduction of 90p (with the highest coefficient being 0.82) compared to 99p (highest coefficient is 0.75). The highest correlation coefficients for both 90p and 99p, relative to CHIRPS, were given by UQAM and Ensmean. Relative to TAMSAT3, CLMcom, and MOHC- HadRM3P and Ensmean and CLMcom recorded the highest correlation coefficients for 90p and 99p, respectively.

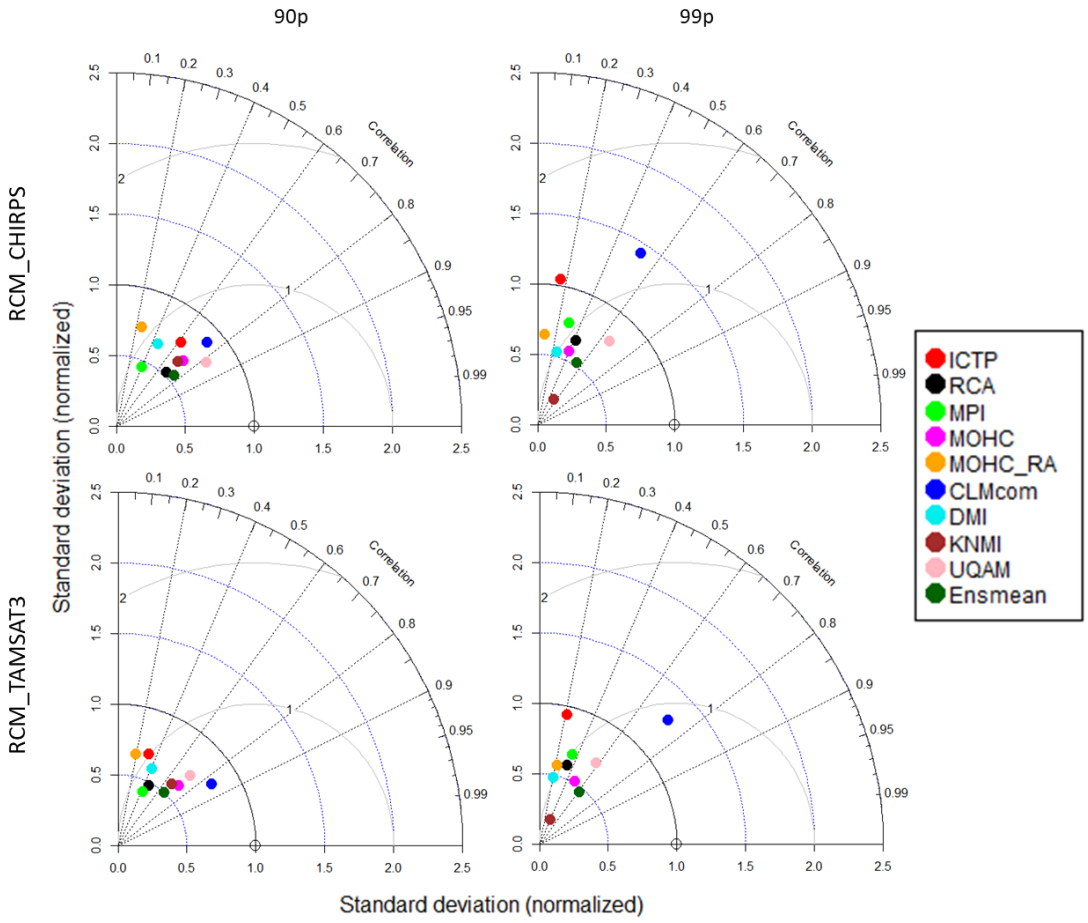

Figure 4.9: As in Figure 4.7 but for 90p and 99p

Overall, the RCMs (forced by ERAINT) showed a good representation of the eight descriptors of rainfall over East Africa. With CHIRPS as the reference data, Ensmean, UQAM, and MOHC- HadRM3P were the top performers in reproducing East Africa's spatial rainfall characteristics. With TAMSAT3 as the reference data, Ensmean, CLMcom, and MOHC- HadRM3P showed superior performance compared to other models under consideration. Given that the current analysis used an ensemble mean of 24 RCM simulations, the recorded differences between RCMs and observations could be because of inter-model differences and uncertainties. However, most parts of the study domain show no significant differences between RCMs and observations across all the seven precipitation descriptors used in the current study.

4.2.2 Simulation of Interannual Variability over East Africa

Using data from RCMs forced by ERAINT, a high interannual precipitation variability and inter-model uncertainties were recorded for the study domain. Nonetheless, the RCMs could follow the general year-to-year rainfall patterns over East Africa relative to observations. TAMSAT3 seemed to over-approximate CDD compared to CHIRPS (Figure 4.10). Most RCMs seemed to agree with CHIRPS with HIRHAM5, and the multi-model ensemble mean giving the closest values to CHIRPS values. TAMSAT3 and CHIRPS, however, agree on CWD approximations (Figure 4.10, bottom row) with MPI, SMH, and CLMcom being the closest fits.

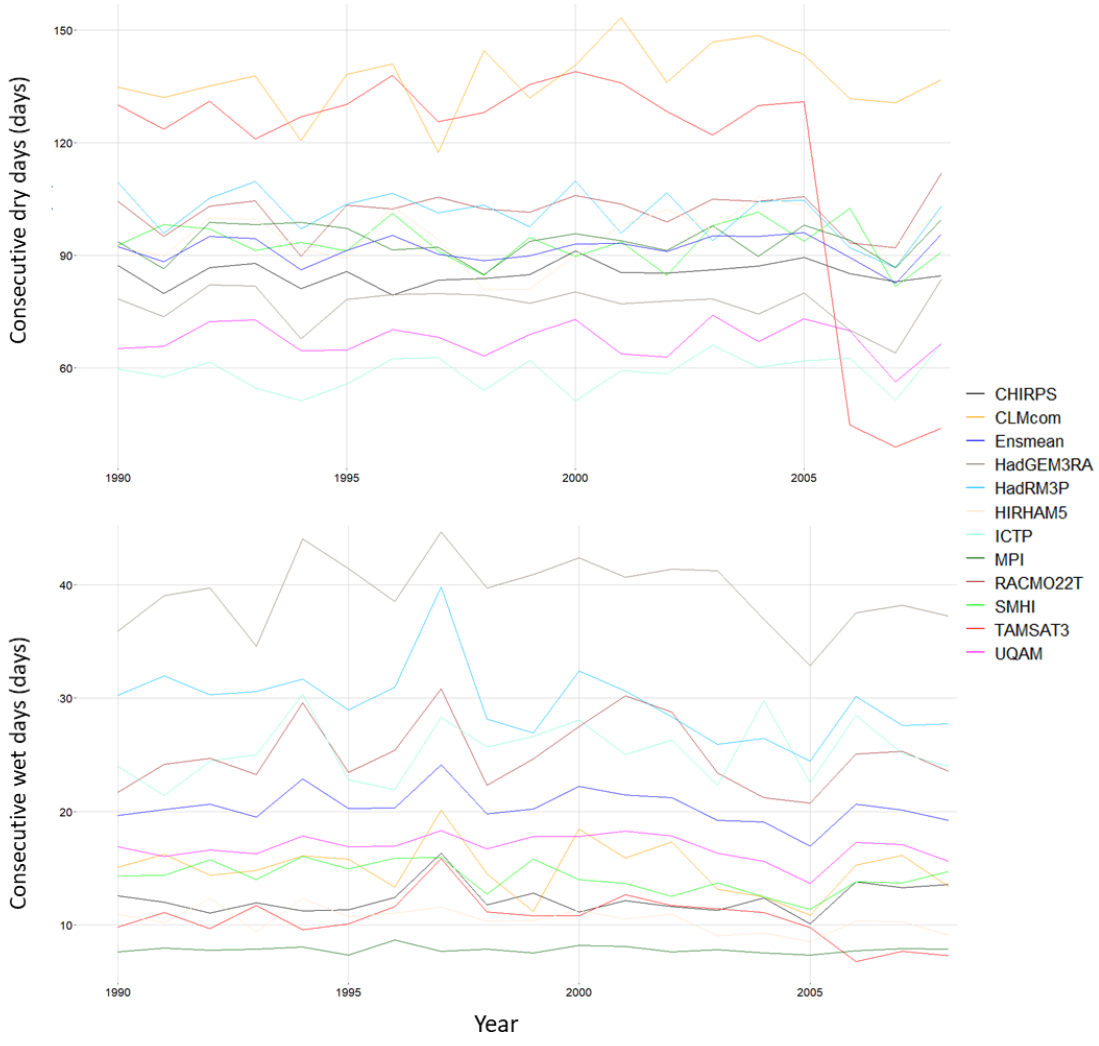

Figure 4.10: Year-to-year CDD (top) and CWD (bottom) variability, spatially averaged for East Africa

All RCMs seemed to under-approximate SDII relative to TAMSAT3 and CHIRPS (Figure 4.11 top row), with values from HIRHAM5, ICTP, and UQAM being closest to observations. Most models under-estimated the mean annual rainfall (ANN), with MOHC-HadRM3p, and the multi-ensemble mean being the closest fits relative to observations (Figure 4.11). Many RCMs could reproduce the 1997/1998 El Niño – induced extreme rainfall recorded in East Africa (Latif et al., 1999; Nicholson, 2017).

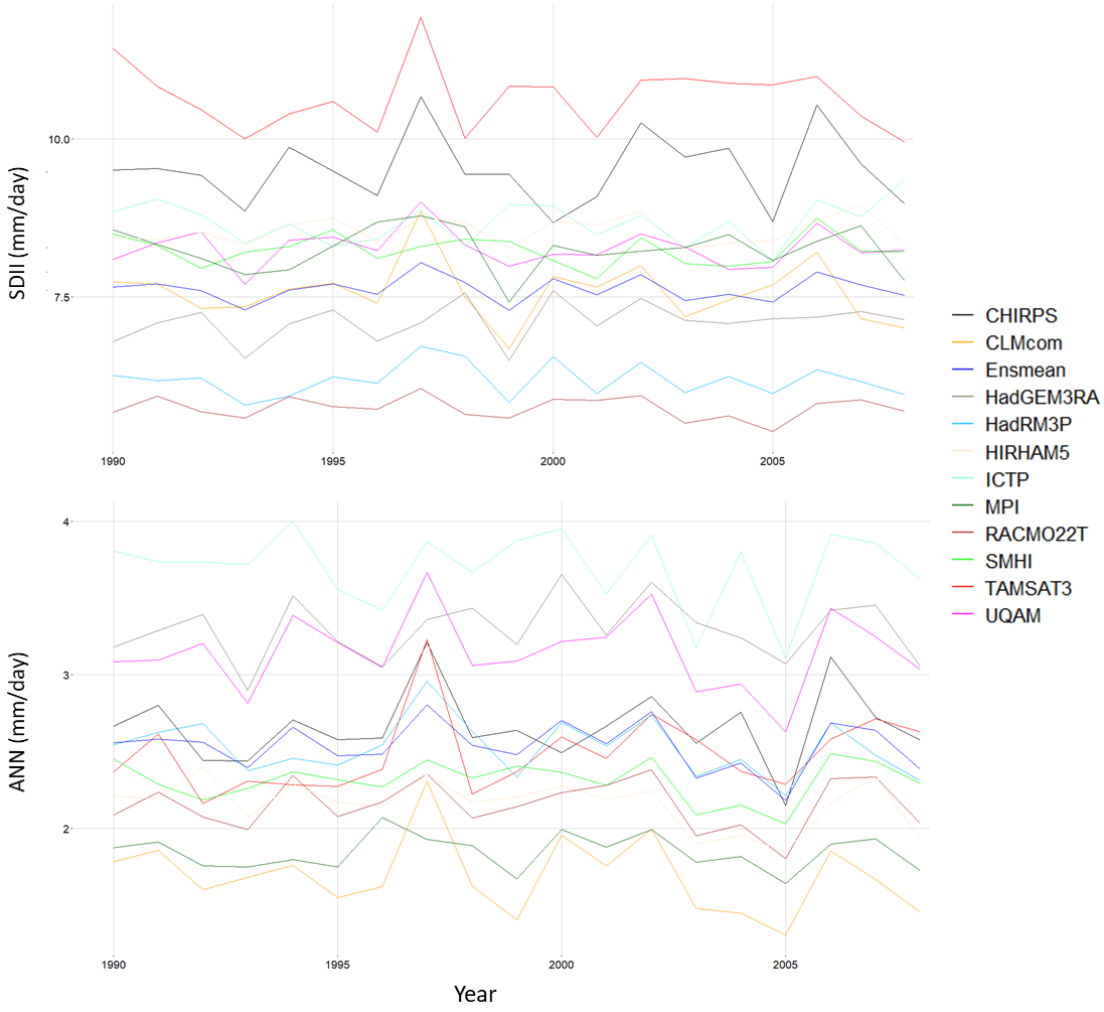

Figure 4.11: As in Figure 4.10 but for SDII and annual daily mean rainfall (ANN)

Discernible inter-model differences were recorded in the MAM season (Figure 4.12 top row), with values from SMHI, MOHC-HadRM3p, and the multi-ensemble mean being closest to observations. However, the OND season was well reproduced across models (Figure 17, bottom row).

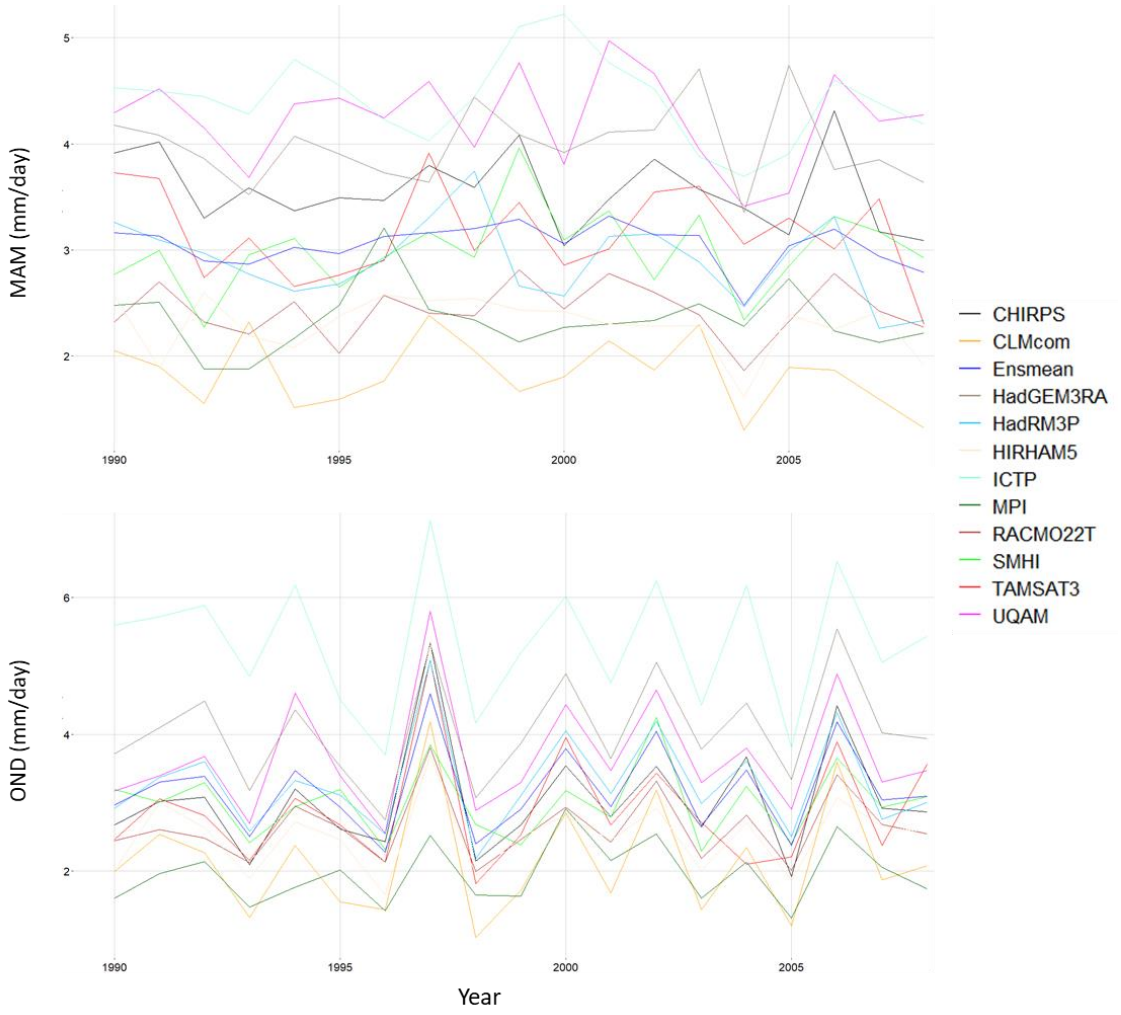

Figure 4.12: As in Figure 4.10 but for MAM and OND daily mean rainfall

The 90p and 99p statistics showed high inter-model uncertainty and inter-annual variability (Figure 4.13). The MOHC-HadGEM3-RA and UQAM gave the best reproduction of 90p while 99p was best reproduced by CLMcom and the multi-model ensemble mean.

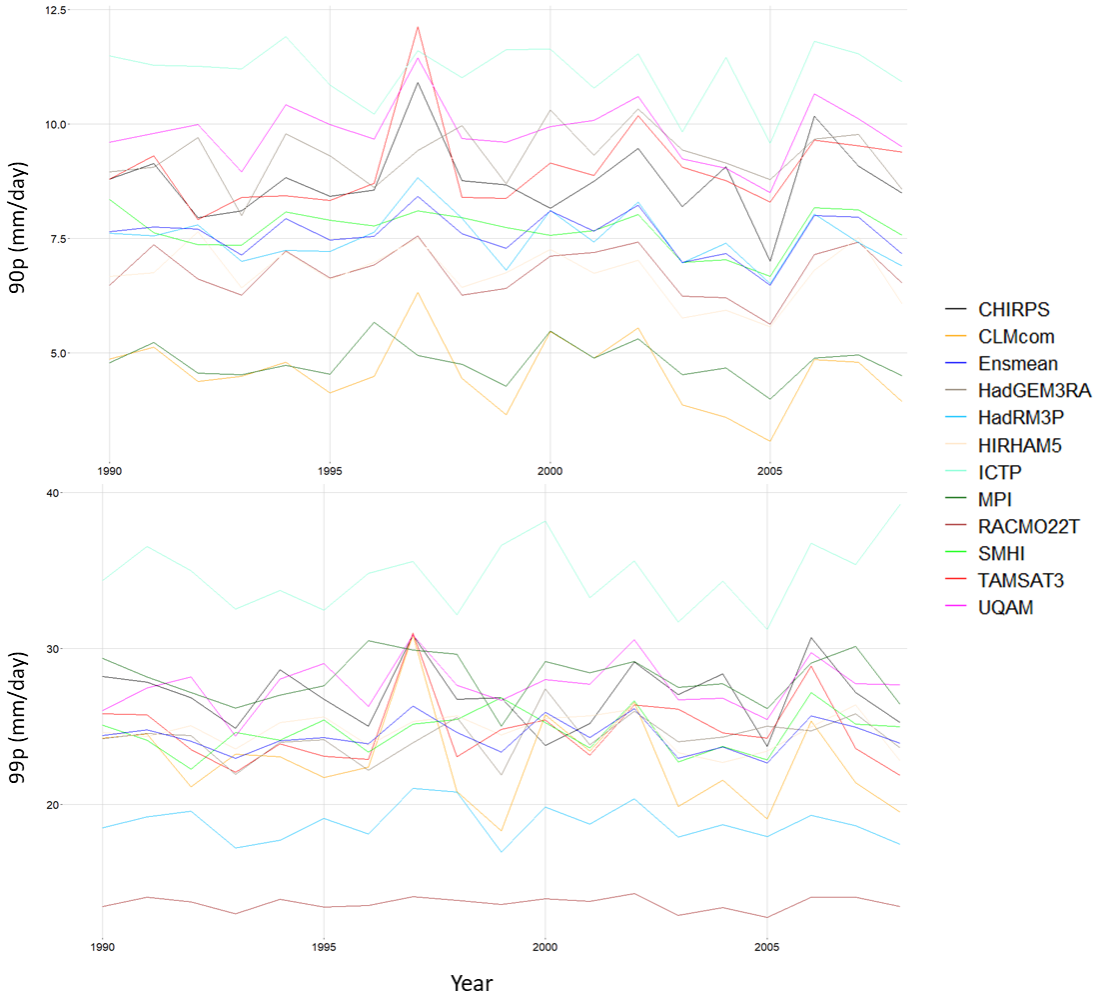

Figure 4.13: As in Figure 4.10 but for 90p and 99p

The next subsection ranks the performance of RCM simulations in reproducing both the spatial and interannual precipitation variability over East Africa.

4.2.3 Model Ranking

Scatter diagrams were plotted to facilitate the assessment of the overall performance of RCMs in simulating both spatial and temporal rainfall characteristics over East Africa, relative to observations. The model ranking was done in two parts; RCMs simulations forced by ERAINT and those forced by GCMs. The model ranking was also done separately with either CHIRPS or TAMSAT3 as the reference dataset.

4.2.3.1 Model simulation ranking using models forced by ERAINT

With CHIRPS as the reference data, ICTP, CLMcom, and MOHC-HadGEM3-RA gave the best reproduction of the interannual variability score (IVS, Figure 4.14). MPI, HIRHAM5, and RACMO22T trailed other models in reproducing the IVS. In terms of spatial correlation (PCC), the top-performing RCMs were MOHC-HadRM3p, CLMcom, and Ensmean, while the least performing models were ICTP, MPI, and MOHC-HadGEM3-RA.

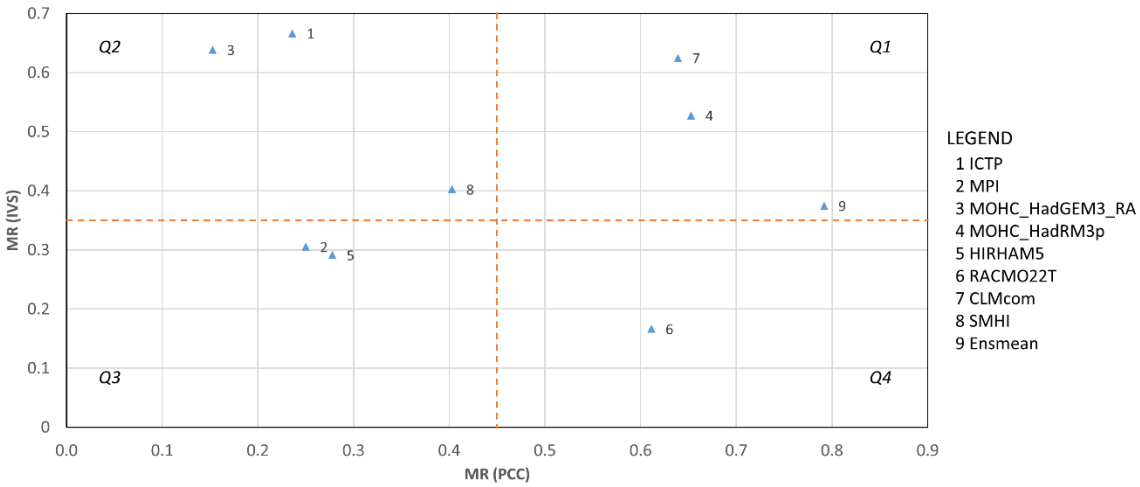

Figure 4.14: Model ranking (MR) based on IVS (y-axis) and correlation coefficients (x-axis), relative to CHIRPS data, using ERAINT-driven RCMs

Model rankings with TAMSAT3 as the reference dataset (Figure 4.15) showed similar results to those with CHIRPS. The similarity in results from both TAMSAT3 and CHIRPS was expected, given that both datasets were used as observational datasets in the current study.

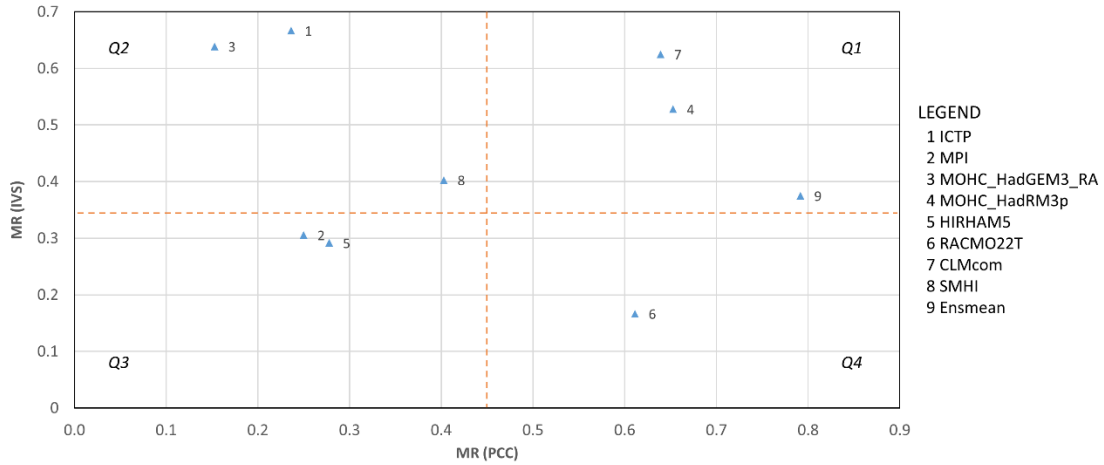

Figure 4.15: As in Figure 4.14 but relative to TAMSAT3 data

The overall top three performing models (with either CHIRPS or TAMSAT3 as the reference dataset) are summarized in Table 4. These findings are consistent with similar assessments that have been done on the study domain where the multi-model ensemble mean has been found to show superior performance (e.g. Endris et al., 2013).

Table 4: Top performing ERAINT-driven RCMs relative to both CHIRPS and TAMSAT3 data

Institute	RCM ID	Acronym
Climate Limited-area Modelling Community (CLM-Community)	CCLM4-8-17.v1	CLMcom
Met Office Hadley Centre	HadRM3P.v1	MOHC
Multi-model ensemble mean for nine ERAINT-forced RCMs used in the study		Ensmean

4.2.3.2 Model simulation ranking using model simulations forced with GCMs

With CHIRPS as the reference data (Figure 4.16), the top five model runs in simulating year-to-year precipitation characteristics over EA are RCA4 (r1i1p1) forced by MPI-M-MPI-ESM-LR, RCA4 (r1i1p1) forced by CNRM-CERFACS-CNRM-CM5, HIRHAM5 (r1i1p1) forced by NCC-NorESM1-M, and RCA4 (r3i1p1) forced by MPI-M-MPI-ESM-LR, respectively. Spatial precipitation characteristics were best simulated by REMO2009 (r1i1p1) forced by MPI-M-MPI-ESM-LR, RCA4 (r1i1p1) forced by CNRM-CERFACS-CNRM-CM5, RCA4 (r1i1p1) forced by MPI-M-MPI-ESM-LR, RCA4 (r1i1p1) forced by ICHEC-EC-EARTH, and an ensemble mean for all GCMs driving RCA4, respectively.

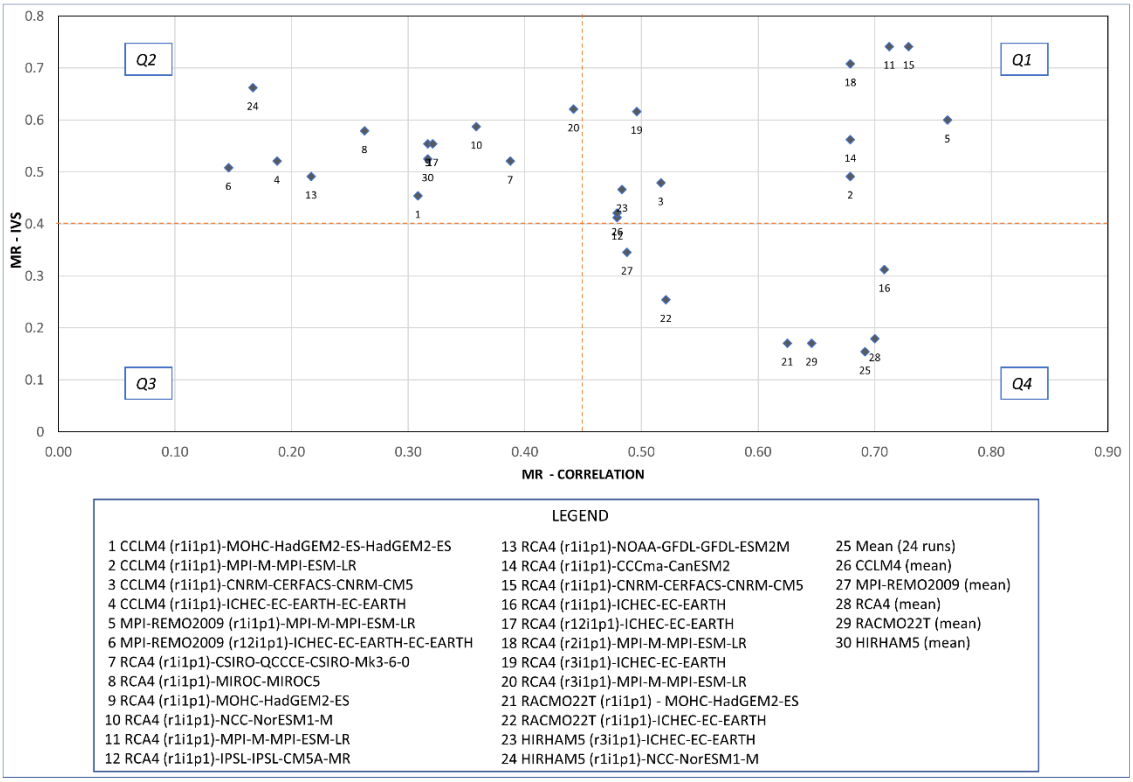

Figure 4.16: Model ranking (MR) for GCM-driven RCMs based on IVS (y-axis) and correlation coefficients (x-axis), relative to CHIRPS data

The best performing model simulations for both criteria (IVS and PCC) are presented in Table 5. Overall, RCA4 (r1i1p1) forced by MPI-M-MPI-ESM-LR and RCA4 (r1i1p1) forced by CNRM-CERFACS-CNRM-CM5 emerged among the top model runs (relatively) in simulating both spatial and year-to-year precipitation characteristics over East Africa.

Table 5: Top five model runs in simulating both spatial and temporal precipitation characteristics with reference to CHIRPS

Institute	RCM	Ensemble	Driving Model
Max Planck Institute (MPI), Germany	REMO2009	r1i1p1	MPI-M-MPI-ESM-LR
Sveriges Meteorologiska och Hydrologiska	SMHI Rossby Center Regional	r1i1p1	MPI-M-MPI-ESM-LR
			CNRM-CERFACS-CNRM-CM5

Institut (SMHI), Sweden	Atmospheric Model (RCA4)		CCCma-CanESM2
		r2i1p1	MPI-M-MPI-ESM-LR

Unlike in the case of CHIRPS as the reference data where models were concentrated in Q1, Q2, and Q4 (with none in the Q3), TAMSAT3 spreads the models in all quadrants (Figure 4.17). The best model runs in simulating year-to-year characteristics are CCLM4 (r1i1p1) forced by CNRM-CERFACS-CNRM-CM5, RCA4 (r1i1p1) forced by MPI-M-MPI-ESM-LR, HIRHAM5 (r1i1p1) forced by NCC-NorESM1-M, CCLM4 (r1i1p1) forced by ICHEC-EC-EARTH, and CCLM4 (r1i1p1) forced by MPI-M-MPI-ESM-LR. The best model runs for spatial characteristics were REMO2009 (r1i1p1) forced by MPI-M-MPI-ESM-LR, RCA4 (r1i1p1) forced by MPI-M-MPI-ESM-LR, RCA4 (r1i1p1) forced by IPSL-IPSL-CM5A-MR, RCA4 (r1i1p1) forced by CNRM-CERFACS-CNRM-CM5, and RCA4 (r2i1p1) forced by MPI-M-MPI-ESM-LR. In terms of both IVS and PCC, RCA4 (r1i1p1) forced by MPI-M-MPI-ESM-LR, RCA4 (r2i1p1) forced by MPI-M-MPI-ESM-LR, RCA4 (r1i1p1) forced by CNRM-CERFACS-CNRM-CM5, CCLM4 (r1i1p1) forced by MPI-M-MPI-ESM-LR, and REMO2009 (r1i1p1) forced by MPI-M-MPI-ESM-LR emerged as the top five model runs, respectively. The RCA4 (r1i1p1) forced by MPI-M-MPI-ESM-LR is the only model run that appeared among the top model runs in simulating both spatial and temporal precipitation characteristics of East Africa.

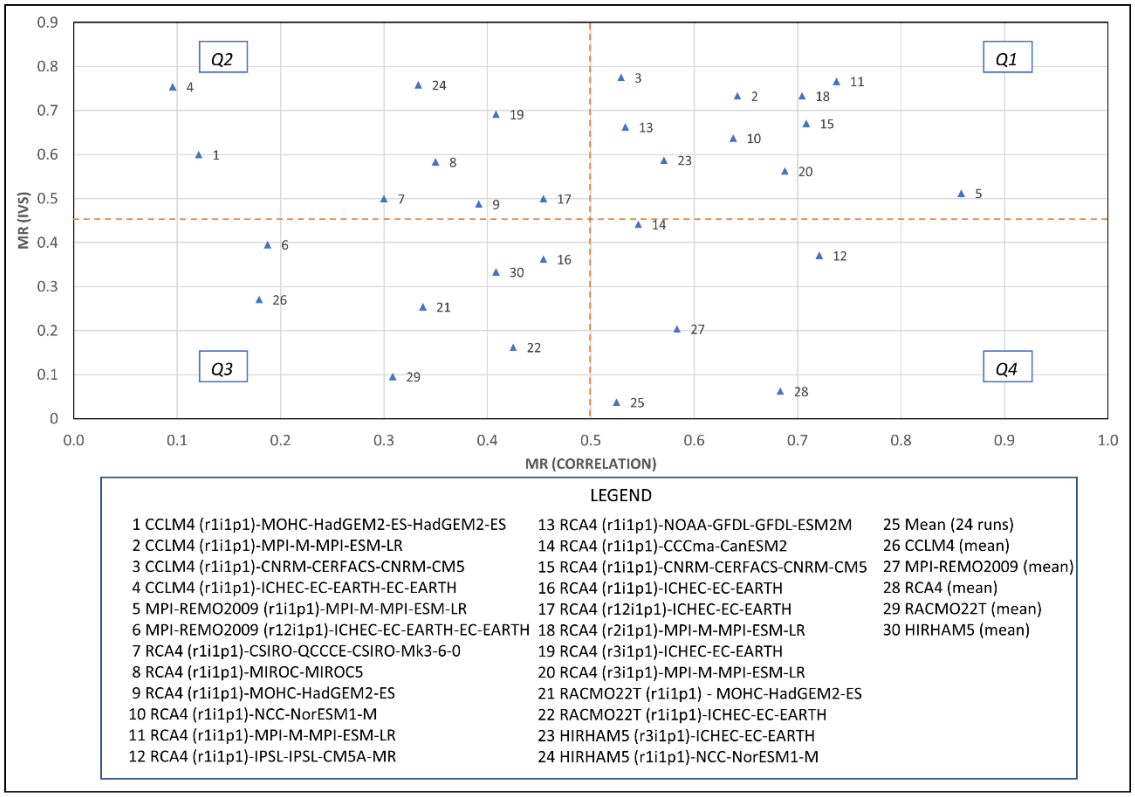

Figure 4.17: Same as Figure 4.16 but using TAMSAT3 as reference data

The top five model runs in simulating spatial and temporal precipitation characteristics (with reference to TAMSAT3 data) are summarized in Table 6. The RCA4 (r1i1p1) forced by MPI-M-MPI-ESM-LR is the only model run that appeared among the top model runs in simulating both spatial and temporal precipitation characteristics of East Africa.

Table 6: Top five model runs in simulating both spatial and temporal precipitation characteristics with reference to TAMSAT3

Institute	RCM	Ensemble	Driving Model
Max Planck Institute (MPI), Germany	REMO2009	r1i1p1	MPI-M-MPI-ESM-LR
Sveriges Meteorologiska och Hydrologiska Institut (SMHI), Sweden	SMHI Rossby Center Regional Atmospheric Model (RCA4)	r1i1p1	MPI-M-MPI-ESM-LR
			CNRM-CERFACS-CNRM-CM5
		r2i1p1	MPI-M-MPI-ESM-LR

Climate Limited-Area Modelling (CLM) Community	CLMcom COSMOCLM (CCLM4)	r1i1p1	MPI-M-MPI-ESM-LR

CHIRPS has been shown to give a better simulation of precipitation over EA than TAMSAT3 relative to observations (Dinku et al. 2018). In the current study, however, both CHIRPS and TAMSAT3 agreed on the top four model runs (Table 7) hence posing no need to choose between ranking results.

Table 7: Top four model runs in simulating EA's precipitation characteristics

Institute	RCM	Ensemble	Driving Model
Max Planck Institute (MPI), Germany	REMO2009	r1i1p1	MPI-M-MPI-ESM-LR
Sveriges Meteorologiska och Hydrologiska Institut (SMHI), Sweden	SMHI Rossby Center Regional Atmospheric Model (RCA4)	r1i1p1	MPI-M-MPI-ESM-LR
			CNRM-CERFACS-CNRM-CM5
		r2i1p1	MPI-M-MPI-ESM-LR

Comparatively, the RCA4 and CCLM4 were the top RCMs in reproducing East Africa's spatio-temporal rainfall characteristics, whether forced by ERAINT or GCMs. Previous studies over the current study domain suggest that a multi-model ensemble mean for RCMs forced by GCMs represents the climatology of precipitation over East Africa fairly well (e.g. Endris et al. 2013; Shiferaw et al. 2018; Kisembe et al., 2018). However, these studies either used RCMs driven by re-analysis data (ERAINT) or an ensemble mean of RCMs but not an ensemble mean of individual model runs. Results from the current study showed that an ensemble mean for the top four model runs performed better (ranked 5th after the top four model runs) than the multi-model ensemble mean for 24 model runs (Figure 4.18). Comparatively, the multi-model ensemble mean (24 runs), and ensemble means for each RCM did not make it to the 1st quadrant. Therefore, a multi-model ensemble mean for a big set of model runs seems to be less competent in simulating both spatial and temporal precipitation characteristics for East Africa. Additional information on model simulation rankings is available in appendices 7.1, 7.2, 7.3, 7.4, 7.5, 7.6, 7.7, and 7.8.

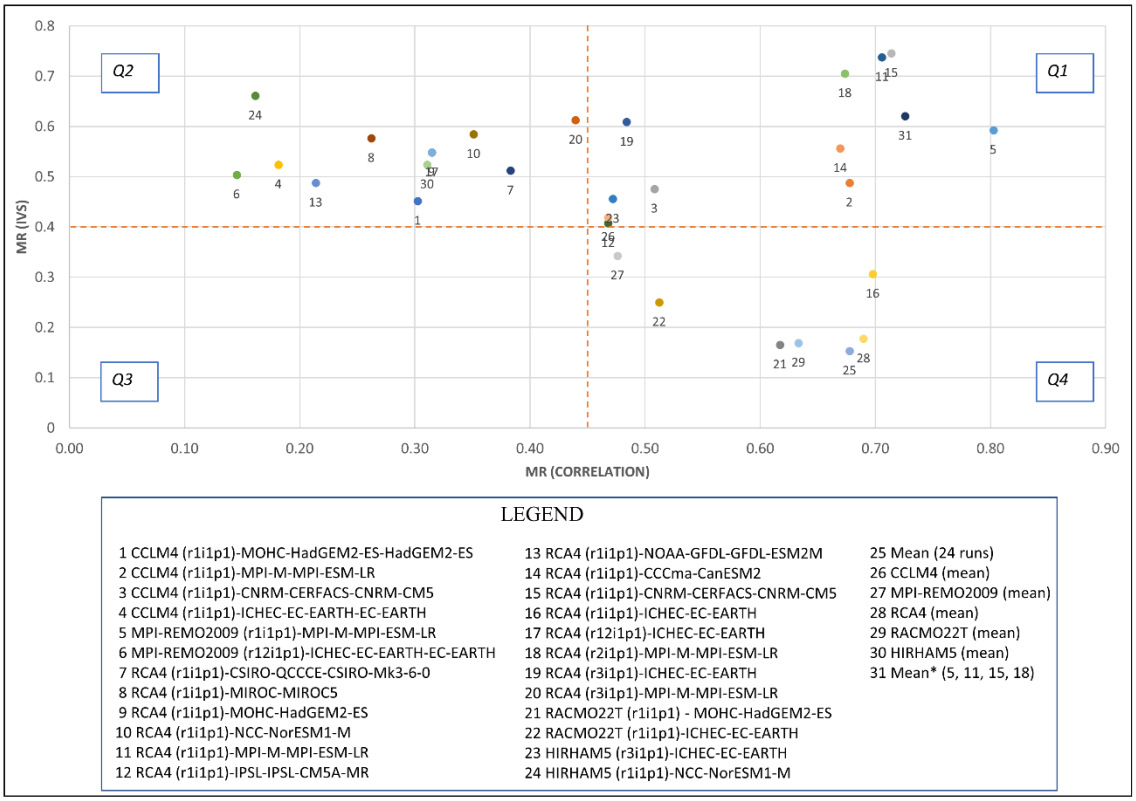

Figure 4.18: Same as Figure 4.16 but now incorporating an ensemble mean (Mean) of the best 4 models*

The results from the current study agree with those from Dosio et al. (2019) who inferred that differences in RCM and GCM simulations make it challenging to subsample a particular model ensemble sufficient to produce a more robust result or reduce uncertainty. The multi-model ensemble mean's relative dismal performance (24 runs) in simulating East Africa's spatial and temporal precipitation characteristics could be attributed to various factors, including a generally high variability in East Africa's year-to-year precipitation patterns (e.g. Endris et al. 2013). The complexity of East Africa's weather and climate caused by a blend of local and external systems such as topography and large inland water bodies (Nicholson 1997) could also be responsible for varied model simulations for East Africa. The current resolution and parameterization of RCMs could be missing the impact of some of the local features, leading to reduced performance in simulation (Dosio & Panitz, 2016).

4.3 Future Precipitation Events over East Africa in a Changing Climate

Future changes in precipitation, under RCP8.5, were analysed using an ensemble mean of the top model runs identified in section 4.2. A plot of changes in future precipitation (FUT) relative to the reference period (HIST) showed a generally drying trend for ANN, MAM, and OND precipitation (Figure 4.19). However, the OND season showed a wetting trend with mean changes of up to 5 mm/day recorded over parts of Lake Victoria.

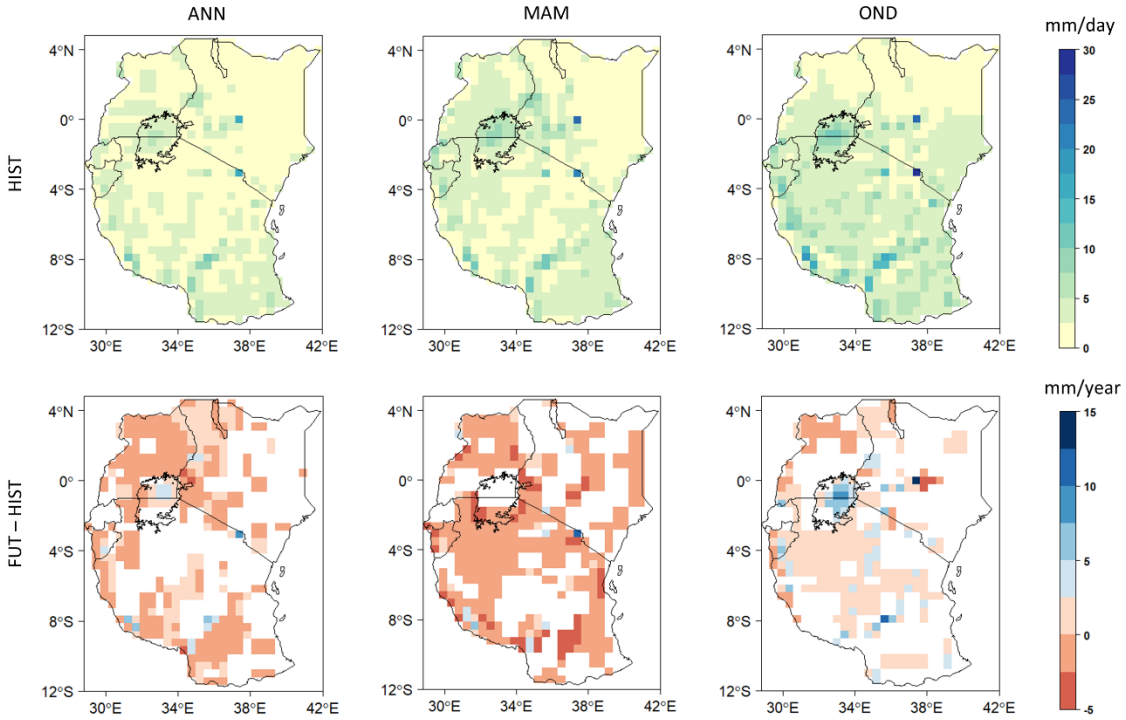

Figure 4.19: The climatology of East Africa (1977-2005, HIST) and significant differences (at 95% confidence interval) between mean precipitation values in the future period and the historical period (FUT-HIST), using an ensemble mean of top four model runs under the RCP8.5 scenario. All units are in mm/day

An analysis of the climate indices (Figure 4.20) showed no discernible changes for the 99p-90p statistic except on a few areas over Lake Victoria where changes exceeding 15 mm/day were recorded. Generally, the 99p-90p statistic showed a drying trend with areas over southern Tanzania recording changes exceeding -15 mm/day. Discernible changes were recorded for the CDD index especially over Uganda where changes exceeding 20 days per year were recorded. At the same time, areas northeast of Kenya and central Tanzania recorded a significant decrease in the CDD index with values exceeding -40

days per year. The CWD index showed a generally wetting trend with values exceeding 10 days per year recorded over most of the study domain. The SDII index showed a general decrease over most of the study domain, with central Kenya recording mean values of up to -10 mm/day. However, some areas over Lake Victoria, parts of Uganda and western Kenya recorded an increase in SDII of up-to 5 mm/day.

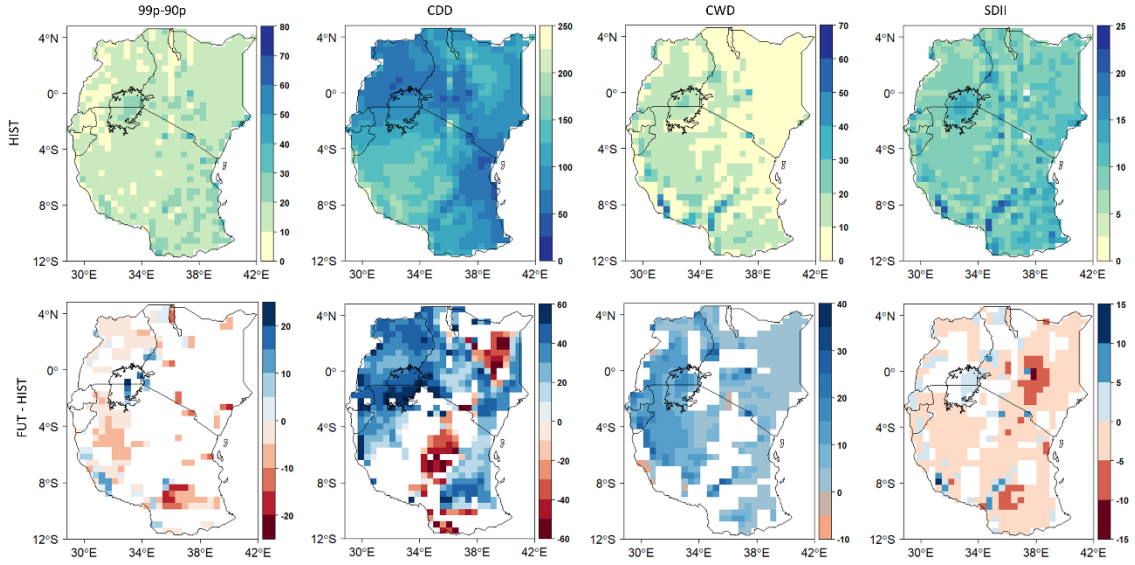

Figure 4.20: Same as Figure 4.19 but for 99p-90p, CDD, CWD, and SDII

Box plots (Figure 4.21 and Figure 4.22) were used to show mean changes over the study domain. As shown in Figure 4.21, no significant changes in mean daily precipitation were recorded for ANN. A marginal drop of about 0.2 mm/day was shown for the MAM season while the OND precipitation showed an increase of about 0.5 mm/day to a daily average of 4 mm by 2100. A reduction in future MAM daily mean rainfall could be caused by projected earlier onset/cessation dates for MAM precipitation hence potentially affecting (relative to the baseline) the MAM season length (Dunning et al. 2018; Wainwright et al. 2019). The SDII index recorded an increase of about 3 mm/day implying a potential for more intense precipitation over the study domain by end of the 21st century.

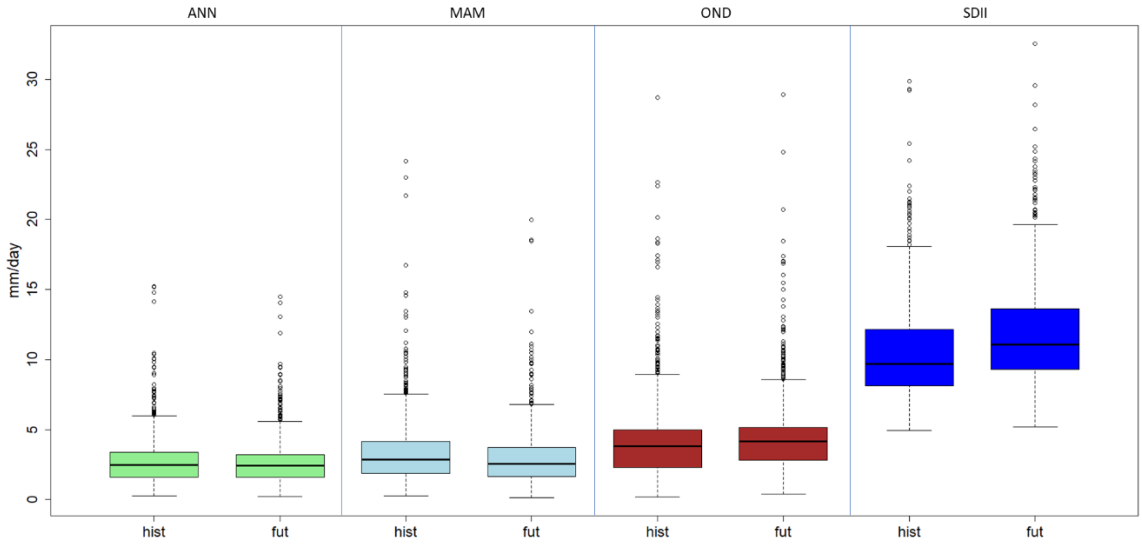

Figure 4.21: Mean future (fut) precipitation changes over the study domain relative to the historical period for ANN, MAM, OND, and SDII. Outliers represent grid-cells with projected changes exceeding 1.5 x Inter-Quartile Range (IQR) above the upper quartile. All units are in mm/day

Projections for the CDD index (Figure 4.22) showed an increase of about ten days to around 105 days compared to CWD, which showed a marginal decrease of about three days. Projections for heavy precipitation events (90p) showed no discernible changes, while projections for very intense precipitation (99p) showed an increase of about five days in a year. The precipitation distribution's right tail width (99p-90p) showed an increase of about 5 mm/day to an average of 20 mm/day. More details of the model performance and future precipitation changes over East Africa were published in a journal article named Appendix 7.9.

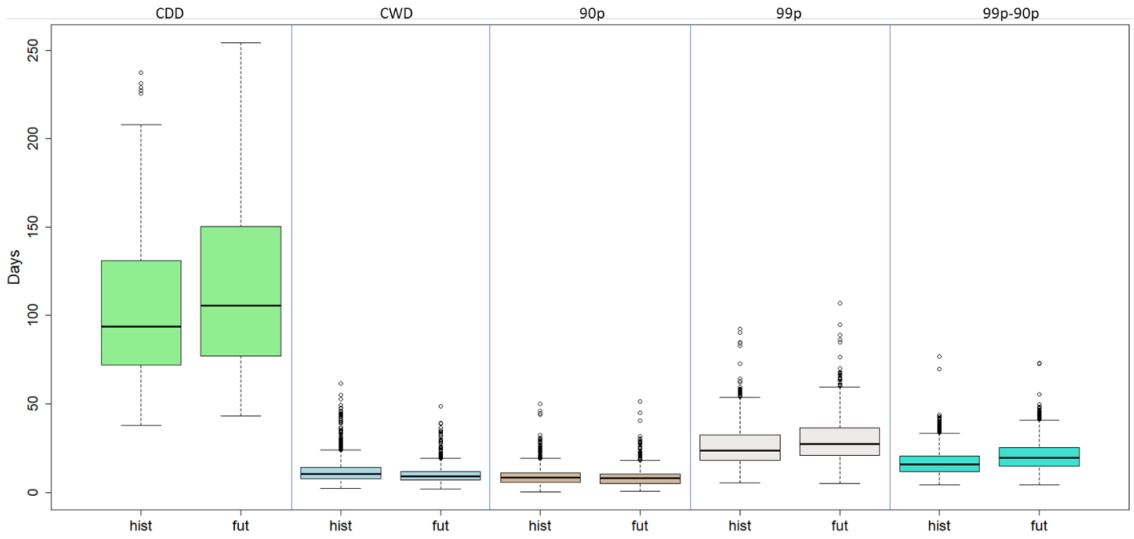

Figure 4.22: Same as Figure 4.21 but for CDD, CWD, 90p, 99p, and 99p-90p

These results complement other works showing a projected increase in OND seasonal precipitation over EA (e.g. Cook & Vizy 2013; Muhati et al., 2018; Gebrechorkos 2019) by showing the distribution at the daily timescale. An increased OND season length due to late precipitation onset and cessation (Wainwright et al., 2019) could explain the high OND precipitation. A warming western Indian Ocean (Lazenby et al. 2018) potentially enhancing other conditions for OND precipitation could also be responsible for the projected increase in OND precipitation. Additionally, the results from the current study agreed with, and complemented, other recent works in the study domain (e.g. Osima et al. 2018; Gudoshava et al. 2020) but showed slight differences in details – possibly because the two studies computed the indices at seasonal timescales under global warming scenarios of 1.5 ^{o}C and 2.0 ^{o}C. The future changes in CDD and CWD could be as a result of a shift in general circulation patterns such as the El Niño Southern Oscillation (ENSO), the Indian Ocean Dipole (IOD) (Shonk et al. 2018; Endris et al. 2019). Future changes in the distribution and occurrence of precipitation have also been linked to changes in southward and northward movement patterns of the intertropical convergence zone (ITCZ) over EA (Dunning et al., 2018). Projections show a decline in June to August (JJA), and MAM mean precipitation (Endris et al. 2019) hence increasing CDD events in the study domain.

Consistent with similar studies in the study domain (e.g. Shongwe et al. 2011; Vizy & Cook 2012; Dunning et al., 2018), findings of the current study show an increase in SDII of up-to 2.5 mm/day (about 25%) over most of the study domain except for Burundi and northern Kenya and east African coast where no significant changes are recorded. Increased CDD events, decreasing CWD events, the drying MAM and JJA seasons, and an increase in SDII imply a possibility of fewer rainy days with above-normal daily precipitation. This observation poses a threat to agricultural activities and socio-economic well-being in East Africa, whose economy is primarily driven by rainfed smallholder farming (Salami et al., 2010; Alessandro et al. 2015).

East Africa's economy is mainly supported by agriculture, tourism, and related sectors, which predominantly depend on rainfall (Alessandro et al. 2015; Hawinkel et al. 2016). Given that the study domain is already facing the impacts of a changing climate (e.g. Morton 2007; Ochieng et al., 2016; Mubiru et al. 2018), an increase in heavy and intense precipitation events in the future is likely to affect the socio-economic well-being of the region adversely. Therefore, there is a need to design and implement effective climate services for adaptive capacity enhancement and sustainable socio-economic development in a changing climate.

4.4 Building Foundations for Climate Services for Sustainability

This subsection samples the use of climate services in the agriculture, health, and tourism sectors. It contributes to effort being dispensed by various actors to build foundations for the design and use of climate services for sustainability in multiple sectors.

4.4.1 Impact of 1.5 oC and 2 oC Global Warming Scenarios on Malaria Transmission in East Africa

This subsection analysed the impact of 1.5 ^{o}C and 2 ^{o}C Global Warming Scenarios on Malaria Transmission in East Africa. Results from this subsection shows how climate information can be used to inform decisions in the health sector and were published in a journal article attached to this thesis as Appendix 7.10.

4.4.1.1 Assessing the Relationship Between Precipitation, Temperature, and Malaria Vectors

Climatic factors significantly influence *An. funestus*, *An. gambiae* s.s., and *An. arabiensis*; the most potent malaria vectors in East Africa (Dida et al., 2018; Karungu et al., 2019). For instance, *An. funestus* tends to be adversely affected by temperatures exceeding 28 ^{o}C (Charlwood, 2017). Its wing-size has a high correlation with elevation and temperature and a low correlation with wind speed and rainfall (Ayala et al., 2011). The survival of *An. gambiae* s.s is significantly influenced by temperature during the larval development (Christiansen-Jucht et al. 2014). Additionally, the mortality of adult *An. gambiae* s.s. increases with temperatures above 27 ^{o}C.

In areas with high malaria transmission by *An. funestus*, precipitation tends to be positively correlated with transmissions caused by *An. arabiensis* and *An. gambiae* s.s. while temperature tends to be negatively correlated (Kelly-Hope et al., 2009). Further, a temperature-dependent and stage-structured delayed differential equation developed by Beck-Johnson et al. (2013) showed that mosquito population abundance is strongly influenced by the dynamics of juvenile mosquito stages which are temperature-dependent. Their model places a peak in abundance of mosquitoes old enough to transmit malaria at around 25 °C. Generally, studies have shown that significant malaria transmission in Africa occurs in areas with temperature ranging from 18 °C to 28 °C, with 25 °C as the optimum temperature (e.g. Craig et al., 1999; Mordecai et al., 2013). Hence, our study adopted the 18 °C – 28 °C as the temperature range within which significant malaria transmission occurs.

While no distinct annual precipitation thresholds have been established for malaria transmission, precipitation plays a vital role in both mosquito abundance and spatial and temporal malaria transmission. It does so by providing good aquatic environments to host malaria vectors. Indeed, heavy and extreme precipitation events have been associated with higher malaria cases in East Africa (e.g. Brown et al., 1998; Hashizume et al., 2009; Kilian et al., 1999). For instance, a study by Gilioli & Mariani (2011) established that a

10 percent increase in precipitation can result in about 6 percent increase in mosquito population in Kenya.

The current assessed the climatology for mean annual precipitation and how it may change under GWL1.5 and GWL2.0. The changes in precipitation patterns were used to estimate the intensity and extent of malaria transmission in East Africa under the two warming scenarios.

4.4.1.2 Trends in Temperature, Precipitation, and Clinical Malaria Cases in East Africa

Despite heavy investments (Head et al., 2017) made to combat and eliminate malaria in the study domain, clinical malaria cases showed some correlation with precipitation and temperature. Siaya and Kigali (b and d, respectively, in Figure 4.23) are good examples where clinical malaria cases corresponded to trends in climate variables, especially the mean temperature.

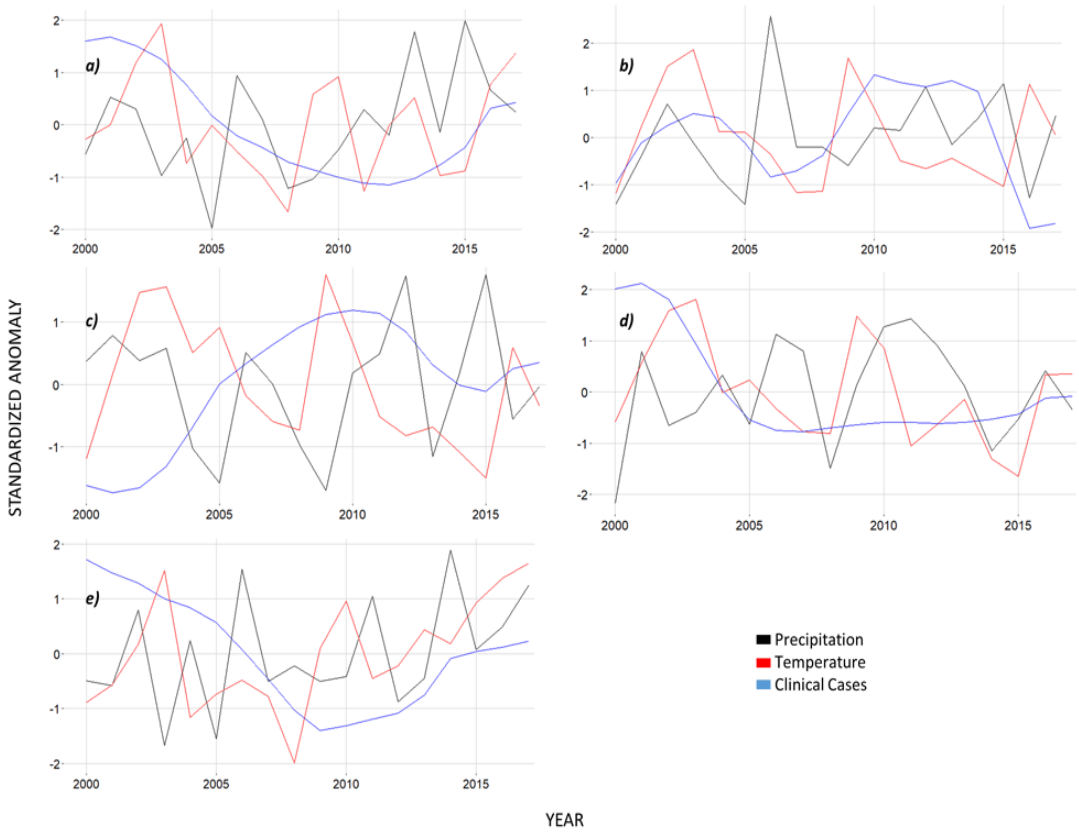

Figure 4.23: Year-to-year anomalies (standardized) for annual precipitation (black), mean temperature (red), and clinical malaria cases (blue) for Gitega, Burundi (a), Siaya, Kenya (b), Jinja, Uganda (c), Kigali, Rwanda (d), and Morogoro, Tanzania (e), for the period 2000–2017, using CHIRPS data

Pearson correlation coefficients (PCCs) for five administrative areas recording the highest number of clinical malaria cases per country (Table 8) showed a positive relationship between temperature and clinical cases, in 22 out of 25 areas under consideration. Burundi recorded the highest positive PCCs (up-to 0.6) between temperature and clinical cases while Uganda recorded the highest negative PCCs (up-to -0.4). Most areas (16 out of 25) recorded a negative correlation between precipitation and clinical malaria cases, with the highest negative correlation being -0.4. The rest showed a marginal positive correlation with the highest being 0.3.

*Table 8: Pearson correlation coefficients for de-trended precipitation (pr) and mean temperature (tmp) values relative to clinical malaria cases. Values marked with * are significant at 95% significance interval*

	Kenya					Rwanda				
	Busia	Kisumu	Siaya	Kakamega	Bungoma	Kigali	North	South	East	West
pr	-0.01	0.1	0.14	0.19	-0.13	-0.31	-0.3	-0.1	-0.2	-0.1
tmp	0.19	0.23	0.07	0.23	0.4	0.2	0.3	0.4	0.4	0.23
	Tanzania					Burundi				
	Geita	Kagera	Mwanza	Mbeya	Morogoro	Gitega	Kirundo	Muyinga	Ngozi	Ruyigi
pr	0.03	-0.35	-0.18	0.29	0.24	0.24	-0.09	-0.13	0.07	0.07
tmp	0	0.55*	0.25	0.4	0.44	0.5*	0.5*	0.6*	0.5*	0.36
	Uganda									
	Iganga	Jinja	Kaabong	Kamuli	Wakiso					
pr	-0.21	-0.33	-0.35	-0.23	-0.21					
tmp	-0.11	0.1	-0.39	-0.03	0.3					

As shown in Table 8, most areas (16 out of 25) recorded a negative correlation between precipitation and clinical malaria cases, with the highest negative correlation being -0.4. The rest showed a marginal positive correlation with the highest being 0.3. Given that precipitation regimes over the study domain are well-defined (e.g. Nicholson, 2017; Schreck & Semazzi, 2004), the observed negative correlation between precipitation and clinical malaria cases could be due to deliberate intensification efforts to combat malaria during the rainy seasons. Nonetheless, areas that record a positive correlation between rainfall and malaria cases (9 out of 25) imply a need for more interventions to minimize malaria transmission.

4.4.1.3 Future Changes in Precipitation and Temperature under 1.5 ^{o}C and 2.0 ^{o}C GWLs

Most of the study domain (except northern Kenya) received at least 400 mm/year of precipitation – the minimum annual precipitation threshold for mosquito vector survival (Figure 4.24). Many areas such as the Lake Victoria region, most of Tanzania and

Uganda, and coastal Kenya recorded more than 800 mm/year of precipitation; the threshold for maximum survival suitability for malaria vectors. Under 1.5 ^{o}C and 2.0 ^{o}C GWLs, the study domain did not record (except for a few places over Tanzania) any significant changes in precipitation (at 95% confidence interval). While global warming of up-to 2.0 ^{o}C may not necessarily significantly change East Africa's mean annual rainfall, the region already received enough precipitation for malaria vector abundance.

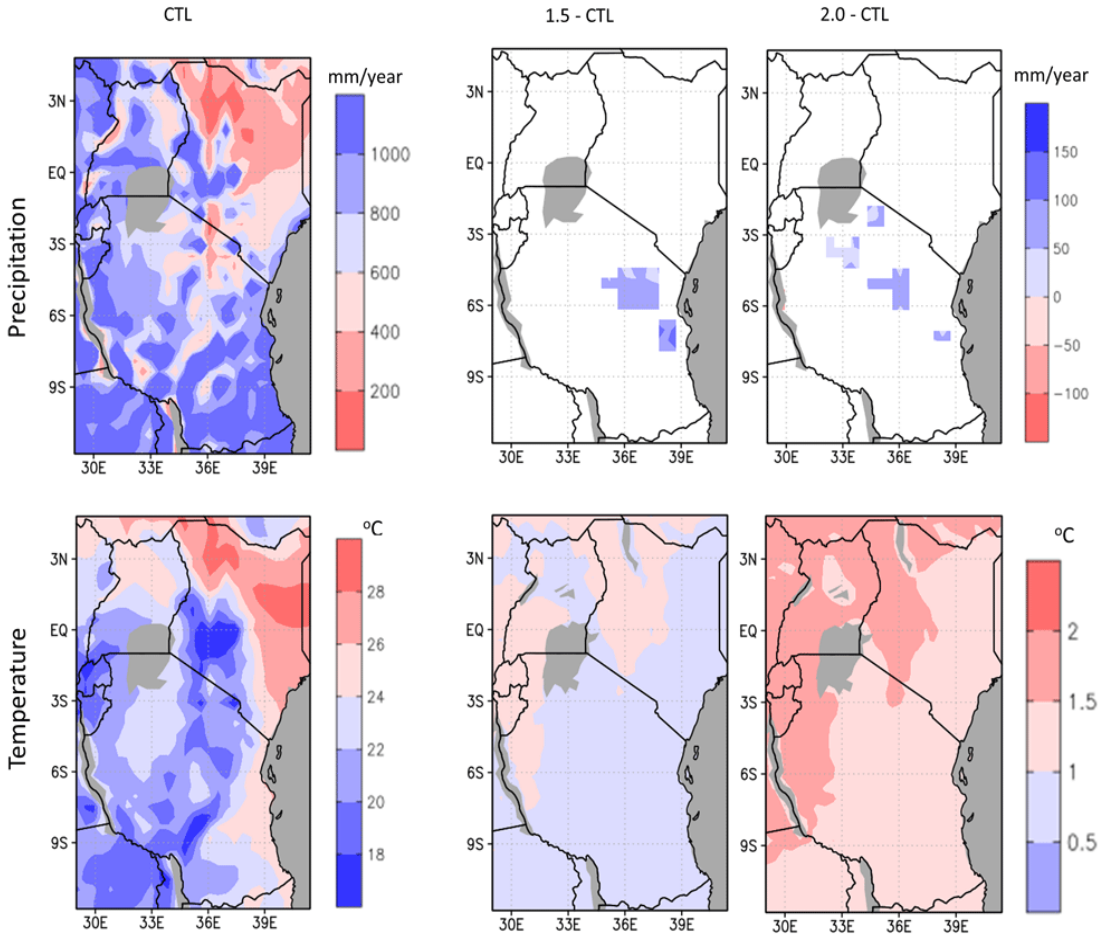

Figure 4.24: Climatology and future changes (at 95% confidence interval) in precipitation (top row) and temperature (bottom row) thresholds under GWL1.5 and GWL2.0 scenarios relative to the control period (1977-2005). Water bodies are shown in grey

In terms of temperature, all areas in the study domain recorded temperatures within the suitability threshold (13-30 ^{o}C) for malaria vectors. Areas in red (Figure 4.33, bottom

row) recorded a temperature range within which maximum suitability (20-25 ^{o}C) occurs for malaria vectors. Below/above the 20-25 ^{o}C threshold (shown in white), the suitability for malaria vector abundance decreases towards none. Under GWL1.5, the study domain recorded a temperature change ranging from 0.5 to 1.5 ^{o}C, potentially increasing the portion of East Africa with the maximum suitability threshold for malaria vector abundance. This was particularly true for Burundi, Rwanda, and central Kenya (Central and Nairobi provinces), where clinical malaria cases were relatively low. A mean temperature increase of between 1 - 2 ^{o}C was expected over the study domain under the GWL2.0. The temperature increase was likely to affect many parts of western Kenya and Tanzania, most of Rwanda, Burundi, and Uganda hence potentially increasing the area recording the maximum suitability threshold (20-25 ^{o}C) for malaria vectors in East Africa. Results from the current study are consistent with findings from similar studies done over the study domain (e.g. Gudoshava et al., 2020; Osima et al., 2018; Ogega et al. 2020).

Existing literature indicates that global warming is likely to increase the seasons and geographical extents for malaria transmission resulting in more cases and newer malaria hotspots (e.g. Ebi et al., 2018; Himeidan & Kweka, 2012; Karungu et al., 2019; Peterson, 2009). While big investments have been made towards eliminating malaria in East Africa, sustaining the gains made so far remains a significant challenge (Bashir et al., 2019; Nkumama et al., 2017). The current study established that despite the ongoing interventions in East Africa, the occurrence of clinical malaria cases was still being influenced by climatic factors. Therefore, a warming globe was likely to make it difficult to sustain gains made and slow down the match towards malaria elimination in East Africa.

4.4.2 Exploring the Future of Nairobi National Park in a Changing Climate and Urban Growth

This subsection analysed the impact of climate change and variability and urban growth on Nairobi National Park, as an example of the impacts of climate change on tourism.

Results from this subsection were published in a journal article enclosed to this thesis as Appendix 7.11.

4.4.2.1 Historical Rainfall Trends over Nairobi Metropolis

A time series analysis for Nairobi showed a high year-to-year rainfall variability (Figure 4.25 and Figure 4.26) in both temperature and precipitation. While no discernible trends were shown for rainfall, the temperature showed a positive trend from below normal during 1981-1990 to above normal from 2000 – 2018. The wettest year for Nairobi was 2018, while the driest year was 2000. The warmest year for Nairobi was 2016, while the coolest year was 1989.

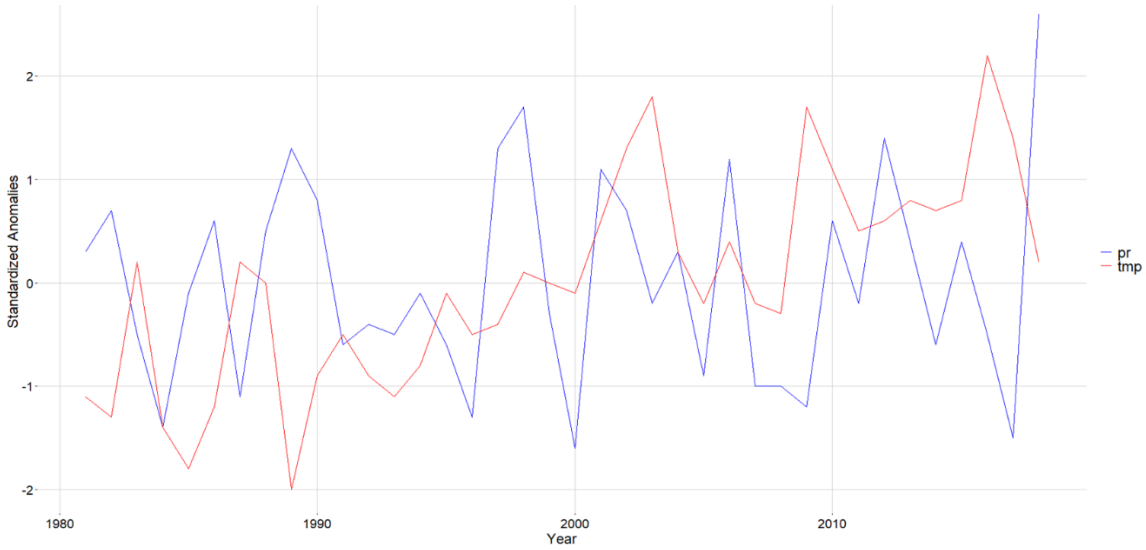

Figure 4.25: Standardized anomalies for year-to-year cycles for precipitation (top row) and temperature (bottom row) for Dagoretti Station, Nairobi

A plot of standardized anomalies for mean annual temperature for Nairobi (Figure 4.26 and Figure 4.27) showed a bimodal temperature regime with March and October as the peaks. July was the coldest month for Nairobi. A bi-modal rainfall was also recorded with April and November being the peaks. The lowest rainfall is recorded between June and September.

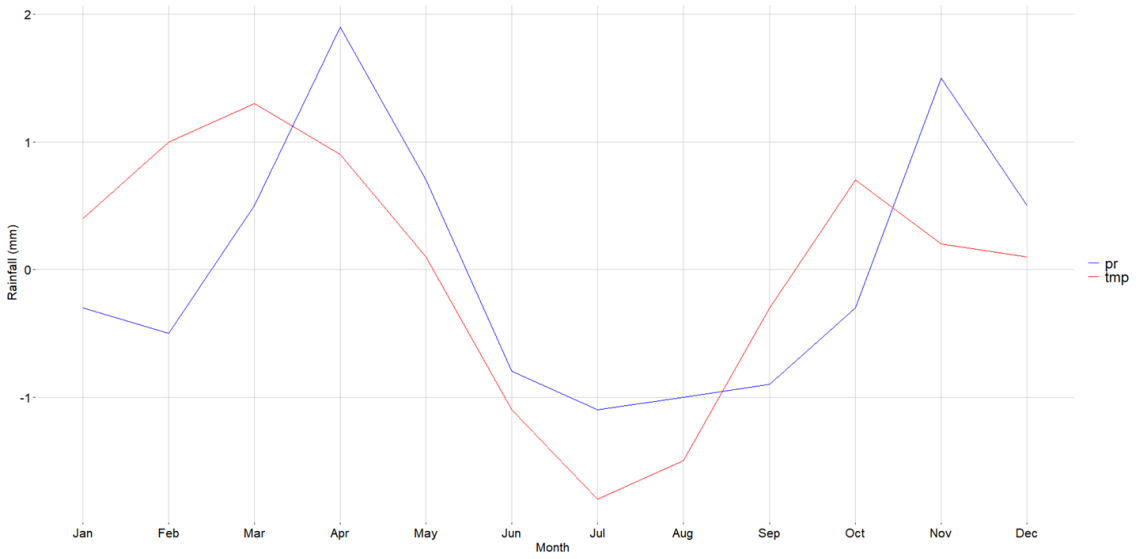

Figure 4.26: As in Figure 4.25 but for annual cycles

While Kenya lies in the tropics, it (as well as the entire east African region) does not experience either a wet climate in annual mean precipitation terms or a monsoonal climate in annual precipitation cycle terms. East Africa, instead, experiences a semi-arid or arid climate characterized by a bimodal yearly variability of precipitation. The bimodal annual precipitation variability has been attributed to the combined yearly cycles of monsoonal winds and the Indian Ocean sea-surface temperature (SST, Yang et al., 2015).

Rainfall variability has differential effects on wildlife (Gandiwa et al., 2016). This includes changes in grazing patterns and the movement of wildlife in and around the conservation areas. Given Nairobi National Park (NNP) 's relatively small spatial extent (about 117 km^2) and the encroachment into the wildlife dispersal areas in Kajiado and Machakos counties, rainfall variability adversely affects wildlife and wildlife activities in and around the park. This variability may have contributed to the recorded cases of human-wildlife conflict in Nairobi and Kitengela. In the recent past, lions have been spotted roaming Nairobi's streets and neighbourhoods adjacent to NNP (Karimi, 2016). This calls for close monitoring of rainfall trends and outlooks to pre-empt any potential risk of human-wildlife cases. In so doing, better management of the park is possible to ensure the prosperity and sustainability of NNP.

4.4.2.2 Future Rainfall Changes for Nairobi Metropolis

Relative to the baseline, no significant MAM and JJA precipitation changes were shown for Nairobi by the end of the 21st century (Figure 4.27). OND season showed a positive shift of up to 150 mm/year in rainfall. An increase in annual rainfall totals of at least 150 mm was shown in the projections for Nairobi. The potential increase in rainfall poses good news for wildlife in the park as it implies a possible rise in water and pasture availability. On the flip side, the presence of more wildlife in the park may bring with it a risk of increased human-wildlife conflict, especially with park-adjacent communities.

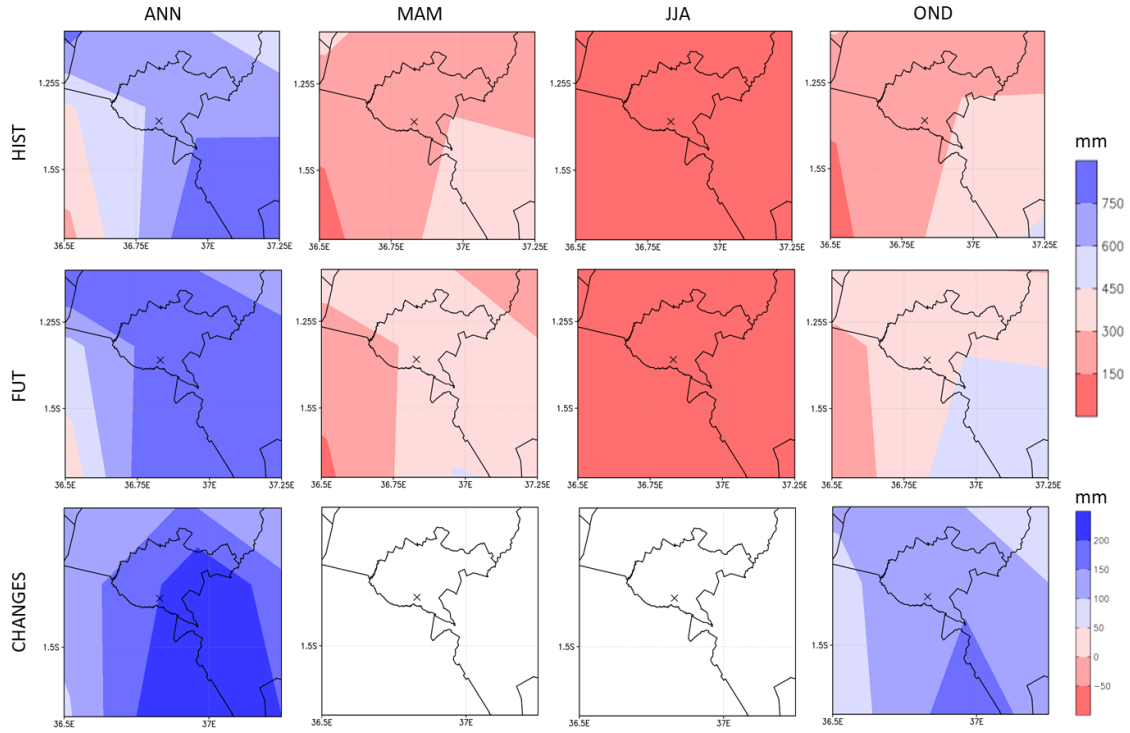

Figure 4.27: Historical climatology and future changes (at 95% confidence level) in precipitation for Nairobi Metropolis. NNP is marked with 'x'

Temperature projections showed a potential rise of at least 3 ^{o}C over Nairobi by the end of the 21st century (Figure 4.28 and). The warming is likely to increase the average annual temperature from the current 20 ^{o}C to about 24 ^{o}C, MAM temperature from 20 ^{o}C to 23 ^{o}C, JJA temperature from 18 ^{o}C to 22 ^{o}C, and OND temperature from 19 ^{o}C to 22.5 ^{o}C. This temperature change may affect the hydrological drought patterns (e.g. Van Loon, 2015) in NNP and, consequently, influence movement of wildlife in and out of the park

in search of shelter. As a result, the potential for human-wildlife conflict, especially with park-adjacent communities and those along the wildlife dispersal areas, is likely to be enhanced under a changing climate. Therefore, more resources may need to be allocated towards monitoring climatic changes and adjust accordingly to minimize the human-wildlife risk.

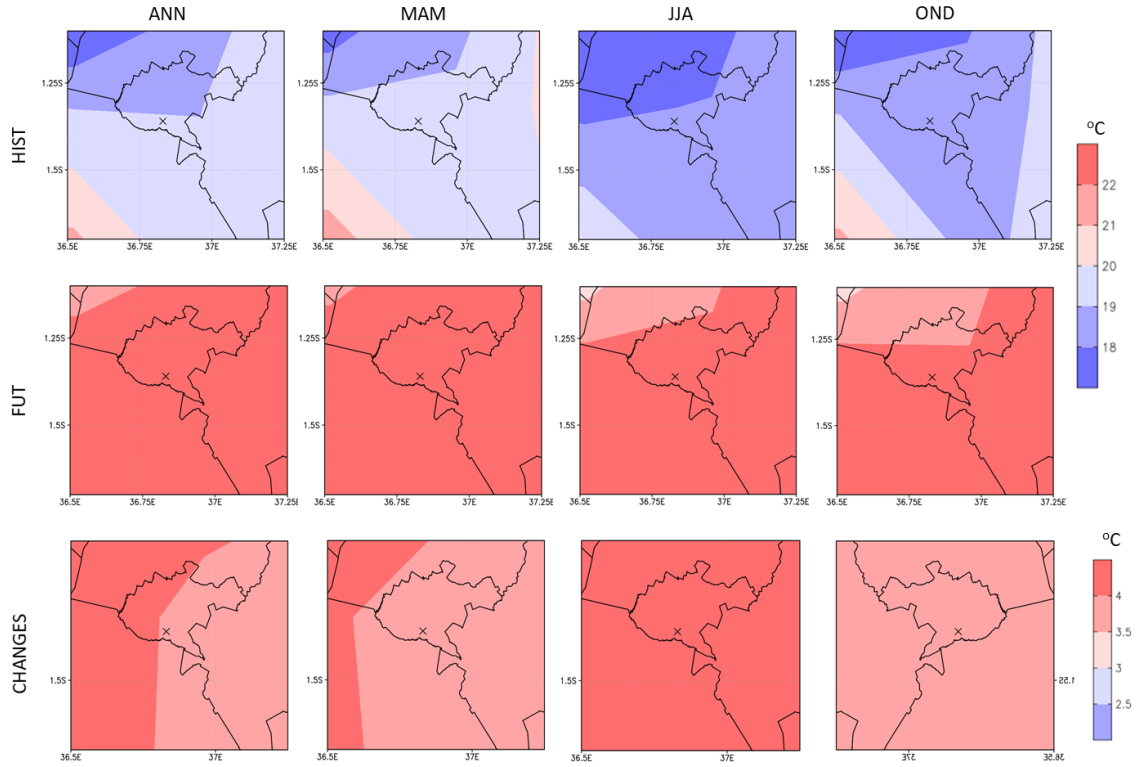

Figure 4.28: As in Figure 4.27 but for temperature

4.4.2.3 Assessment of Historical Urban Growth Patterns in Nairobi Metropolis

An exponential population growth was observed in the three counties surrounding NNP (Nairobi, Kajiado, and Machakos counties; Figure 4.29). With reference to 1989, Nairobi's population had grown 3.6-fold to 4.4 million, Machakos 1.8-fold to 1.4 million, and Kajiado 3.7-fold to 1.1 million people. Consequently, the rapid population growth had increased residential, and transportation needs within the Nairobi metropolis.

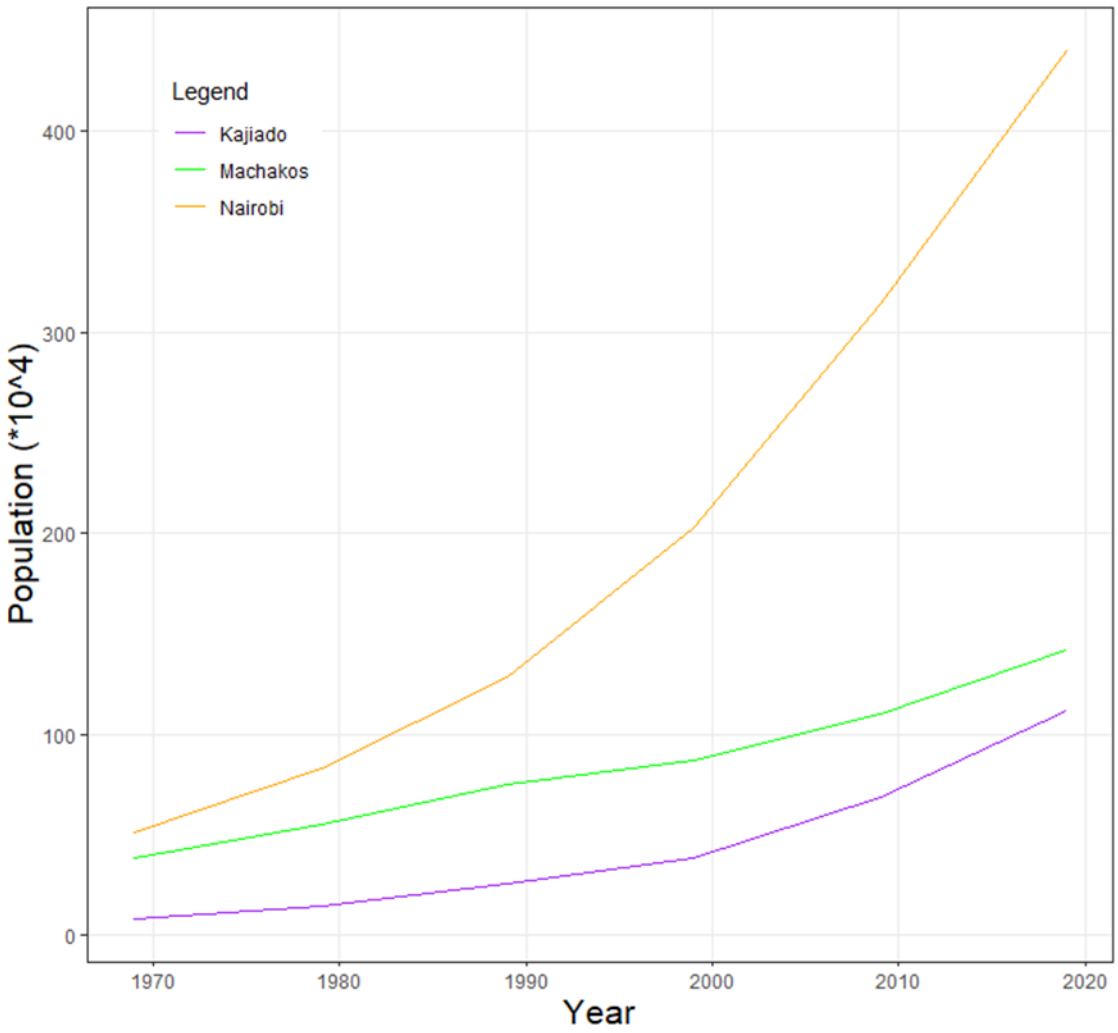

Figure 4.29: Population growth in Nairobi and counties surrounding Nairobi National Park

While NNP is fenced along its borders with the rest of Nairobi and Machakos Counties, satellite imagery analysis showed clear encroachment into the park by residential and transportation infrastructure (Figure 4.30 and Figure 4.31). Enhanced human activities in Nairobi and its environs is have gradually replaced vegetative cover, especially in Nairobi and Kajiado counties, with built-up urban areas.

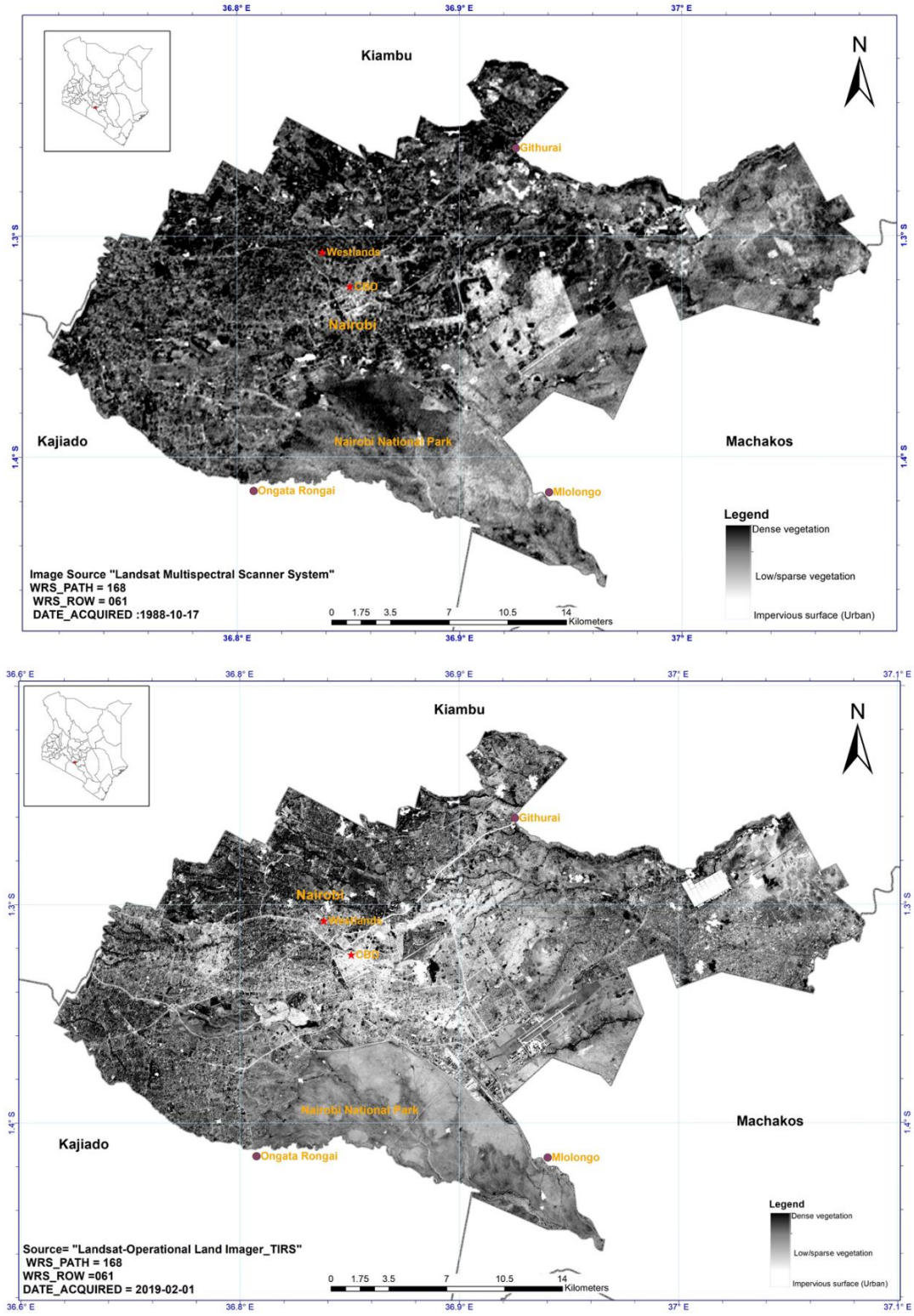

Figure 4.30: Spatial plots for Nairobi County showing vegetation and impervious area distribution over time showing differences in healthy vegetation (dark red), sparse vegetation (light red) and impervious surfaces (in grey) between 1988 and in 2019

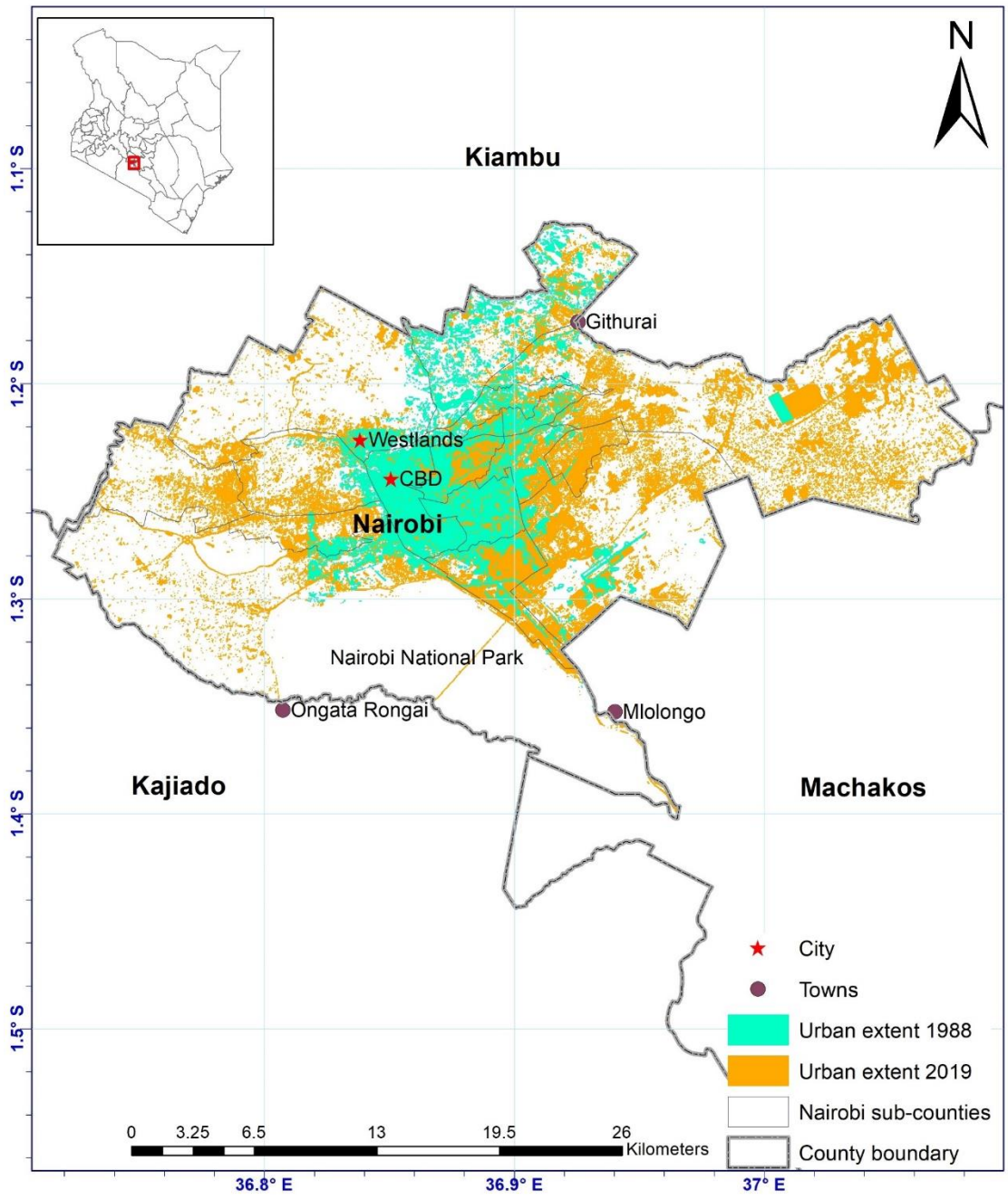

Figure 4.31: Same as Figure 4.30 but highlighting the growth of Nairobi in 2019 compared to 1988

Large-scale transportation projects have shaped the structure of urban development around the NNP while encroaching on the park. The Southern Bypass, for instance, was one of the roads identified in Nairobi's Master Plan of 1973 as a crucial transportation artery for the city. Over the years, however, land allocated for construction of the bypass,

particularly along the northern border of the Nairobi National Park, was grabbed and residential units built on the land. A 7-km long Standard Gauge Railway (SGR) line has been constructed right through the park. Additionally, there are plans to connect the Internal Container Depot just outside the park by a 4 km road corridor measuring 21 meters in width within the Southern Bypass Park. The intensification of development, high levels of sub-division of land coupled with the fencing within the southern border county of Kajiado poses the risk of increasingly blocking migration routes for wildlife while increasing human-wildlife conflict opportunities.

Some efforts have been made to address urban development's sprawl into previously pastoral areas in Kajiado County. In the year 2000, the Wildlife Lease Conservation Programme run by the World-Wide Fund for Nature was initiated. In the programme, landowners along migratory corridors were paid KES 300 per acre annually (Nkedianye, 2004) to allow unrestricted passage for wildlife. In 2011, a master plan for the Kitengela-Isinya-Kipeto area was launched, aiming at curbing sub-division along wildlife migration corridors. Besides, the Kajiado County government in 2018 released new zoning guidelines that seek to limit the ongoing land fragmentation in the county's rural sections. In Nairobi County, however, there has been little policy direction to protect the park from encroachment.

In summary, there is a need for the administrators of NNP to engage the administrators of the Nairobi metropolis to ensure that the future survival and prosperity of NNP is guaranteed. There is evidence of a rapidly growing population in the Nairobi metropolis areas and increased human activity around NNP and the wildlife dispersal areas. Analysis of the climate data also shows significant historical rainfall variability as well as in the outlook. Therefore, a concerted effort from all stakeholders is required to formulate and implement robust policies that will check human activities around NNP and its wildlife dispersal areas. In so doing, human-wildlife conflict cases will be reduced, the NNP ecosystem conserved, and the socio-economic benefits of the NNP fostered.

4.4.3 Climate Services for Sustainability in the Agriculture Sector

This subsection analysed past and future climate patterns and their impacts on smallholder farmers in Kilifi County. Based on the results of the analysis and information provided by the smallholder farmers in Kilifi County, a customized climate change adaptation approach was co-produced. The work done on this section was published in a journal article enclosed to this thesis as Appendix 7.12.

4.4.3.1 Historical and future precipitation patterns over Kilifi County

A year-to-year plot of standardized anomalies (Figure 4.32) showed a generally decreasing trend for the three seasons (MAM, JJA, and OND). MAM rainfall variability was, largely, within the normal range (-1 to -1) except for a few cases of above normal (1981, 1986, 2007 and 2017) and below normal (1992, 2001, 2004, 2009, 2011, and 2012) precipitation. The OND season showed variability mainly within the normal range except for 1997 and 2006 when the area experienced extreme rainfall (above 2). While JJA season recorded the least rainfall in Kilifi County, its year-to-year variability showed a tendency towards above and below normal rainfall.

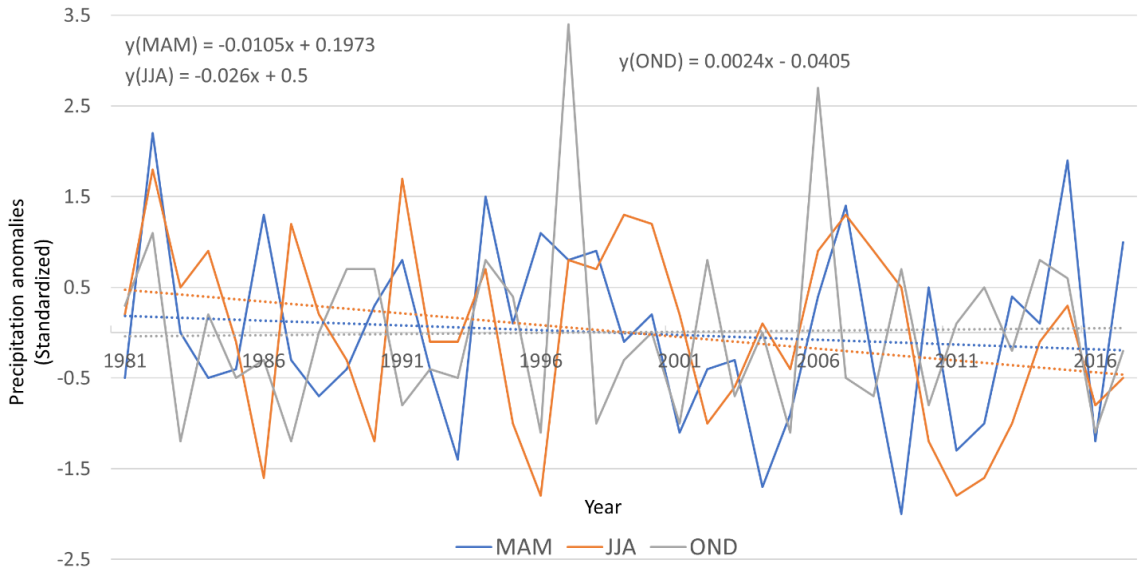

Figure 4.32: Year-to-year standardized seasonal precipitation anomalies for Kilifi County, averaged for the period 1981 to 2018

The climatology plots for annual (ANN) and seasonal (MAM and OND) rainfall over Kilifi (Figure *4.33*) showed no significant rainfall changes in the future period (FUT,

2071 to 2100) relative to the baseline (HIST, 1976 to 2005) for ANN and MAM, under the RCP 8.5. A slight increase of up to 3 mm/day in OND rainfall, especially in the northern part of Kilifi County, was recorded. Kilifi County seemed to receive its highest rainfall during the OND season compared to MAM season.

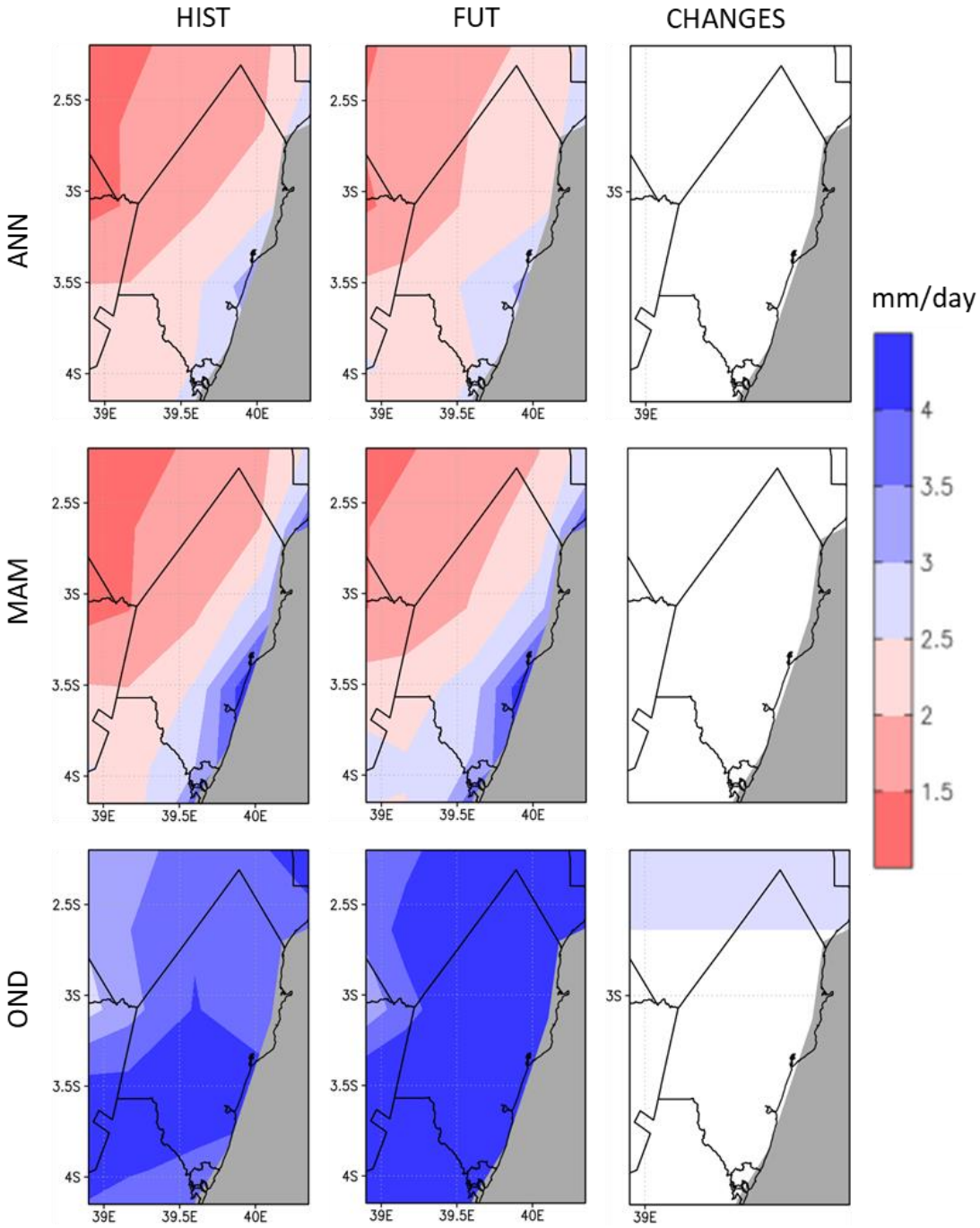

Figure 4.33: Climatology of mean daily rainfall for the baseline period (HIST), future period (FUT) and significant (at 95% confidence level) changes between FUT and HIST for ANN, MAM, and OND (top, middle, and bottom rows, respectively). Water bodies are shown in grey

For climate indices (Figure 4.34), no significant changes were shown for CDD. While CWD recorded some reduction in the FUT period compared to the baseline, the changes

were not significant at a 95% confidence level. SDII showed an increase in the FUT period, especially at the coastal strip. A reduction in the number of CWD events and an increase in SDII implies a possibility of heavier rainy events than normal. The increased daily rainfall intensity may lead to cases of flooding hence potentially disrupting normal life in Kilifi – especially during the OND season.

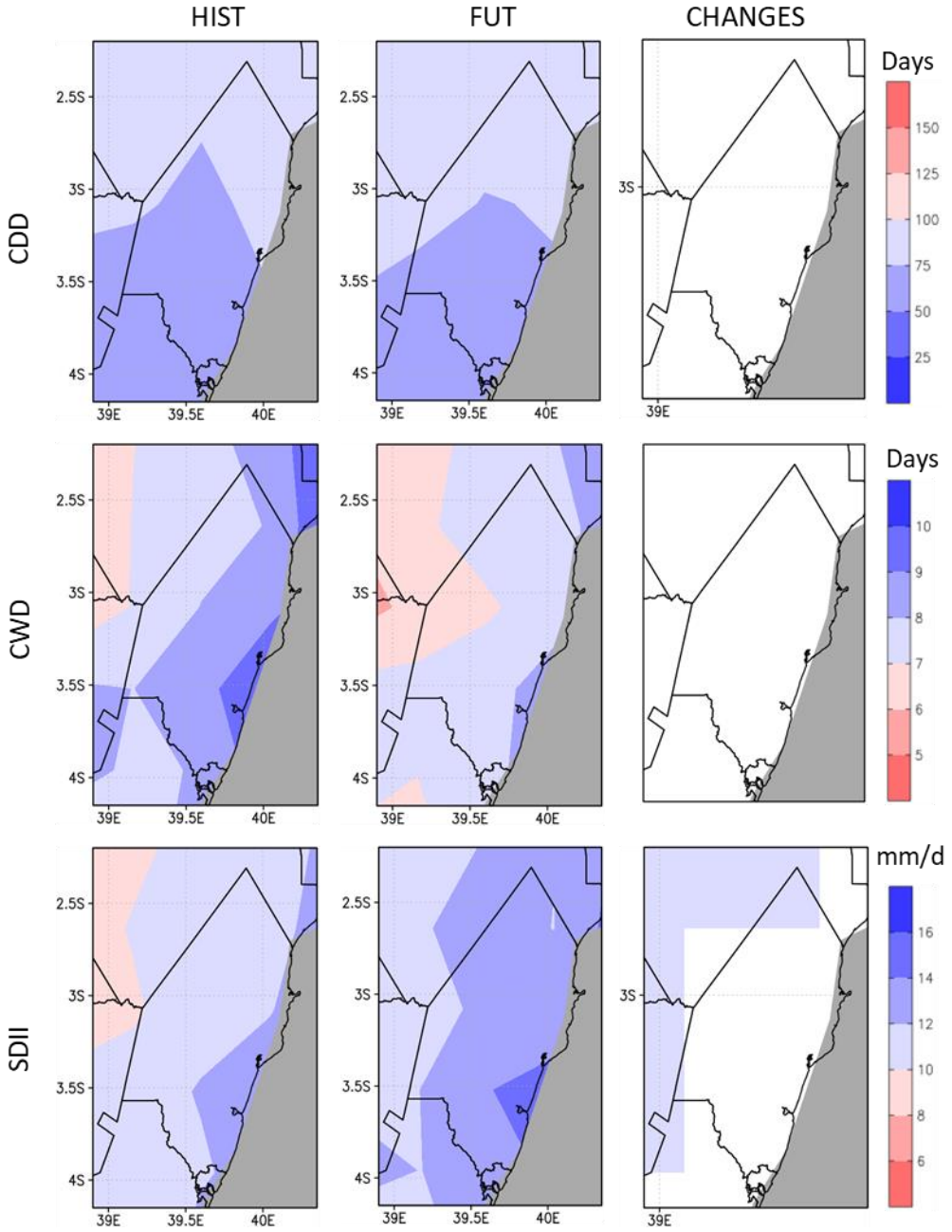

Figure 4.34: As in Figure 4.33 but for CDD, CWD, and SDII

4.4.3.2 Smallholder Farmers' Perception and Response to Climate Change and Variability in Kilifi County

Knowledge of weather and climate variability over time for smallholder farmers in Kilifi County is presented in Figure 4.35. Most farmers (78 percent) cited crop failure (attributed to changing rainfall patterns) as the main consequence of a changing climate in Kilifi County. Specifically, inconsistency - in terms of onset and cessation timing, frequency, and intensity - of the rains during crop growing seasons was identified as a perennial impediment to good crop yields. Respondents did not perceive temperature change as an issue in Kilifi County (results not shown).

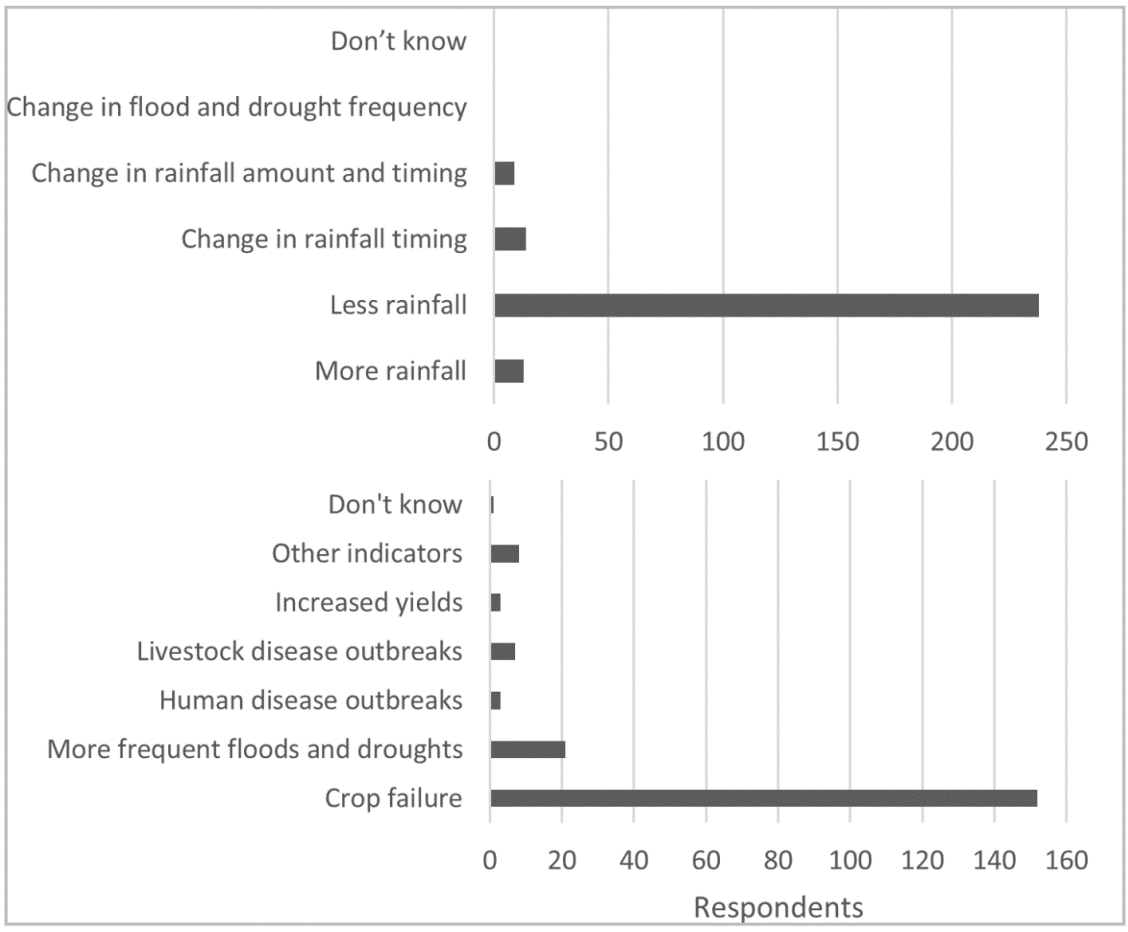

Figure 4.35: Farmers' perceptions (top row) and effects (bottom row) of climate change and variability in Kilifi County. Multiple responses were allowed

In response to changes in rainfall, farmers had made adjustments to their farming practices over time (Figure 4.36). Most respondents had diversified crop variety (33

percent) followed by the introduction of fertilizer or manure to farming (25 percent). The farmers informed that the use fertilizer/manure was now necessary unlike before when good yields were possible even without fertilizer/manure. Diversification of crop variety and irrigation initiatives were also identified as other farming adjustments made in response to changing weather and climate patterns.

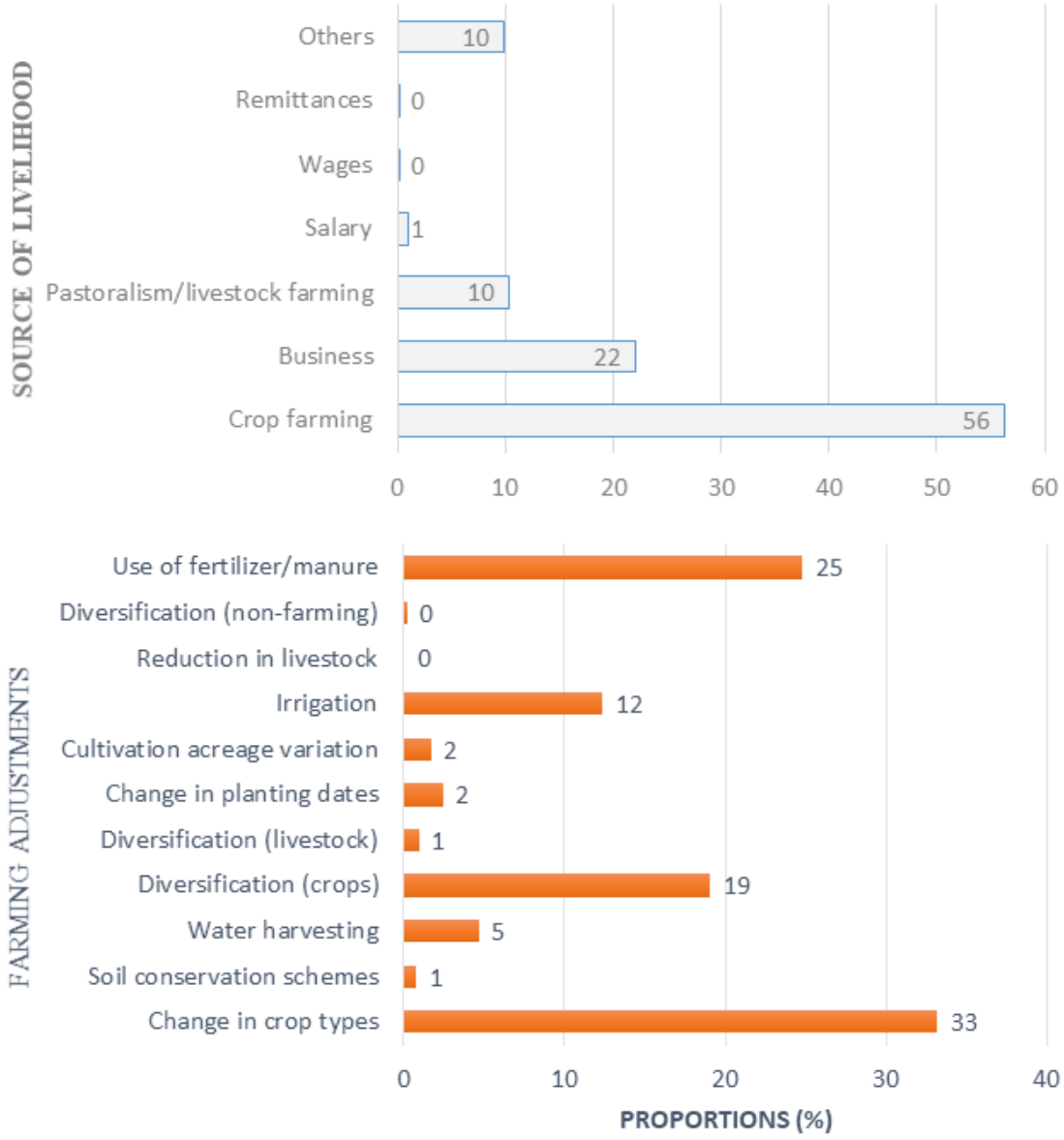

Figure 4.36: Farmers' main source of livelihood (top row) and their adjustment to a changing climate (bottom row) in Kilifi County

Notably, hardly any farmers were diversifying to non-farming sources of livelihood (Figure 4.36). A few farmers (22 percent) were engaged in some form of business. However, farming remained their primary source of livelihood. Findings on the farmers' perceptions agree with the seasonal (OND and MAM) rainfall time series for Kilifi County.

Results from the questionnaire and key-informant interviews were shared with participants through a focus group discussion (FGD). The sharing was done to facilitate knowledge co-production and dissemination. Membership of the FGD was composed of farmers, local administration, academia, civil society organizations, and the media. Potential solutions to issues raised in the social survey were exhaustively discussed, key among them being the need for a robust and well-coordinated climate change adaptation approach as a pathway to sustainable farming activities in Kilifi County. Outcomes from the focus-group discussions and knowledge from the literature were used to propose an innovative climate change adaptation model for Kilifi (Figure 4.37). The model, building on earlier works by Ogega (2017) and Ojwang et al. (2017), uses climate services as a critical input for effective climate change adaptation and sustainability.

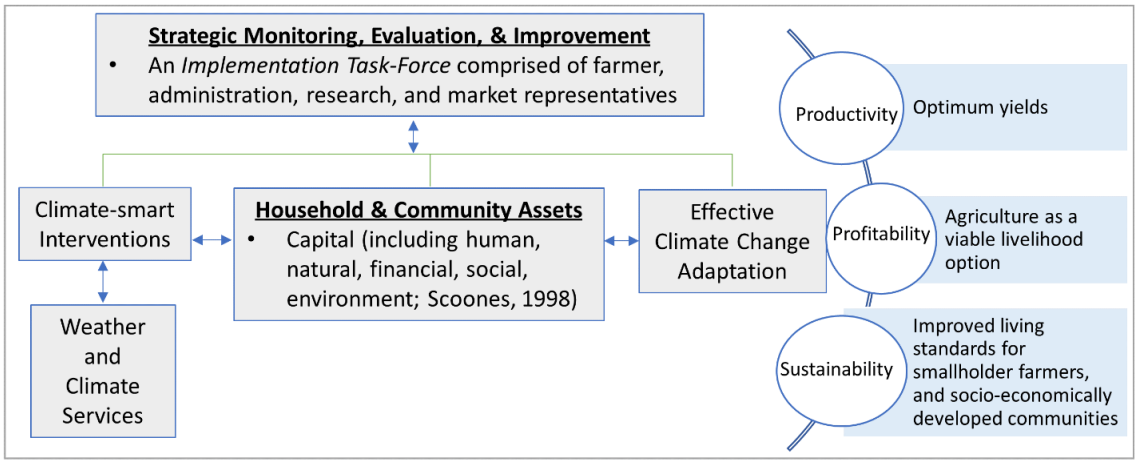

Figure 4.37: An integrated climate change adaptation approach (adapted from Máñez et al., 2014; Scoones, 1998)

The proposed climate change adaptation model (Figure 4.37) puts climate services at the centre of interventions made in response to weather and climate variability. Notably, the model is driven by a trans-sector implementation task force comprised of representatives

of farmers, researchers, local administration, and the market. The taskforce ensures that farmers get the best climate services, helps implement interventions, and links farmers to the pre-arranged market. This model is formed against a backdrop of a Capital Approach Framework detailed in Máñez et al. (2014) and Ojwang et al. (2017). The framework considers adaptation from five critical lenses; financial, social, human, political, and environmental capitals, which provide an enabling environment for interventions to lead to sustainable adaptation.

CHAPTER 5: SUMMARY, CONCLUSIONS, AND RECOMMENDATIONS

This chapter gives a summary of the work done (5), conclusions (5.2), and recommendations for policy and further research (5.3).

5.1 Summary

The study set out to assess historical intraseasonal rainfall variability, generate future intraseasonal rainfall scenarios, and build on climate service foundations for sustainable climate change adaptation in East Africa. An assessment of the performance of CORDEX RCMs in simulating East Africa's rainfall spatial and temporal variability was done, after which the best performing models were used to assess projections for future rainfall changes over the study domain under a global warming scenario. After that, examples of how sector-specific climate services could be used to enhance climate change adaptation.

Specifically, the first objective evaluated the performance of CORDEX RCMs in simulating observed spatial and temporal intraseasonal rainfall characteristics and heavy precipitation events over East Africa. Here, two sets of CORDEX RCM data were used: one driven by reanalysis data (ERAINT) and the other group driven by CMIP 5 GCMs. Overall, RCA4 (r1i1p1) forced by CNRM-CERFACS-CNRM-CM5 and MPI-M-MPI-ESM-LR, REMO2009 (r1i1p1) forced by MPI-M-MPI-ESM-LR, and RCA4 (r2i1p1) forced by MPI-M-MPI-ESM-LR emerged as the top four model runs in simulating both spatial and temporal characteristics of precipitation over East Africa.

Contrary to earlier studies (e.g. Endris et al., 2013; Kisembe et al., 2018; Nikulin et al., 2012) that showed that a multi-model ensemble mean could sufficiently simulate East Africa's precipitation characteristics, results from the current study showed a dismal performance of the multi-model ensemble (for a large number of ensemble members) when assessed against a big set of criteria compared to a smaller ensemble mean of the top-performing models. In this study, an ensemble mean of the top four model runs outperformed an ensemble mean of 24 model simulations and ensemble means for all runs in an RCM. Of the top four model simulations, three are from the RCA4 model, while the other is from the REMO2009 model. Comparatively, the RCA4 and CCLM4 emerge as the top RCMs in reproducing East Africa's spatio-temporal rainfall

characteristics, whether forced by ERAINT or GCMs.

The second objective was to investigate whether observed rainfall characteristics change in the future under a global warming scenario. Here, the top four model runs (and their ensemble mean) were used to assess future changes in all the eight rainfall descriptors under the RCP 8.5 scenario. Consistent with recent studies in the study area that had shown a decrease/increase in future mean MAM/OND precipitation (e.g. Endris et al., 2019), results from this study showed a reduction/increase in mean daily precipitation for MAM/OND for the period 2071-2099. An increase/decrease in CDD/CWD events in the study domain was also recorded consistent with findings from similar studies in the study domain (e.g. Gudoshava et al., 2020; Osima et al., 2018; Wainwright et al., 2019). Projections for SDII and the width of the right tail of the precipitation distribution (99p-90p) showed an increase in most parts of the study domain. An increase in SDII and 99p-90p implies a potential for heavy and extreme precipitation incidences by the year 2100 relative to the baseline (1977-2005).

The third objective aimed at building on foundations for the use of climate services for sustainability in the agriculture, tourism, and health sectors. On health, the study sought to establish the relationship between climatic and clinical malaria cases in East Africa. It also assessed how these trends might change under the 1.5 ^{o}C and 2.0 ^{o}C global warming (1.5GWL and 2.0GWL, respectively). An analysis of trends during the period 2000-2017 showed a predominantly positive/negative correlation between clinical malaria cases and temperature/precipitation in East Africa. The relationship was well defined for temperature than precipitation, possibly due to enhanced malaria control interventions during the rainy seasons. Relative to the control period (1977-2005), no significant precipitation changes were to be expected in East Africa under 1.5GWL and 2.0GWL. However, temperature seemed to increase by 0.5 - 1.5 ^{o}C and 1.0 - 2.0 ^{o}C under 1.5GWL and 2.0GWL, respectively. The increasing temperature was likely to increase the portion of East Africa, recording annual average temperatures within the thresholds where maximum suitability for malaria vector abundance occurs.

An analysis of the impact of a changing climate on coastal smallholder farmers in Kilifi

County was also done. Here, a social survey was done to establish the farmers' perception of climate change in their area and their adaptive capacity against the changing climate. Historical rainfall trends were reviewed, and an outlook of future rainfall changes analysed. Here, enhanced within-season rainfall variability was observed, a phenomenon that had adversely affected smallholder farming in Kilifi. Future rainfall projections also pointed to more intraseasonal rainfall variability over Kilifi hence posing a threat to disrupt cropping seasons. Information from the climate data and the social survey was used to design an innovative, robust, and effective climate change adaptation approach. The climate change adaptation approach would enhance smallholder farmers' adaptive capacity for prosperity and sustainability in the changing climate.

An assessment of historical seasonal rainfall variability over Nairobi was done. The results show significant variability, especially for the MAM and OND seasons. An analysis of historical urban growth patterns in the Nairobi metropolis showed a considerable increase in population. The study also showed a loss of vegetative cover over time and increasing settlement activities around the Nairobi National Park (NNP) and its wildlife dispersal areas. While the Nairobi metropolis's need to source for additional space for its ever-growing population is appreciated, a balance between social, economic, and environmental factors is paramount in safeguarding the prosperity and survival NNP. In so doing, the park will be conserved as it continues to provide vital ecosystem goods and services to the residents of Nairobi.

5.2 Conclusions

1. RCA4 (r1i1p1) forced by CNRM-CERFACS-CNRM-CM5 and MPI-M-MPI-ESM-LR, REMO2009 (r1i1p1) forced by MPI-M-MPI-ESM-LR, and RCA4 (r2i1p1) forced by MPI-M-MPI-ESM-LR (and their ensemble mean) emerged as the top RCM model simulations (from a pool of 30 candidates) that adequately reproduce East Africa's rainfall characteristics
2. The intensity of rainfall received in a rainy day has been increasing in many parts of East Africa. However, the length of rainy seasons has been decreasing over time, leading to shorter rainy seasons but with more intense rainfall on rainy days.

Additionally, East Africa is likely to receive fewer rainy days under global warming but with more intense rainfall in the future. This is likely to cause more frequent and severe flooding events in the region

3. The current interventions to help smallholder farmers adapt to climate change are not sufficient. There is a need for a well-planned, coordinated, and implemented adaptation approach to boost the smallholder farmers' adaptive capacity for sustainability.
4. Global warming scenarios of 1.5 ^{o}C and 2 ^{o}C are likely to increase temporal and spatial malaria transmission in East Africa. Therefore, interventions should be intensified to sustain gains made towards malaria elimination in the region.
5. At the current trends and situation, the future of Nairobi National Park is not guaranteed. Increasing Park encroachment activities coupled with changing weather and climate trends may not only diminish the park but is also likely to drive wildlife out of the park in search of better habitat.

5.3 Recommendations

1. With the projected increase in daily rainfall intensity and heavy rainfall events, East Africa should strengthen its resilience against floods and heavy rains to minimize the negative impacts. On the flip side, more investment should be made in water harvesting schemes to ensure adequate water availability during droughts.
2. For a more appropriate climate change adaptation for smallholder farmers, the use of an integrated climate change adaptation approach produced in this thesis is recommended.
3. Global warming is likely to increase the season and geographical extent of malaria transmission in East Africa. Therefore, the world should collectively work towards keeping global warming below 1.5 ^{o}C. Meanwhile, investment should be intensified hasten and sustain gains made towards malaria elimination in the region. Further, more research is required to enhance the understanding of the influence of other environmental factors (e.g. altitude and humidity) on malaria transmission in East Africa.

4. With the increased encroachment that the park has experienced over time, there is an urgent need for all stakeholders to work together in safeguarding the park's survival and prosperity. While infrastructural development is necessary for Nairobi's prosperity, the growth must not be done at the expense of the world's only national park adjacent to a capital city. A strategic balance between environmental, economic, and social considerations is imperative for sustainability.

REFERENCES

Ahmad, C. B., Jaafar, J., & Abdullah, J. (2011). Buffer zone characteristics for protected areas: a preliminary study of Krau Wildlife Reserve. *WIT Press*. https://doi.org/10.2495/RAV110031

Akdag, S., & Yıldırım, H. (2020). Toward a sustainable mitigation approach of energy efficiency to greenhouse gas emissions in the European countries. *Heliyon*, 6(3), e03396. https://doi.org/10.1016/j.heliyon.2020.e03396

Albert, S., Bronen, R., Tooler, N., Leon, J., Yee, D., Ash, J., Boseto, D., & Grinham, A. (2018). Heading for the hills: climate-driven community relocations in the Solomon Islands and Alaska provide insight for a 1.5 °C future. *Regional Environmental Change*, 18(8), 2261–2272. https://doi.org/10.1007/s10113-017-1256-8

Alessandro, S. D., Caballero, J., Simpkin, S., & Lichte, J. (2015). Kenya Agricultural Risk Assessment. October. https://bit.ly/2RnCyhP

Allen, M. R., Fuglestvedt, J. S., Shine, K. P., Reisinger, A., Pierrehumbert, R. T., & Forster, P. M. (2016). New use of global warming potentials to compare cumulative and short-lived climate pollutants. *Nature Climate Change*, 6(8), 773–776. https://doi.org/10.1038/nclimate2998

Alola, A. A., Bekun, F. V., & Sarkodie, S. A. (2019). Dynamic impact of trade policy, economic growth, fertility rate, renewable and non-renewable energy consumption on ecological footprint in Europe. *Science of The Total Environment*, 685, 702–709. https://doi.org/10.1016/j.scitotenv.2019.05.139

Arab, A., Jackson, M. C., & Kongoli, C. (2014). Modelling the effects of weather and climate on malaria distributions in West Africa. *Malaria Journal*, 13(1), 126. https://doi.org/10.1186/1475-2875-13-126

Ayala, D., Caro-Riaño, H., Dujardin, J.-P., Rahola, N., Simard, F., & Fontenille, D. (2011). Chromosomal and environmental determinants of morphometric variation in natural populations of the malaria vector Anopheles funestus in Cameroon. *Infection, Genetics and Evolution*, 11(5), 940–947. https://doi.org/10.1016/j.meegid.2011.03.003

Bashir, I. M., Nyakoe, N., & Van Der Sande, M. (2019). Targeting remaining pockets of malaria transmission in Kenya to hasten progress towards national elimination goals: An assessment of prevalence and risk factors in children from the Lake endemic region. *Malaria Journal*, 18(1), 1–10. https://doi.org/10.1186/s12936-019-2876-x

Battle, K. E., Lucas, T. C. D., Nguyen, M., Howes, R. E., Nandi, A. K., Twohig, K. A., Pfeffer, D. A., Cameron, E., Rao, P. C., Casey, D., Gibson, H. S., Rozier, J. A., Dalrymple, U., Keddie, S. H., Collins, E. L., Harris, J. R., Guerra, C. A., Thorn, M. P., Bisanzio, D., … Gething, P. W. (2019). Mapping the global endemicity and clinical burden of Plasmodium vivax, 2000–17: a spatial and temporal modelling study. *The Lancet*, *394*(10195), 332–343. https://doi.org/10.1016/S0140-6736(19)31096-7

Beck, H. E., Wood, E. F., Pan, M., Fisher, C. K., Miralles, D. G., van Dijk, A. I. J. M., McVicar, T. R., & Adler, R. F. (2019). MSWEP V2 Global 3-Hourly 0.1° Precipitation: Methodology and Quantitative Assessment. *Bulletin of the American*

Meteorological Society, *100*(3), 473–500. https://doi.org/10.1175/BAMS-D-17-0138.1

Beck-Johnson, L. M., Nelson, W. A., Paaijmans, K. P., Read, A. F., Thomas, M. B., & Bjørnstad, O. N. (2013). The Effect of Temperature on Anopheles Mosquito Population Dynamics and the Potential for Malaria Transmission. *PLoS ONE*, 8(11), e79276. https://doi.org/10.1371/journal.pone.0079276

Berhane, F., & Zaitchik, B. (2014). Modulation of Daily Precipitation over East Africa by the Madden–Julian Oscillation. *Journal of Climate*, 27(15), 6016–6034. https://doi.org/10.1175/JCLI-D-13-00693.1

Bindoff, N.L., Stott, P.A., AchutaRao, K.M., Allen, M.R., Gillett, N., Gutzler, D., Hansingo, K., Hegerl, G., Hu, Y., Jain, S., Mokhov, I.I., Overland, J., Perlwitz, J., Sebbari, R., & Zhang, X. (2013). Detection and attribution of climate change: From global to regional. In *Climate Change 2013: The Physical Science Basis. Contribution of Working Group I to the Fifth Assessment Report of the Intergovernmental Panel on Climate Change*. [Stocker, T.F., Qin, D., Plattner, G.-K., Tignor, M., Allen, S.K., Doschung, J., Nauels, A., Xia, Y., Bex, V., & Midgley, P.M. (eds.)]. Cambridge University Press, pp. 867-952. https://bit.ly/3bDpbRH

Bjerknes, J. (1966). A possible response of the atmospheric Hadley circulation to equatorial anomalies of ocean temperature. *Tellus*, 18(4), 820–829. https://doi.org/10.1111/j.2153-3490.1966.tb00303.x

Boyard-Micheau, J., Camberlin, P., Philippon, N., & Moron, V. (2013). Regional-scale rainy season onset detection: A new approach based on multivariate analysis. *Journal of Climate*, 26(22), 8916–8928. https://doi.org/10.1175/JCLI-D-12-00730.1

Breil, M., Panitz, H. J., & Schädler, G. (2017). Impact of soil-vegetation-atmosphere interactions on the spatial rainfall distribution in the Central Sahel. *Meteorologische Zeitschrift*, 26(4), 379–389. https://doi.org/10.1127/metz/2017/0819

Buontempo, C., Mathison, C., Jones, R., Williams, K., Wang, C., & McSweeney, C. (2015). An ensemble climate projection for Africa. *Climate Dynamics*, 44(7–8), 2097–2118. https://doi.org/10.1007/s00382-014-2286-2

Cai, W., Wang, G., Santoso, A., McPhaden, M. J., Wu, L., Jin, F.-F., Timmermann, A., Collins, M., Vecchi, G., Lengaigne, M., England, M. H., Dommenget, D., Takahashi, K., & Guilyardi, E. (2015). Increased frequency of extreme La Niña events under greenhouse warming. *Nature Climate Change*, 5(2), 132–137. https://doi.org/10.1038/nclimate2492

Cai, W., Zheng, X.-T., Weller, E., Collins, M., Cowan, T., Lengaigne, M., Yu, W., & Yamagata, T. (2013). Projected response of the Indian Ocean Dipole to greenhouse warming. *Nature Geoscience*, 6(12), 999–1007. https://doi.org/10.1038/ngeo2009

Camberlin, P., Fontaine, B., Louvet, S., Oettli, P., & Valimba, P. (2010). Climate Adjustments over Africa Accompanying the Indian Monsoon Onset. *Journal of Climate*, 23(8), 2047–2064. https://doi.org/10.1175/2009JCLI3302.1

Camberlin, Pierre, & Camberlin, P. (2018). Climate of Eastern Africa. In *Oxford Research Encyclopedia of Climate Science (Issue April)*. https://doi.org/10.1093/acrefore/9780190228620.013.512

Camberlin, Pierre, Boyard-Micheau, J., Philippon, N., Baron, C., Leclerc, C., & Mwongera, C. (2014). Climatic gradients along the windward slopes of Mount Kenya and their implication for crop risks. Part 1: climate variability. *International Journal of Climatology*, 34(7), 2136–2152. https://doi.org/10.1002/joc.3427

Camberlin, Pierre, Moron, V., Okoola, R., Philippon, N., & Gitau, W. (2009). Components of rainy seasons' variability in Equatorial East Africa: Onset, cessation, rainfall frequency and intensity. *Theoretical and Applied Climatology*, *98*(3–4), 237–249. https://doi.org/10.1007/s00704-009-0113-1

Camberlin, Pierre. (1997). Rainfall Anomalies in the Source Region of the Nile and Their Connection with the Indian Summer Monsoon. *Journal of Climate*, 10(6), 1380–1392. https://doi.org/10.1175/1520-0442(1997)010<1380:RAITSR>2.0.CO;2

Caminade, C., Medlock, J. M., Ducheyne, E., McIntyre, K. M., Leach, S., Baylis, M., & Morse, A. P. (2012). Suitability of European climate for the Asian tiger mosquito Aedes albopictus : recent trends and future scenarios. *Journal of The Royal Society Interface*, 9(75), 2708–2717. https://doi.org/10.1098/rsif.2012.0138

Cattani, E., Merino, A., Guijarro, J. A., & Levizzani, V. (2018). East Africa Rainfall trends and variability 1983-2015 using three long-term satellite products. *Remote Sensing*, 10(6), 1–26. https://doi.org/10.3390/rs10060931

CBS (1996). Kenya Population Census 1989: Analytical Report Volume IV: Migration and Urbanization. *Central Bureau of Statistics (CBS)*. Nairobi

CBS (2002). Kenya 1999 Population and Housing Census: Migration and Urbanization. *Central Bureau of Statistics (CBS)*. Nairobi

Chadwick, R., Boutle, I., & Martin, G. (2013). Spatial Patterns of Precipitation Change in CMIP5: Why the Rich Do Not Get Richer in the Tropics. *Journal of Climate*, 26(11), 3803–3822. https://doi.org/10.1175/JCLI-D-12-00543.1

Charlwood, J. D. (2017). Some like it hot: a differential response to changing temperatures by the malaria vectors Anopheles funestus and An. gambiae s.l. *PeerJ*, 5, e3099. https://doi.org/10.7717/peerj.3099

Chen, W., Jiang, Z., & Li, L. (2011). Probabilistic projections of climate change over China under the SRES A1B scenario using 28 AOGCMs. *Journal of Climate*, 24(17), 4741–4756. https://doi.org/10.1175/2011JCLI4102.1

Christiansen-Jucht, C., Parham, P. E., Saddler, A., Koella, J. C., & Basáñez, M.-G. (2014). Temperature during larval development and adult maintenance influences the survival of Anopheles gambiae s.s. *Parasites & Vectors*, 7(1), 489. https://doi.org/10.1186/s13071-014-0489-3

Collins, C. S., & Stockton, C. M. (2018). The Central Role of Theory in Qualitative Research. *International Journal of Qualitative Methods*, 17(1), 160940691879747. https://doi.org/10.1177/1609406918797475

Collins, M., An, S.-I., Cai, W., Ganachaud, A., Guilyardi, E., Jin, F.-F., Jochum, M., Lengaigne, M., Power, S., Timmermann, A., Vecchi, G., & Wittenberg, A.

(2010). The impact of global warming on the tropical Pacific Ocean and El Niño. *Nature Geoscience*, 3(6), 391–397. https://doi.org/10.1038/ngeo868

Colón-González, F. J., Fezzi, C., Lake, I. R., & Hunter, P. R. (2013). The Effects of Weather and Climate Change on Dengue. *PLoS Neglected Tropical Diseases*, 7(11), e2503. https://doi.org/10.1371/journal.pntd.0002503

Cook, K. H., & Vizy, E. K. (2013). Projected changes in east african rainy seasons. *Journal of Climate*, 26(16), 5931–5948. https://doi.org/10.1175/JCLI-D-12-00455.1

Cooper, P. J. M., Dimes, J., Rao, K. P. C., Shapiro, B., Shiferaw, B., & Twomlow, S. (2008). Coping better with current climatic variability in the rain-fed farming systems of sub-Saharan Africa: An essential first step in adapting to future climate change? *Agriculture, Ecosystems & Environment*, 126(1–2), 24–35. https://doi.org/10.1016/j.agee.2008.01.007

Dabernig, M., Mayr, G. J., Messner, J. W., & Zeileis, A. (2017). Spatial ensemble post-processing with standardized anomalies. *Quarterly Journal of the Royal Meteorological Society*, 143(703), 909–916. https://doi.org/10.1002/qj.2975

Davis, R., Gichere, S., Mogaka, H., & Hirji, R. (2009). Climate Variability and Water Resources in Kenya : The Economic Cost of Inadequate Management. *Water P-Notes*, 22, 4. https://bit.ly/2U8k6Lr

Dee, D. P., Uppala, S. M., Simmons, A. J., Berrisford, P., Poli, P., Kobayashi, S., Andrae, U., Balmaseda, M. A., Balsamo, G., Bauer, P., Bechtold, P., Beljaars, A. C. M., van de Berg, L., Bidlot, J., Bormann, N., Delsol, C., Dragani, R., Fuentes, M., Geer, A. J., … Vitart, F. (2011). The ERA-Interim reanalysis: Configuration and performance of the data assimilation system. *Quarterly Journal of the Royal Meteorological Society*, *137*(656), 553–597. https://doi.org/10.1002/qj.828

Descamps, S., Aars, J., Fuglei, E., Kovacs, K. M., Lydersen, C., Pavlova, O., Pedersen, Å. Ø., Ravolainen, V., & Strøm, H. (2017). Climate change impacts on wildlife in a High Arctic archipelago - Svalbard, Norway. *Global Change Biology*, 23(2), 490–502. https://doi.org/10.1111/gcb.13381

Deshmukh, I. (1985). Decomposition of grasses in Nairobi National Park, Kenya. *Oecologia*, 67(1), pp. 147-149

Diaconescu, E. P., Gachon, P., & Laprise, R. (2015). On the Remapping Procedure of Daily Precipitation Statistics and Indices Used in Regional Climate Model Evaluation. *Journal of Hydrometeorology*, *16*(6), 2301–2310. https://doi.org/10.1175/JHM-D-15-0025.1

Dida, G. O., Anyona, D. N., Abuom, P. O., Akoko, D., Adoka, S. O., Matano, A.-S., Owuor, P. O., & Ouma, C. (2018). Spatial distribution and habitat characterization of mosquito species during the dry season along the Mara River and its tributaries, in Kenya and Tanzania. *Infectious Diseases of Poverty*, 7(1), 2. https://doi.org/10.1186/s40249-017-0385-0

Dinku, T., Peterson, P., Barbara, S., Maidment, R., & Tadesse, T. (2018). *Validation of the CHIRPS Satellite Rainfall Estimates over Eastern of Africa: Validation of the CHIRPS satellite rainfall estimates over eastern. April*. https://doi.org/10.1002/qj.3244

Dosio, A., & Panitz, H. J. (2016). Climate change projections for CORDEX-Africa with COSMO-CLM regional climate model and differences with the driving global climate models. *Climate Dynamics*, 46(5–6), 1599–1625. https://doi.org/10.1007/s00382-015-2664-4

Dosio, A., Jones, R. G., Jack, C., Lennard, C., Nikulin, G., & Hewitson, B. (2019). What can we know about future precipitation in Africa? Robustness, significance and added value of projections from a large ensemble of regional climate models. *Climate Dynamics*, 53(9–10), 5833–5858. https://doi.org/10.1007/s00382-019-04900-3

Dunning, C. M., Black, E., & Allan, R. P. (2018). Later wet seasons with more intense rainfall over Africa under future climate change. *Journal of Climate*, 31(23), 9719–9738. https://doi.org/10.1175/JCLI-D-18-0102.1

Ebi, K. L., Hasegawa, T., Hayes, K., Monaghan, A., Paz, S., & Berry, P. (2018). Health risks of warming of 1.5 °c, 2 °c, and higher, above pre-industrial temperatures. *Environmental Research Letters*, 13(6). https://doi.org/10.1088/1748-9326/aac4bd

Eden, J. M., Widmann, M., Maraun, D., & Vrac, M. (2014). Comparison of GCM- and RCM-simulated precipitation following stochastic postprocessing. *Journal of Geophysical Research: Atmospheres*, 119(19), 11,040-11,053. https://doi.org/10.1002/2014JD021732

Endris, H. S., Lennard, C., Hewitson, B., Dosio, A., Nikulin, G., & Artan, G. A. (2019). Future changes in rainfall associated with ENSO, IOD and changes in the mean state over Eastern Africa. *Climate Dynamics*, 52(3–4), 2029–2053. https://doi.org/10.1007/s00382-018-4239-7

Endris, H. S., Lennard, C., Hewitson, B., Dosio, A., Nikulin, G., & Panitz, H.-J. (2016). Teleconnection responses in multi-GCM driven CORDEX RCMs over Eastern Africa. *Climate Dynamics*, 46(9–10), 2821–2846. https://doi.org/10.1007/s00382-015-2734-7

Endris, H. S., Omondi, P., Jain, S., Lennard, C., Hewitson, B., Chang'a, L., Awange, J. L., Dosio, A., Ketiem, P., Nikulin, G., Panitz, H.-J., Büchner, M., Stordal, F., & Tazalika, L. (2013). Assessment of the Performance of CORDEX Regional Climate Models in Simulating East African Rainfall. *Journal of Climate*, 26(21), 8453–8475. https://doi.org/10.1175/JCLI-D-12-00708.1

Fishman, R. (2016). More uneven distributions overturn benefits of higher precipitation for crop yields. *Environmental Research Letters*, 11(2), 024004. https://doi.org/10.1088/1748-9326/11/2/024004

Fiwa, L., Vanuytrecht, E., Wiyo, K., & Raes, D. (2014). Effect of rainfall variability on the length of the crop growing period over the past three decades in central Malawi. *Climate Research*, 62(1), 45–58. https://doi.org/10.3354/cr01263

Folland, C. K., Colman, A. W., Rowell, D. P., & Davey, M. K. (2001). Predictability of Northeast Brazil Rainfall and Real-Time Forecast Skill, 1987–98. *Journal of Climate*, 14(9), 1937–1958. https://doi.org/10.1175/1520-0442(2001)014<1937:PONBRA>2.0.CO;2

Frings, M., Lakes, T., Müller, D., Khan, M. M. H., Epprecht, M., Kipruto, S., Galea, S., & Gruebner, O. (2018). Modelling and mapping the burden of disease in Kenya. *Scientific Reports*, 8(1), 9826. https://doi.org/10.1038/s41598-018-28266-4

Funk, C., Peterson, P., Landsfeld, M., Pedreros, D., Verdin, J., Shukla, S., Husak, G., Rowland, J., Harrison, L., Hoell, A., & Michaelsen, J. (2015). The climate hazards infrared precipitation with stations—a new environmental record for monitoring extremes. *Scientific Data*, *2*(1), 150066. https://doi.org/10.1038/sdata.2015.66

Gandiwa, E., Heitkonig, I. M., Eilers, P. H. & Prins, H. H., 2016. Rainfall variability and its impact on large mammal populations in a complex of semi-arid African savanna protected areas. *Tropical Ecology*, 57(2), pp. 163-180

Gao, X., & Giorgi, F. (2017). Use of the RegCM System over East Asia: Review and Perspectives. *Engineering*, 3(5), 766–772. https://doi.org/10.1016/J.ENG.2017.05.019

Gbegbelegbe, S., Serem, J., Stirling, C., Kyazze, F., Radeny, M., Misiko, M., Tongruksawattana, S., Nafula, L., Gakii, M., & Sonder, K. (2018). Smallholder farmers in eastern Africa and climate change: a review of risks and adaptation options with implications for future adaptation programmes. *Climate and Development*, 10(4), 289–306. https://doi.org/10.1080/17565529.2017.1374236

Gebbie, G., Eisenman, I., Wittenberg, A., & Tziperman, E. (2007). Modulation of Westerly Wind Bursts by Sea Surface Temperature: A Semistochastic Feedback for ENSO. *Journal of the Atmospheric Sciences*, 64(9), 3281–3295. https://doi.org/10.1175/JAS4029.1

Gebrechorkos, S. H. (2019). Changes in temperature and precipitation extremes in Ethiopia, Kenya, and Tanzania. *International Journal of Climatology*. https://doi.org/10.1002/joc.5777

Gebremeskel Haile, G., Tang, Q., Sun, S., Huang, Z., Zhang, X., & Liu, X. (2019). Droughts in East Africa: Causes, impacts and resilience. *Earth-Science Reviews*, 193, 146–161. https://doi.org/10.1016/j.earscirev.2019.04.015

GERICS (2017). MPI-CSC CORDEX data for Africa (AFR-44) based on REMO2009 model simulations. *World Data Center for Climate (WDCC) at DKRZ*. https://bit.ly/3bfGlVu

Gizaw, M. S., & Gan, T. Y. (2017). Impact of climate change and El Niño episodes on droughts in sub-Saharan Africa. *Climate Dynamics*, 49(1–2), 665–682. https://doi.org/10.1007/s00382-016-3366-2

Grant, C., & Osanloo, A. (2014). Understanding, selecting, and integrating a theoretical framework in dissertation research: creating the blueprint for your "house." *Administrative Issues Journal Education Practice and Research*. https://doi.org/10.5929/2014.4.2.9

Guan, K., Sultan, B., Biasutti, M., Baron, C., & Lobell, D. B. (2015). What aspects of future rainfall changes matter for crop yields in West Africa? *Geophysical Research Letters*, 42(19), 8001–8010. https://doi.org/10.1002/2015GL063877

Gudoshava, M., Misiani, H. O., Segele, Z. T., Jain, S., Ouma, J. O., Otieno, G., Anyah, R., Indasi, V. S., Endris, H. S., Osima, S., Lennard, C., Zaroug, M., Mwangi, E., Nimusiima, A., Kondowe, A., Ogwang, B., Artan, G., & Atheru, Z. (2020). Projected effects of 1.5 °C and 2 °C global warming levels on the intraseasonal rainfall characteristics over the Greater Horn of Africa. *Environmental Research Letters*, 15(3), 034037. https://doi.org/10.1088/1748-9326/ab6b33

Hassanali, K. (2017). Challenges in mainstreaming climate change into productive coastal sectors in a Small Island State – The case of Trinidad and Tobago. *Ocean & Coastal Management*, 142, 136–142. https://doi.org/10.1016/j.ocecoaman.2017.04.001

Hastenrath, S., & Polzin, D. (2003). Circulation mechanisms of climate anomalies in the equatorial Indian Ocean. *Meteorologische Zeitschrift*, 12(2), 81–93. https://doi.org/10.1127/0941-2948/2003/0012-0081

Hastenrath, S., Polzin, D., & Camberlin, P. (2004). Exploring the predictability of the'Short Rains' at the coast of East Africa. *International Journal of Climatology*, 24(11), 1333–1343. https://doi.org/10.1002/joc.1070

Hastenrath, S., Polzin, D., & Mutai, C. (2011). Circulation Mechanisms of Kenya Rainfall Anomalies. *Journal of Climate*, 24(2), 404–412. https://doi.org/10.1175/2010JCLI3599.1

Hawinkel, P., Thiery, W., Lhermitte, S., Swinnen, E., Verbist, B., Van Orshoven, J., & Muys, B. (2016). Vegetation response to precipitation variability in East Africa controlled by biogeographical factors. *Journal of Geophysical Research*: Biogeosciences, 121(9), 2422–2444. https://doi.org/10.1002/2016JG003436

Hay, S. I., & Snow, R. W. (2006). The Malaria Atlas Project: Developing Global Maps of Malaria Risk. *PLoS Medicine*, *3*(12), e473. https://doi.org/10.1371/journal.pmed.0030473

Head, M. G., Goss, S., Gelister, Y., Alegana, V., Brown, R. J., Clarke, S. C., Fitchett, J. R. A., Atun, R., Scott, J. A. G., Newell, M.-L., Padmadas, S. S., & Tatem, A. J. (2017). Global funding trends for malaria research in sub-Saharan Africa: a systematic analysis. *The Lancet Global Health*, 5(8), e772–e781. https://doi.org/10.1016/S2214-109X(17)30245-0

Heron, L., Wilkinson, C., Spiegel, P., White, J. M., Carter, J., & Mason, J. B. (2012). Child Acute Malnutrition and Mortality in Populations Affected by Displacement in the Horn of Africa, 1997–2009. *International Journal of Environmental Research and Public Health*, 9(3), 791–806. https://doi.org/10.3390/ijerph9030791

Hession, S. L., & Moore, N. (2011). A spatial regression analysis of the influence of topography on monthly rainfall in East Africa. *International Journal of Climatology*, 31(10), 1440–1456. https://doi.org/10.1002/joc.2174

Hewitt, C., Mason, S., & Walland, D. (2012). The Global Framework for Climate Services. *Nature Climate Change*, 2(12), 831–832. https://doi.org/10.1038/nclimate1745

Himeidan, Y. E., & Kweka, E. J. (2012). Malaria in East African highlands during the past 30 years: Impact of environmental changes. *Frontiers in Physiology*, 3 AUG(August), 1–11. https://doi.org/10.3389/fphys.2012.00315

Homan, T., Maire, N., Hiscox, A., Di Pasquale, A., Kiche, I., Onoka, K., Mweresa, C., Mukabana, W. R., Ross, A., Smith, T. A., & Takken, W. (2016). Spatially variable risk factors for malaria in a geographically heterogeneous landscape, western Kenya: an explorative study. *Malaria Journal*, 15(1), 1. https://doi.org/10.1186/s12936-015-1044-1

Hudson, D., Alves, O., Hendon, H. H., & Marshall, A. G. (2011). Bridging the gap between weather and seasonal forecasting: Intraseasonal forecasting for Australia. *Quarterly Journal of the Royal Meteorological Society*, 137(656), 673–689. https://doi.org/10.1002/qj.769

Huffman, G. J., Adler, R. F., Bolvin, D. T., & Gu, G. (2009). Improving the global precipitation record: GPCP Version 2.1. *Geophysical Research Letters*, *36*(17), L17808. https://doi.org/10.1029/2009GL040000

Indeje, M., Semazzi, F. H. M., & Ogallo, L. J. (2000). ENSO signals in East African rainfall seasons. *International Journal of Climatology*, 20(1), 19–46. https://doi.org/10.1002/(SICI)1097-0088(200001)20:1<19::AID-JOC449>3.0.CO;2-0

IPCC (2001). Climate Change: Synthesis Report. *Intergovernmental Panel on Climate Change*. Cambridge University Press, New York, NY, USA; Cambridge, UK, 2001

IPCC (2018). Annex I: Glossary [Matthews, J.B.R. (ed.)]. In: *Global Warming of 1.5°C. An IPCC Special Report on the impacts of global warming of 1.5°C above pre-industrial levels and related global greenhouse gas emission pathways, in the context of strengthening the global response to the threat of climate change, sustainable development, and efforts to eradicate poverty* [Masson-Delmotte, V., P. Zhai, H.-O. Pörtner, D. Roberts, J. Skea, P.R. Shukla, A. Pirani, W. Moufouma-Okia, C. Péan, R. Pidcock, S. Connors, J.B.R. Matthews, Y. Chen, X. Zhou, M.I. Gomis, E. Lonnoy, T. Maycock, M. Tignor, and T. Waterfield (eds.)]. In Press

Jackson, B., Nicholson, S. E., & Klotter, D. (2009). Mesoscale Convective Systems over Western Equatorial Africa and Their Relationship to Large-Scale Circulation. *Monthly Weather Review*, 137(4), 1272–1294. https://doi.org/10.1175/2008MWR2525.1

Jiang, Z., Li, W., Xu, J., & Li, L. (2015). Extreme precipitation indices over China in CMIP5 models. Part I: Model evaluation. *Journal of Climate*, 28(21), 8603–8619. https://doi.org/10.1175/JCLI-D-15-0099.1

Jin, F.-F., Boucharel, J., & Lin, I.-I. (2014). Eastern Pacific tropical cyclones intensified by El Niño delivery of subsurface ocean heat. *Nature*, 516(7529), 82–85. https://doi.org/10.1038/nature13958

Jin, Fei-Fei, Kim, S. T., & Bejarano, L. (2006). A coupled-stability index for ENSO. *Geophysical Research Letters*, 33(23), L23708. https://doi.org/10.1029/2006GL027221

Jones, G. S., Stott, P. A., & Christidis, N. (2013). Attribution of observed historical near-surface temperature variations to anthropogenic and natural causes using CMIP5 simulations. *Journal of Geophysical Research: Atmospheres*, 118(10), 4001–4024. https://doi.org/10.1002/jgrd.50239

Karimi, F., 2016. Mohawk the lion shot dead in Kenya after attacking man. *CNN*, 03 April

Karungu, S., Atoni, E., Ogalo, J., Mwaliko, C., Agwanda, B., Yuan, Z., & Hu, X. (2019). Mosquitoes of etiological concern in Kenya and possible control strategies. *Insects*, 10(6), 1–23. https://doi.org/10.3390/insects10060173

Kelly-Hope, L. A., Hemingway, J., & McKenzie, F. E. (2009). Environmental factors associated with the malaria vectors Anopheles gambiae and Anopheles funestus in Kenya. *Malaria Journal*, 8(1), 268. https://doi.org/10.1186/1475-2875-8-268

Kiboro, L.M. & Kiboro, C.N. (2015). Impact of land use changes on wildlife population in Nairobi National Park and Kitengela dispersal areas in Kenya. *International Journal of Science and Research (IJSR)* , pp. 2319-7064

Kiladis, G. N., von Storch, H., & Loon, H. (1989). Origin of the South Pacific Convergence Zone. *Journal of Climate*, 2(10), 1185–1195. https://doi.org/10.1175/1520-0442(1989)002<1185:OOTSPC>2.0.CO;2

Kilavi, M., MacLeod, D., Ambani, M., Robbins, J., Dankers, R., Graham, R., Helen, T., Salih, A. A. M., & Todd, M. C. (2018). Extreme rainfall and flooding over Central Kenya Including Nairobi City during the long-rains season 2018: Causes, predictability, and potential for early warning and actions. *Atmosphere*, 9(12). https://doi.org/10.3390/atmos9120472

Kim, J., Waliser, D. E., Mattmann, C. A., Goodale, C. E., Hart, A. F., Zimdars, P. A., Crichton, D. J., Jones, C., Nikulin, G., Hewitson, B., Jack, C., Lennard, C., & Favre, A. (2014). Evaluation of the CORDEX-Africa multi-RCM hindcast: systematic model errors. *Climate Dynamics*, 42(5–6), 1189–1202. https://doi.org/10.1007/s00382-013-1751-7

Kiros, G., Shetty, A., & Nandagiri, L. (2017). Extreme rainfall signatures under changing climate in semi-arid northern highlands of Ethiopia. *Cogent Geoscience*, 3(1), 1–20. https://doi.org/10.1080/23312041.2017.1353719

Kisembe, J., Dosio, A., Lennard, C., Sabiiti, G., Nimusiima, A., & Favre, A. (2018). Evaluation of rainfall simulations over Uganda in CORDEX regional climate models. *Theoretical and Applied Climatology*, 1995, 1–18. https://doi.org/10.1007/s00704-018-2643-x

KNMI (2017). KNMI CORDEX data for Africa (AFR-44) based on RACMO22T model simulations. *World Data Center for Climate (WDCC) at DKRZ*. https://bit.ly/3bo2bpP

Knox, J., Hess, T., Daccache, A., & Wheeler, T. (2012). Climate change impacts on crop productivity in Africa and South Asia. *Environmental Research Letters*, 7(3), 034032. https://doi.org/10.1088/1748-9326/7/3/034032

Kongsager, R. (2018). Linking Climate Change Adaptation and Mitigation: A Review with Evidence from the Land-Use Sectors. *Land*, 7(4), 158. https://doi.org/10.3390/land7040158

Kutatoi, S.K. & Waweru, A. (2018). The causes of human and wildlife conflict within Kajiado south sub county. *Journal of Conflict Management*, pp. 23-33

Landman, W. A., & Beraki, A. (2012). Multi-model forecast skill for mid-summer rainfall over southern Africa. *International Journal of Climatology*, 32(2), 303–314. https://doi.org/10.1002/joc.2273

Lashkari, H., Mohammadi, Z., & Keikhosravi, G. (2017). Annual Fluctuations and Displacements of Inter Tropical Convergence Zone (ITCZ) within the Range of Atlantic Ocean-India. *Open Journal of Ecology*, 07(01), 12–33. https://doi.org/10.4236/oje.2017.71002

Latif, M., Dommenget, D., Dima, M., & Grötzner, A. (1999). The Role of Indian Ocean Sea Surface Temperature in Forcing East African Rainfall Anomalies during December–January 1997/98. *Journal of Climate*, 12(12), 3497–3504. https://doi.org/10.1175/1520-0442(1999)012<3497:TROIOS>2.0.CO;2

Lau, N.-C., Leetmaa, A., & Nath, M. J. (2008). Interactions between the Responses of North American Climate to El Niño–La Niña and to the Secular Warming Trend in the Indian–Western Pacific Oceans. *Journal of Climate*, 21(3), 476–494. https://doi.org/10.1175/2007JCLI1899.1

Lazenby, M. J., Todd, M. C., Chadwick, R., & Wang, Y. (2018). Future precipitation projections over central and Southern Africa and the adjacent Indian Ocean: What causes the changes and the uncertainty? *Journal of Climate*, 31(12), 4807–4826. https://doi.org/10.1175/JCLI-D-17-0311.1

Li, C., Chai, Y., Yang, L., & Li, H. (2016). Spatio-temporal distribution of flood disasters and analysis of influencing factors in Africa. *Natural Hazards*, 82(1), 721–731. https://doi.org/10.1007/s11069-016-2181-8

Luo, L., & Wood, E. F. (2006). Assessing the idealized predictability of precipitation and temperature in the NCEP Climate Forecast System. *Geophysical Research Letters*, 33(4), 2–5. https://doi.org/10.1029/2005GL025292

Lyon, B., & Dewitt, D. G. (2012). A recent and abrupt decline in the East African long rains. *Geophysical Research Letters*, 39(2), 1–5. https://doi.org/10.1029/2011GL050337

Maidment, R. I., Grimes, D., Black, E., Tarnavsky, E., Young, M., Greatrex, H., Allan, R. P., Stein, T., Nkonde, E., Senkunda, S., & Alcántara, E. M. U. (2017). A new, long-term daily satellite-based rainfall dataset for operational monitoring in Africa. *Scientific Data*, *4*(1), 170063. https://doi.org/10.1038/sdata.2017.63

Masih, I., Maskey, S., Mussá, F. E. F., & Trambauer, P. (2014). A review of droughts on the African continent: a geospatial and long-term perspective. *Hydrology and Earth System Sciences*, 18(9), 3635–3649. https://doi.org/10.5194/hess-18-3635-2014

McPhaden, M. J., Busalacchi, A. J., Cheney, R., Donguy, J.-R., Gage, K. S., Halpern, D., Ji, M., Julian, P., Meyers, G., Mitchum, G. T., Niiler, P. P., Picaut, J., Reynolds, R. W., Smith, N., & Takeuchi, K. (1998). The Tropical Ocean-Global Atmosphere observing system: A decade of progress. *Journal of Geophysical Research: Oceans*, 103(C7), 14169–14240. https://doi.org/10.1029/97JC02906

MEA (2005). Appendix D: Glossary. In: *Ecosystems and Human Well-being: Current States and Trends. Findings of the Condition and Trends Working Group* [Hassan, R., R. Scholes, and N. Ash (eds.)]. *Millennium Ecosystem Assessment (MEA)*. Island Press, Washington DC, USA, pp. 893–900

Menne, M. J., Durre, I., Vose, R. S., Gleason, B. E., & Houston, T. G. (2012). An Overview of the Global Historical Climatology Network-Daily Database. *Journal of Atmospheric and Oceanic Technology*, *29*(7), 897–910. https://doi.org/10.1175/JTECH-D-11-00103.1

Met Office Hadley Centre (MOHC) (2017). MOHC CORDEX data for Africa (AFR-44) based on HadGEM3-RA model simulations. *World Data Center for Climate (WDCC) at DKRZ*. https://bit.ly/2yDbyoq

Met Office Hadley Centre (MOHC) (2017). MOHC CORDEX data for Africa (AFR-44) based on HadGEM3-RA model simulations. *World Data Center for Climate (WDCC) at DKRZ*. https://bit.ly/2yDbyoq

Metelmann, S., Caminade, C., Jones, A. E., Medlock, J. M., Baylis, M., & Morse, A. P. (2019). The UK's suitability for Aedes albopictus in current and future climates. *Journal of the Royal Society Interface*, 16(152). https://doi.org/10.1098/rsif.2018.0761

Miles, M.B. & Huberman, A.M. (1994). Qualitative data analysis: An expanded sourcebook (2nd ed.). *Thousand Oaks: Sage*.

Mohammadkhani, M., Khanjani, N., Bakhtiari, B., & Sheikhzadeh, K. (2016). The relation between climatic factors and malaria incidence in Kerman, South East of Iran. *Parasite Epidemiology and Control*, 1(3), 205–210. https://doi.org/10.1016/j.parepi.2016.06.001

Morton, J. F. (2007). The impact of climate change on smallholder and subsistence agriculture. *Proceedings of the National Academy of Sciences of the United States of America*, 104(50), 19680–19685. https://doi.org/10.1073/pnas.0701855104

Moss, R. H., Edmonds, J. A., Hibbard, K. A., Manning, M. R., Rose, S. K., van Vuuren, D. P., Carter, T. R., Emori, S., Kainuma, M., Kram, T., Meehl, G. A., Mitchell, J. F. B., Nakicenovic, N., Riahi, K., Smith, S. J., Stouffer, R. J., Thomson, A. M., Weyant, J. P., & Wilbanks, T. J. (2010). The next generation of scenarios for climate change research and assessment. *Nature*, 463(7282), 747–756. https://doi.org/10.1038/nature08823

Mpelasoka, F., Awange, J. L., & Zerihun, A. (2018). Influence of coupled ocean-atmosphere phenomena on the Greater Horn of Africa droughts and their implications. *Science of The Total Environment*, 610–611, 691–702. https://doi.org/10.1016/j.scitotenv.2017.08.109

Mubiru, D. N., Radeny, M., Kyazze, F. B., Zziwa, A., Lwasa, J., Kinyangi, J., & Mungai, C. (2018). Climate trends, risks and coping strategies in smallholder farming systems in Uganda. *Climate Risk Management*, 22(October 2016), 4–21. https://doi.org/10.1016/j.crm.2018.08.004

Muhati, G. L., Olago, D., & Olaka, L. (2018). Past and projected rainfall and temperature trends in a sub-humid Montane Forest in Northern Kenya based on the CMIP5 model ensemble. *Global Ecology and Conservation*, 16, e00469. https://doi.org/10.1016/j.gecco.2018.e00469

Muthoni, F. K., Odongo, V. O., Ochieng, J., Mugalavai, E. M., Mourice, S. K., Hoesche-Zeledon, I., Mwila, M., & Bekunda, M. (2019). Long-term spatial-temporal trends and variability of rainfall over Eastern and Southern Africa. *Theoretical and Applied Climatology*, 137(3–4), 1869–1882. https://doi.org/10.1007/s00704-018-2712-1

Mwaniki, M. W., Agutu, N. O., Mbaka, J. G., Ngigi, T. G., & Waithaka, E. H. (2015). Landslide scar/soil erodibility mapping using Landsat TM/ETM+ bands 7 and 3 Normalised Difference Index: A case study of central region of Kenya. *Applied Geography*, 64, 108–120. https://doi.org/10.1016/j.apgeog.2015.09.009

Mwaniki, M. W., Agutu, N. O., Mbaka, J. G., Ngigi, T. G., & Waithaka, E. H. (2015). Landslide scar/soil erodibility mapping using Landsat TM/ETM+ bands 7 and 3

Normalised Difference Index: A case study of central region of Kenya. *Applied Geography*, *64*, 108–120. https://doi.org/10.1016/j.apgeog.2015.09.009
Mweya, C. N., Kimera, S. I., Stanley, G., Misinzo, G., & Mboera, L. E. G. (2016). Climate Change Influences Potential Distribution of Infected Aedes aegypti Co-Occurrence with Dengue Epidemics Risk Areas in Tanzania. *PLOS ONE*, 11(9), e0162649. https://doi.org/10.1371/journal.pone.0162649
Mysiak, J., Surminski, S., Thieken, A., Mechler, R., & Aerts, J. (2016). Brief communication: Sendai framework for disaster risk reduction – success or warning sign for Paris? *Natural Hazards and Earth System Sciences*, 16(10), 2189–2193. https://doi.org/10.5194/nhess-16-2189-2016
Naab, F. Z., Abubakari, Z., & Ahmed, A. (2019). The role of climate services in agricultural productivity in Ghana: The perspectives of farmers and institutions. *Climate Services*, 13, 24–32. https://doi.org/10.1016/j.cliser.2019.01.007
Nairobi City County (2018). County Integrated Development Plan (CIDP) 2018 – 2022. *Nairobi City County*. https://bit.ly/2ZWCfQe
Nakakana, U. N., Mohammed, I. A., Onankpa, B. O., Jega, R. M., & Jiya, N. M. (2020). A validation of the Malaria Atlas Project maps and development of a new map of malaria transmission in Sokoto, Nigeria: a cross-sectional study using geographic information systems. *Malaria Journal*, *19*(1), 149. https://doi.org/10.1186/s12936-020-03214-8
National Research Council (2001) A Climate Services Vision: First Steps Toward the Future. *Washington, DC: The National Academies Press*. https://doi.org/10.17226/10198
Ngotho, W. & Kangu, M. (2016). Influence of land tenure system on social economic development of households in Kajiado North District. *Journal of Poverty, Investment and Development,* 1(1), pp. 1-15
Nicholson, S. E. (2014). A detailed look at the recent drought situation in the Greater Horn of Africa. *Journal of Arid Environments*, 103, 71–79. https://doi.org/10.1016/j.jaridenv.2013.12.003
Nicholson, S. E. (2017). Climate and climatic variability of rainfall over eastern Africa. *Reviews of Geophysics*, 55(3), 590–635. https://doi.org/10.1002/2016RG000544
Nicholson, S. E. (2018). The ITCZ and the Seasonal Cycle over Equatorial Africa. *Bulletin of the American Meteorological Society*, 99(2), 337–348. https://doi.org/10.1175/BAMS-D-16-0287.1
Nicholson, S. E., & Kim, J. (1997). The relationship of the el nino oscillation to african rainfall. *International Journal of Climatology*, 17, 117–135. https://doi.org/10.1002/(SICI)1097-0088(199702)17:2<117::AID-JOC84>3.0.CO;2-O
Nicholson, S. E., Funk, C., & Fink, A. H. (2018). Rainfall over the African continent from the 19th through the 21st century. *Global and Planetary Change*, 165, 114–127. https://doi.org/10.1016/j.gloplacha.2017.12.014
Nikulin, G., Jones, C., Giorgi, F., Asrar, G., Büchner, M., Cerezo-Mota, R., Christensen, O. B., Déqué, M., Fernandez, J., Hänsler, A., van Meijgaard, E., Samuelsson, P., Sylla, M. B., & Sushama, L. (2012). Precipitation Climatology in

an Ensemble of CORDEX-Africa Regional Climate Simulations. *Journal of Climate*, 25(18), 6057–6078. https://doi.org/10.1175/JCLI-D-11-00375.1

Nikulin, G., Lennard, C., Dosio, A., Kjellström, E., Chen, Y., Hänsler, A., Kupiainen, M., Laprise, R., Mariotti, L., Maule, C. F., van Meijgaard, E., Panitz, H.-J., Scinocca, J. F., & Somot, S. (2018). The effects of 1.5 and 2 degrees of global warming on Africa in the CORDEX ensemble. *Environmental Research Letters*, 13(6), 065003. https://doi.org/10.1088/1748-9326/aab1b1

Nkedianye, D. (2004). Testing the attitudinal impact of a conservation tool outside a protected area: the case of the Kitengela Wildlife Conservation Lease Programme for Nairobi National Park. *University of Nairobi*. Nairobi

Nkedianye, D. (2005). Payment for biodiversity gains and challenges from Kitengela. *International Livestock Research Institute (ILRI).* Nairobi, Kenya

Nkumama, I. N., O'Meara, W. P., & Osier, F. H. A. (2017). Changes in Malaria Epidemiology in Africa and New Challenges for Elimination. *Trends in Parasitology*, 33(2), 128–140. https://doi.org/10.1016/j.pt.2016.11.006

Nsoesie, E. O., Kraemer, M. U. G., Golding, N., Pigott, D. M., Brady, O. J., Moyes, C. L., Johansson, M. A., Gething, P. W., Velayudhan, R., Khan, K., Hay, S. I., & Brownstein, J. S. (2016). Global distribution and environmental suitability for chikungunya virus, 1952 to 2015. *Eurosurveillance*, 21(20), 1–12. https://doi.org/10.2807/1560-7917.ES.2016.21.20.30234

Ochieng, J., Kirimi, L., & Mathenge, M. (2016). Effects of climate variability and change on agricultural production: The case of small scale farmers in Kenya. *NJAS - Wageningen Journal of Life Sciences*, 77(2016), 71–78. https://doi.org/10.1016/j.njas.2016.03.005

Ogutu, G. E. O., Franssen, W. H. P., Supit, I., Omondi, P., & Hutjes, R. W. A. (2018). Probabilistic maize yield prediction over East Africa using dynamic ensemble seasonal climate forecasts. *Agricultural and Forest Meteorology*, 250–251, 243–261. https://doi.org/10.1016/j.agrformet.2017.12.256

Ogutu, J. O., Piepho, H.-P., Said, M. Y., Ojwang, G. O., Njino, L. W., Kifugo, S. C., & Wargute, P. W. (2016). Extreme Wildlife Declines and Concurrent Increase in Livestock Numbers in Kenya: What Are the Causes? *PLOS ONE*, 11(9), e0163249. https://doi.org/10.1371/journal.pone.0163249

Ojwang, L., Rosendo, S., Celliers, L., Obura, D., Muiti, A., Kamula, J., & Mwangi, M. (2017). Assessment of Coastal Governance for Climate Change Adaptation in Kenya. *Earth's Future*, 5(11), 1119–1132. https://doi.org/10.1002/2017EF000595

Olima, W.H.A. (2011). The Dynamics and Implications of Sustaining Urban Spatial Segregation in Kenya: Experiences from Nairobi Metropolis. Cambridge, MA, USA, s.n.

Omondi, P., Awange, J. L., Ogallo, L. A., Okoola, R. A., & Forootan, E. (2012). Decadal rainfall variability modes in observed rainfall records over East Africa and their relations to historical sea surface temperature changes. *Journal of Hydrology*, 464–465, 140–156. https://doi.org/10.1016/j.jhydrol.2012.07.003

Oppewal, H. (2010). Causal Research. In *Wiley International Encyclopedia of Marketing. John Wiley & Sons, Ltd*. https://doi.org/10.1002/9781444316568.wiem02001

Osima, S., Kondowe, A. L., Indasi, V. S., Zaroug, M., Lennard, C., Endris, H. S., Gudoshava, M., Misiani, H. O., Otieno, G., Anyah, R. O., Nimusiima, A., Ogwang, B. A., Mwangi, E., Jain, S., Nikulin, G., & Dosio, A. (2018). Projected climate over the Greater Horn of Africa under 1.5 °c and 2 °c global warming. *Environmental Research Letters*, 13(6). https://doi.org/10.1088/1748-9326/aaba1b

Owiti, Zablone, Ogallo, L. A. (2008). Linkages between the Indian Ocean Dipole and East African Seasonal Rainfall Anomalies. 2(April), 3–17.

Pal, J. S., Giorgi, F., Bi, X., Elguindi, N., Solmon, F., Gao, X., Rauscher, S. A., Francisco, R., Zakey, A., Winter, J., Ashfaq, M., Syed, F. S., Bell, J. L., Diffenbaugh, N. S., Karmacharya, J., Konaré, A., Martinez, D., da Rocha, R. P., Sloan, L. C., & Steiner, A. L. (2007). Regional Climate Modelling for the Developing World: The ICTP RegCM3 and RegCNET. *Bulletin of the American Meteorological Society*, 88(9), 1395–1410. https://doi.org/10.1175/BAMS-88-9-1395

Panitz, H-J, Schubert-Frisius, M., & Dosio, A. (2015). CORDEX simulations (evaluation, historical, rcp85, and rcp45) on a ca. 50 km grid over Africa based on CCLM4-8-17 forced by MPI-ESM-LR, EC-EARTH, CNRM-CM5 and HadGEM2-ES. *World Data Center for Climate (WDCC) at DKRZ*. https://doi.org/10.1594/WDCC/CXAF44CLCL

Peterson, A. T. (2009). Shifting suitability for malaria vectors across Africa with warming climates. *BMC Infectious Diseases*, 9, 1–6. https://doi.org/10.1186/1471-2334-9-59

Peterson, T. C., Folland, C., Gruza, G., Hogg, W., & Plummer, N. (2001). *Report on the Activities of the Working Group on Climate Change Detection and Related Rapporteurs*. *March*.

Philippon, N., Camberlin, P., & Fauchereau, N. (2002). Empirical predictability study of October–December East African rainfall. Quarterly Journal of the Royal Meteorological Society, 128(585), 2239–2256. https://doi.org/10.1256/qj.01.190

Power, S. B., & Callaghan, J. (2016). Variability in Severe Coastal Flooding, Associated Storms, and Death Tolls in Southeastern Australia since the Mid–Nineteenth Century. *Journal of Applied Meteorology and Climatology*, 55(5), 1139–1149. https://doi.org/10.1175/JAMC-D-15-0146.1

Reid, J. (2017). There is no significant trend in global average temperature. Energy & Environment, 28(3), 302–315. https://doi.org/10.1177/0958305X16686447

Ren, Z., Wang, D., Ma, A., Hwang, J., Bennett, A., Sturrock, H. J. W., Fan, J., Zhang, W., Yang, D., Feng, X., Xia, Z., Zhou, X.-N., & Wang, J. (2016). Predicting malaria vector distribution under climate change scenarios in China: Challenges for malaria elimination. *Scientific Reports*, 6(1), 20604. https://doi.org/10.1038/srep20604

Rockström, J., Karlberg, L., Wani, S. P., Barron, J., Hatibu, N., Oweis, T., Bruggeman, A., Farahani, J., & Qiang, Z. (2010). Managing water in rainfed agriculture—The need for a paradigm shift. *Agricultural Water Management*, 97(4), 543–550. https://doi.org/10.1016/j.agwat.2009.09.009

Rodriguez, L. C., Henson, D., Herrero, M., Nkedianye, D., & Reid, R. (2012). Private farmers' compensation and viability of protected areas: the case of Nairobi

National Park and Kitengela dispersal corridor. *International Journal of Sustainable Development & World Ecology*, *19*(1), 34–43. https://doi.org/10.1080/13504509.2011.587549

Rowell, D. P., Booth, B. B. B., Nicholson, S. E., & Good, P. (2015). Reconciling Past and Future Rainfall Trends over East Africa. *Journal of Climate*, 28(24), 9768–9788. https://doi.org/10.1175/JCLI-D-15-0140.1

Roy, D. P., Wulder, M. A., Loveland, T. R., C.E., W., Allen, R. G., Anderson, M. C., Helder, D., Irons, J. R., Johnson, D. M., Kennedy, R., Scambos, T. A., Schaaf, C. B., Schott, J. R., Sheng, Y., Vermote, E. F., Belward, A. S., Bindschadler, R., Cohen, W. B., Gao, F., … Zhu, Z. (2014). Landsat-8: Science and product vision for terrestrial global change research. *Remote Sensing of Environment*, 145, 154–172. https://doi.org/10.1016/j.rse.2014.02.001

Said, M. Y., Ogutu, J. O., Kifugo, S. C., Makui, O., Reid, R. S., & de Leeuw, J. (2016). Effects of extreme land fragmentation on wildlife and livestock population abundance and distribution. *Journal for Nature Conservation*, 34, 151–164. https://doi.org/10.1016/j.jnc.2016.10.005

Saji, N. H., Goswami, B. N., Vinayachandran, P. N., & Yamagata, T. (1999). A dipole mode in the tropical Indian Ocean. *Nature*, 401(6751), 360–363. https://doi.org/10.1038/43854

Salami, A., Kamara, A. B., & Brixiova, Z. (2010). Smallholder Agriculture in East Africa : Trends , Constraints and Opportunities Smallholder Agriculture in East Africa : Trends , Constraints and Opportunities Adeleke Salami , Abdul B . Kamara and. *African Development Bank Group Working Paper No. 105*, January.

Santoso, A., Mcphaden, M. J., & Cai, W. (2017). The Defining Characteristics of ENSO Extremes and the Strong 2015/2016 El Niño. *Reviews of Geophysics*, 55(4), 1079–1129. https://doi.org/10.1002/2017RG000560

Schneider, T., Bischoff, T., & Haug, G. H. (2014). Migrations and dynamics of the intertropical convergence zone. *Nature*, 513(7516), 45–53. https://doi.org/10.1038/nature13636

Schreck, C. J., & Semazzi, F. H. M. (2004). Variability of the recent climate of eastern Africa. *International Journal of Climatology*, 24(6), 681–701. https://doi.org/10.1002/joc.1019

Schulman, L. L. (1973). On the summer hemisphere Hadley cell. *Quarterly Journal of the Royal Meteorological Society*, 99(419), 197–201. https://doi.org/10.1002/qj.49709941916

Scoccimarro, E., Gualdi, S., Bellucci, A., Zampieri, M., & Navarra, A. (2013). Heavy precipitation events in a warmer climate: Results from CMIP5 models. Journal of Climate, 26(20), 7902–7911. https://doi.org/10.1175/JCLI-D-12-00850.1

Segele, Z. T., Lamb, P. J., & Leslie, L. M. (2009). Seasonal-to-Interannual Variability of Ethiopia/Horn of Africa Monsoon. Part I: Associations of Wavelet-Filtered Large-Scale Atmospheric Circulation and Global Sea Surface Temperature. *Journal of Climate*, 22(12), 3396–3421. https://doi.org/10.1175/2008JCLI2859.1

Semakula, H. M., Song, G., Achuu, S. P., Shen, M., Chen, J., Mukwaya, P. I., Oulu, M., Mwendwa, P. M., Abalo, J., & Zhang, S. (2017). Prediction of future malaria

hotspots under climate change in sub-Saharan Africa. *Climatic Change*, 143(3–4), 415–428. https://doi.org/10.1007/s10584-017-1996-y

Seno, S. K., & Shaw, W. W. (2002). Land Tenure Policies, Maasai Traditions, and Wildlife Conservation in Kenya. *Society & Natural Resources*, 15(1), 79–88. https://doi.org/10.1080/089419202317174039

Shiferaw, A., Tadesse, T., Rowe, C., & Oglesby, R. (2018). Precipitation extremes in dynamically downscaled climate scenarios over the greater horn of Africa. *Atmosphere*, 9(3), 1–28. https://doi.org/10.3390/atmos9030112

Shongwe, M. E., van Oldenborgh, G. J., van den Hurk, B., & van Aalst, M. (2011). Projected changes in mean and extreme precipitation in Africa under global warming. Part II: East Africa. *Journal of Climate*, 24(14), 3718–3733. https://doi.org/10.1175/2010JCLI2883.1

Shonk, J. K. P., Guilyardi, E., Toniazzo, T., Woolnough, S. J., & Stockdale, T. (2018). Identifying causes of Western Pacific ITCZ drift in ECMWF System 4 hindcasts. *Climate Dynamics*, 50(3–4), 939–954. https://doi.org/10.1007/s00382-017-3650-9

Shunlin Liang, Hongliang Fang, Morisette, J. T., Mingzhen Chen, Shuey, C. J., Walthall, C. L., & Daughtry, C. S. T. (2002). Atmospheric correction of Landsat ETM+ land surface imagery. II. Validation and applications. *IEEE Transactions on Geoscience and Remote Sensing*, 40(12), 2736–2746. https://doi.org/10.1109/TGRS.2002.807579

Sillmann, J., Kharin, V. V., Zwiers, F. W., Zhang, X., & Bronaugh, D. (2013). Climate extremes indices in the CMIP5 multimodel ensemble: Part 2. Future climate projections. *Journal of Geophysical Research: Atmospheres*, *118*(6), 2473–2493. https://doi.org/10.1002/jgrd.50188

Silungwe, F., Graef, F., Bellingrath-Kimura, S., Tumbo, S., Kahimba, F., & Lana, M. (2019). Analysis of Intra and Interseasonal Rainfall Variability and Its Effects on Pearl Millet Yield in a Semiarid Agroclimate: Significance of Scattered Fields and Tied Ridges. *Water*, 11(3), 578. https://doi.org/10.3390/w11030578

Slingo, J., Spencer, H., Hoskins, B., Berrisford, P., & Black, E. (2005). The meteorology of the Western Indian Ocean, and the influence of the East African Highlands. *Philosophical Transactions of the Royal Society A: Mathematical, Physical and Engineering Sciences*, 363(1826), 25–42. https://doi.org/10.1098/rsta.2004.1473

SMHI (2017). cordex AFR-44 SMHI RCA4. *World Data Center for Climate (WDCC) at DKRZ*. https://bit.ly/2YRklha

Souverijns, N., Thiery, W., Demuzere, M., & Lipzig, N. P. M. Van. (2016b). Drivers of future changes in East African precipitation. *Environmental Research Letters*, 11(11), 114011. https://doi.org/10.1088/1748-9326/11/11/114011

Stevenson, S., Fox-Kemper, B., Jochum, M., Neale, R., Deser, C., & Meehl, G. (2012). Will There Be a Significant Change to El Niño in the Twenty-First Century? *Journal of Climate*, 25(6), 2129–2145. https://doi.org/10.1175/JCLI-D-11-00252.1

Tàbara, J., Jäger, J., Mangalagiu, D., & Grasso, M. (2019). Defining transformative climate science to address high-end climate change. *Regional Environmental Change*, 19(3), 807–818. https://doi.org/10.1007/s10113-018-1288-8

Tall, A., Coulibaly, J. Y., & Diop, M. (2018). Do climate services make a difference? A review of evaluation methodologies and practices to assess the value of climate information services for farmers: Implications for Africa. *Climate Services*, 11, 1–12. https://doi.org/10.1016/j.cliser.2018.06.001

Taylor, K. E. (2001). Summarizing multiple aspects of model performance in a single diagram. *Journal of Geophysical Research: Atmospheres*, 106(D7), 7183–7192. https://doi.org/10.1029/2000JD900719

Tierney, J. E., Ummenhofer, C. C., & DeMenocal, P. B. (2015). Past and future rainfall in the Horn of Africa. *Science Advances*, 1(9), e1500682. https://doi.org/10.1126/sciadv.1500682

Tjaden, N. B., Suk, J. E., Fischer, D., Thomas, S. M., Beierkuhnlein, C., & Semenza, J. C. (2017). Modelling the effects of global climate change on Chikungunya transmission in the 21st century. *Scientific Reports*, 7(1), 3813. https://doi.org/10.1038/s41598-017-03566-3

Uhe, P., Philip, S., Kew, S., Shah, K., Kimutai, J., Mwangi, E., van Oldenborgh, G. J., Singh, R., Arrighi, J., Jjemba, E., Cullen, H., & Otto, F. (2018). Attributing drivers of the 2016 Kenyan drought. *International Journal of Climatology*, 38, e554–e568. https://doi.org/10.1002/joc.5389

United Nations (UN) (1992). United Nations Framework Convention on Climate Change. *United Nations*. http://bit.ly/2tFKsKK

Van Loon, A. F. (2015). Hydrological drought explained. *Wiley Interdisciplinary Reviews: Water*, 2(4), 359–392. https://doi.org/10.1002/wat2.1085

Vaughan, C., Hansen, J., Roudier, P., Watkiss, P., & Carr, E. (2019). Evaluating agricultural weather and climate services in Africa: Evidence, methods, and a learning agenda. *Wiley Interdisciplinary Reviews: Climate Change*, e586. https://doi.org/10.1002/wcc.586

Vigaud, N., Lyon, B., & Giannini, A. (2017). Sub-seasonal teleconnections between convection over the Indian Ocean, the East African long rains and tropical Pacific surface temperatures. *International Journal of Climatology*, 37(3), 1167–1180. https://doi.org/10.1002/joc.4765

Vitousek, P. M. (1997). Human Domination of Earth's Ecosystems. *Science*, 277(5325), 494–499. https://doi.org/10.1126/science.277.5325.494

Vizy, E. K., & Cook, K. H. (2012). Mid-twenty-first-century changes in extreme events over northern and tropical Africa. *Journal of Climate*, 25(17), 5748–5767. https://doi.org/10.1175/JCLI-D-11-00693.1

Vrieling, A., de Leeuw, J., & Said, M. (2013). Length of Growing Period over Africa: Variability and Trends from 30 Years of NDVI Time Series. *Remote Sensing*, 5(2), 982–1000. https://doi.org/10.3390/rs5020982

Wainwright, C. M., Marsham, J. H., Keane, R. J., Rowell, D. P., Finney, D. L., Black, E., & Allan, R. P. (2019). 'Eastern African Paradox' rainfall decline due to shorter not less intense Long Rains. *Npj Climate and Atmospheric Science*, 2(1), 1–9. https://doi.org/10.1038/s41612-019-0091-7

Waliser, D. E., & Jiang, X. (2015). TROPICAL METEOROLOGY AND CLIMATE | Intertropical Convergence Zone. In *Encyclopedia of Atmospheric Sciences (pp. 121–131). Elsevier*. https://doi.org/10.1016/B978-0-12-382225-3.00417-5

Weiss, D. J., Lucas, T. C. D., Nguyen, M., Nandi, A. K., Bisanzio, D., Battle, K. E., Cameron, E., Twohig, K. A., Pfeffer, D. A., Rozier, J. A., Gibson, H. S., Rao, P. C., Casey, D., Bertozzi-Villa, A., Collins, E. L., Dalrymple, U., Gray, N., Harris, J. R., Howes, R. E., … Gething, P. W. (2019). Mapping the global prevalence, incidence, and mortality of Plasmodium falciparum, 2000–17: a spatial and temporal modelling study. *The Lancet*, *394*(10195), 322–331. https://doi.org/10.1016/S0140-6736(19)31097-9

Wenhaji Ndomeni, C., Cattani, E., Merino, A., & Levizzani, V. (2018). An observational study of the variability of East African rainfall with respect to sea surface temperature and soil moisture. *Quarterly Journal of the Royal Meteorological Society*, 144(S1), 384–404. https://doi.org/10.1002/qj.3255

Winger, K. (2017). UQAM CORDEX data for Africa (AFR-44) based on CRCM5 model simulations. *World Data Center for Climate (WDCC) at DKRZ*. https://doi.org/10.1594/WDCC/CXAF44UQAMCR

World Meteorological Organization (WMO) (2020). Frequently asked questions (FAQs). *World Meteorological Organization*. http://bit.ly/38uOWCF

Wu, Z., Huang, N. E., Long, S. R., & Peng, C.-K. (2007). On the trend, detrending, and variability of nonlinear and nonstationary time series. *Proceedings of the National Academy of Sciences*, 104(38), 14889–14894. https://doi.org/10.1073/pnas.0701020104

Yang, W., Seager, R., Cane, M. A., & Lyon, B. (2014). The East African Long Rains in Observations and Models. *Journal of Climate*, 27(19), 7185–7202. https://doi.org/10.1175/JCLI-D-13-00447.1

Yang, W., Seager, R., Cane, M. A., & Lyon, B. (2015). The Annual Cycle of East African Precipitation. *Journal of Climate*, 28(6), 2385–2404. https://doi.org/10.1175/JCLI-D-14-00484.1

Zelle, H., Jan van Oldenborgh, G., Burgers, G., & Dijkstra, H. (2005). El Niño and Greenhouse Warming: Results from Ensemble Simulations with the NCAR CCSM. *Journal of Climate*, 18(22), 4669–4683. https://doi.org/10.1175/JCLI3574.1

Zheng, X.-T., Xie, S.-P., Du, Y., Liu, L., Huang, G., & Liu, Q. (2013). Indian Ocean Dipole Response to Global Warming in the CMIP5 Multimodel Ensemble. *Journal of Climate*, 26(16), 6067–6080. https://doi.org/10.1175/JCLI-D-12-00638.1

Zhou, B., Wen, Q. H., Xu, Y., Song, L., & Zhang, X. (2014). Projected Changes in Temperature and Precipitation Extremes in China by the CMIP5 Multimodel Ensembles. *Journal of Climate*, *27*(17), 6591–6611. https://doi.org/10.1175/JCLI-D-13-00761.1

Zhou, R.-G., Hu, W., Fan, P., & Ian, H. (2017). Quantum realization of the bilinear interpolation method for NEQR. *Scientific Reports*, *7*(1), 2511. https://doi.org/10.1038/s41598-017-02575-6

Ziervogel, G., New, M., Archer van Garderen, E., Midgley, G., Taylor, A., Hamann, R., Stuart-Hill, S., Myers, J., & Warburton, M. (2014). Climate change impacts and adaptation in South Africa. *Wiley Interdisciplinary Reviews: Climate Change*, 5(5), 605–620. https://doi.org/10.1002/wcc.295

APPENDICES

7.1 ERAINT-driven Model Ranking Based on Inter-annual Variability Scores (IVS), for TAMSAT3 Data

RCM	IVS								Ranking based on PCC							
	PR					CDD	CWD	SDII	PR					CDD	CWD	SDII
	ANN	MAM	OND	90p	99p				ANN	MAM	OND	90p	99p			
ICTP	0.004	0.048	0.139	0.594	0.016	31.397	0.458	0.989	2	1	4	2	1	7	3	3
MPI	2.118	0.411	1.698	3.890	0.622	21.042	36.306	0.819	9	5	9	9	3	5	9	2
MOHC_HadGEM3_RA	0.148	0.128	0.015	0.743	1.354	32.176	0.946	1.553	3	4	2	3	5	8	5	4
MOHC_HadRM3p	0.421	0.091	0.035	1.053	2.073	26.772	0.795	2.033	4	3	3	4	6	6	4	5
HIRHAM5	1.045	1.250	0.841	1.153	2.548	17.809	2.841	4.155	7	8	7	5	7	3	8	7
RACMO22T	0.703	1.112	1.030	1.265	25.941	12.075	0.947	7.359	5	7	8	6	9	2	6	9
CLMcom	0.002	0.435	0.014	0.188	0.256	7.749	0.127	0.075	1	6	1	1	2	1	1	1
SMHI	1.871	0.082	0.784	2.600	1.190	19.487	1.051	3.638	8	2	6	8	4	4	7	6
Ensmean	0.746	3.387	0.212	2.190	2.737	43.782	0.215	5.453	6	9	5	7	8	9	2	8

7.2 ERAINT-driven Model Ranking Based on IVS, for CHIRPS Data

RCM	IVS								Ranking based on PCC							
	PR					CDD	CWD	SDII	PR					CDD	CWD	SDII
	ANN	MAM	OND	90p	99p				ANN	MAM	OND	90p	99p			
ICTP	0.004	0.041	0.141	0.332	0.008	0.836	2.124	1.305	2	4	4	2	1	3	5	3
MPI	2.118	0.045	1.690	2.965	0.315	1.801	17.302	1.103	9	5	9	9	2	5	9	2
MOHC_HadGEM3_RA	0.148	0.004	0.014	0.443	0.846	0.791	3.277	1.967	3	1	1	3	5	2	7	4
MOHC_HadRM3p	0.421	0.014	0.034	0.678	1.396	1.170	2.932	2.525	4	2	3	4	6	4	6	5
HIRHAM5	1.045	0.434	0.836	0.756	1.766	2.338	0.756	4.969	7	8	7	5	7	7	3	7
RACMO22T	0.703	0.360	1.024	0.844	20.530	3.949	3.279	8.634	5	7	8	6	9	8	8	9
CLMcom	0.002	0.053	0.015	0.061	0.536	6.504	1.187	0.165	1	6	2	1	3	9	4	1
SMHI	1.871	0.018	0.779	1.912	0.724	2.037	0.089	4.375	8	3	6	8	4	6	2	6
Ensmean	0.746	1.708	0.209	1.580	1.913	0.333	0.052	6.455	6	9	5	7	8	1	1	8

7.3 ERAINT-driven Model Ranking Based on Pearson Correlation Coefficients (PCCs), for TAMSAT3 Data

RCM	Pearson Correlation Coefficient (PCC)								Ranking based on PCC							
	PR					CDD	CWD	SDII	PR					CDD	CWD	SDII
	ANN	MAM	OND	90p	99p				ANN	MAM	OND	90p	99p			
ICTP	0.39	-0.21	0.74	0.33	0.21	0.08	0.11	0.24	8	9	7	8	8	8	6	5
MPI	0.53	0.20	0.71	0.43	0.35	0.37	0.03	0.33	5	8	8	6	5	5	7	4
MOHC_HadGEM3_RA	0.35	0.33	0.79	0.20	0.22	0.05	0.39	0.06	9	4	6	9	7	9	3	9
MOHC_HadRM3p	0.66	0.35	0.86	0.72	0.51	0.38	0.43	0.49	3	3	2	2	3	4	1	2
HIRHAM5	0.39	0.24	0.81	0.41	0.21	0.42	-0.02	0.16	7	7	5	7	9	3	8	8
RACMO22T	0.59	0.27	0.83	0.67	0.41	0.20	0.42	0.19	4	6	4	3	4	6	2	7
CLMcom	0.86	0.61	0.87	0.84	0.73	0.52	0.30	0.61	1	1	1	1	1	1	5	1
SMHI	0.49	0.32	0.66	0.47	0.34	0.10	-0.08	0.23	6	5	9	5	6	7	9	6
Ensmean	0.69	0.39	0.85	0.67	0.62	0.48	0.37	0.46	2	2	3	4	2	2	4	3

7.4 ERAINT-driven Model Ranking Based on PCCs, for CHIRPS Data

RCM	Pearson Correlation Coefficient (PCC)								Ranking based on PCC							
	PR					CDD	CWD	SDII	PR					CDD	CWD	SDII
	ANN	MAM	OND	90p	99p				ANN	MAM	OND	90p	99p			
ICTP	0.57	0.10	0.88	0.62	0.16	-0.06	0.28	0.27	6	6	7	6	8	8	6	8
MPI	0.53	0.09	0.79	0.41	0.31	0.52	0.03	0.36	7	7	8	8	6	2	9	7
MOHC_HadGEM3_RA	0.35	0.06	0.89	0.26	0.08	0.45	0.24	0.13	9	8	5	9	9	5	7	9
MOHC_HadRM3p	0.67	0.55	0.94	0.73	0.40	0.47	0.74	0.45	4	1	2	3	5	4	1	5
HIRHAM5	0.44	-0.02	0.89	0.46	0.27	0.58	0.24	0.42	8	9	6	7	7	1	8	6
RACMO22T	0.74	0.48	0.93	0.70	0.56	0.12	0.34	0.53	1	3	4	4	1	7	5	3
CLMcom	0.71	0.32	0.96	0.75	0.53	0.37	0.45	0.57	3	5	1	2	3	6	4	2
SMHI	0.66	0.41	0.76	0.69	0.43	-0.08	0.52	0.50	5	4	9	5	4	9	3	4
Ensmean	0.73	0.52	0.94	0.76	0.54	0.52	0.52	0.62	2	2	3	1	2	2	2	1

7.5 GCM-driven Model Ranking Based on IVS, for TAMSAT3 Data

RCM	IVS								Ranking based on IVS							
	PR					CDD	CWD	SDII	PR					CDD	CWD	SDII
	ANN	MAM	OND	90p	99p				ANN	MAM	OND	90p	99p			
CCLM4 (r1i1p1)-MOHC-HadGEM2-ES-HadGEM2-ES	0.0	0.9	0.3	4.2	0.0	0.1	0.4	0.6	2	23	9	21	2	11	15	13
CCLM4 (r1i1p1)-MPI-M-MPI-ESM-LR	0.2	0.0	0.1	4.2	0.6	0.0	0.1	0.0	5	9	7	22	12	2	6	1
CCLM4 (r1i1p1)-CNRM-CERFACS-CNRM-CM5	0.0	0.0	0.2	0.6	0.7	0.0	0.2	0.3	1	5	8	1	15	5	10	9
CCLM4 (r1i1p1)-ICHEC-EC-EARTH-EC-EARTH	0.0	0.0	0.0	0.6	0.8	0.3	0.4	0.0	3	1	1	2	18	14	16	4
MPI-REMO2009 (r1i1p1)-MPI-M-MPI-ESM-LR	1.6	0.3	0.5	2.9	0.1	0.8	7.9	0.0	17	18	11	16	4	22	27	2
MPI-REMO2009 (r12i1p1)-ICHEC-EC-EARTH-EC-EARTH	3.2	0.1	0.6	5.1	0.2	0.6	6.6	1.0	22	15	14	23	7	20	26	18
RCA4 (r1i1p1)-CSIRO-QCCCE-CSIRO-Mk3-6-0	1.6	0.1	1.3	3.2	0.9	0.5	0.0	0.9	18	10	18	19	20	18	2	15
RCA4 (r1i1p1)-MIROC-MIROC5	0.5	0.2	1.1	1.7	0.1	0.1	1.2	0.6	10	16	16	8	5	10	21	14
RCA4 (r1i1p1)-MOHC-HadGEM2-ES	1.4	0.3	1.1	2.3	0.6	0.4	0.2	1.2	14	19	17	12	14	17	11	19
RCA4 (r1i1p1)-NCC-NorESM1-M	1.9	0.1	0.9	2.5	0.0	0.3	0.0	0.3	21	12	15	14	3	13	1	8
RCA4 (r1i1p1)-MPI-M-MPI-ESM-LR	0.5	0.0	0.0	0.8	0.6	0.0	0.3	0.3	8	6	2	5	10	6	13	6
RCA4 (r1i1p1)-IPSL-IPSL-CM5A-MR	1.4	0.1	3.7	4.0	16.7	0.3	1.2	0.9	15	11	24	20	28	15	22	16
RCA4 (r1i1p1)-NOAA-GFDL-GFDL-ESM2M	0.5	0.2	0.1	1.4	0.2	1.0	0.2	0.0	11	17	4	7	6	24	9	3
RCA4 (r1i1p1)-CCCma-CanESM2	1.5	0.3	2.7	2.4	1.0	0.3	0.0	1.8	16	20	21	13	21	16	4	23
RCA4 (r1i1p1)-CNRM-CERFACS-CNRM-CM5	0.5	0.1	0.1	0.8	0.5	0.6	0.3	0.4	7	14	5	3	8	19	12	11
RCA4 (r1i1p1)-ICHEC-EC-EARTH	3.9	0.0	8.1	6.2	3.2	0.1	0.4	2.3	24	4	27	24	24	9	17	24
RCA4 (r12i1p1)-ICHEC-EC-EARTH	1.9	0.7	0.4	3.0	1.7	0.2	0.0	0.5	20	22	10	18	23	12	3	12
RCA4 (r2i1p1)-MPI-M-MPI-ESM-LR	0.5	0.0	0.0	0.8	0.6	0.0	0.3	0.3	9	7	3	6	11	7	14	7
RCA4 (r3i1p1)-ICHEC-EC-EARTH	1.2	0.0	0.1	2.1	0.7	0.0	0.2	0.9	12	3	6	11	16	1	8	17
RCA4 (r3i1p1)-MPI-M-MPI-ESM-LR	20.5	0.0	0.5	1.9	0.5	0.8	0.1	0.3	30	8	12	10	9	21	5	10
RACMO22T (r1i1p1) - MOHC-HadGEM2-ES	3.6	2.4	2.6	10.2	24.7	0.0	2.9	14.9	23	26	20	25	29	4	25	27
RACMO22T (r1i1p1)-ICHEC-EC-EARTH	5.3	2.4	2.9	20.9	15.7	1.1	2.0	12.7	25	25	22	27	27	25	24	26
HIRHAM5 (r3i1p1)-ICHEC-EC-EARTH	0.1	0.0	0.5	1.8	1.6	0.1	0.7	1.6	4	2	13	9	22	8	19	22
HIRHAM5 (r1i1p1)-NCC-NorESM1-M	0.2	0.1	2.3	0.8	0.0	0.0	0.1	0.1	6	13	19	4	1	3	7	5
Ensemble mean (24 runs)	11.1	12.1	17.7	38.3	14.3	16.0	14.2	19.5	29	30	30	30	25	30	29	28
CCLM4 (mean)	1.8	3.5	5.2	2.9	0.9	1.1	0.4	4.8	19	27	26	15	19	26	18	25
MPI-REMO2009 (mean)	7.9	1.6	3.3	13.8	0.6	3.5	22.8	1.3	27	24	23	26	13	28	30	20
RCA4 (mean)	5.5	9.8	17.0	35.0	15.0	10.8	12.1	20.8	26	29	29	29	26	29	28	29
RACMO22T (mean)	9.3	5.8	8.8	26.3	30.5	2.8	0.7	22.4	28	28	28	26	30	27	20	30
HIRHAM5 (mean)	1.3	0.5	3.9	3.0	0.8	0.9	1.6	1.4	13	21	25	17	17	23	23	21

7.6 GCM-driven Model Ranking Based on PCCs, for TAMSAT3 Data

RCM	Pearson Correlation Coefficient (PCC)								Ranking based on PCC							
	PR					CDD	CWD	SDII	PR					CDD	CWD	SDII
	ANN	MAM	OND	90p	99p				ANN	MAM	OND	90p	99p			
CCLM4 (r1i1p1)-MOHC-HadGEM2-ES-HadGEM2-ES	-0.4	-0.1	-0.3	-0.2	-0.3	-0.2	-0.3	-0.2	28	23	30	24	27	24	29	26
CCLM4 (r1i1p1)-MPI-M-MPI-ESM-LR	0.2	0.0	0.2	-0.2	0.4	-0.4	0.4	0.3	3	16	3	25	4	29	1	5
CCLM4 (r1i1p1)-CNRM-CERFACS-CNRM-CM5	0.1	0.1	0.1	-0.3	0.1	-0.2	0.0	0.1	8	12	6	26	10	23	14	14
CCLM4 (r1i1p1)-ICHEC-EC-EARTH-EC-EARTH	-0.4	-0.1	-0.2	-0.3	-0.5	-0.1	-0.3	-0.6	29	27	28	27	30	16	30	30
MPI-REMO2009 (r1i1p1)-MPI-M-MPI-ESM-LR	0.2	0.3	0.1	0.2	0.4	0.1	0.2	0.4	4	2	10	3	3	3	6	3
MPI-REMO2009 (r12i1p1)-ICHEC-EC-EARTH-EC-EARTH	-0.3	0.0	-0.3	-0.3	-0.3	0.0	0.0	-0.3	27	21	29	30	28	10	21	29
RCA4 (r1i1p1)-CSIRO-QCCCE-CSIRO-Mk3-6-0	-0.1	-0.1	0.0	-0.1	-0.2	-0.5	0.0	0.1	20	26	15	22	23	30	20	12
RCA4 (r1i1p1)-MIROC-MIROC5	0.0	-0.2	0.2	-0.1	-0.3	-0.2	0.0	-0.1	11	28	20	12	26	19	18	22
RCA4 (r1i1p1)-MOHC-HadGEM2-ES	-0.4	0.2	0.2	-0.3	-0.4	-0.1	0.1	-0.3	30	3	2	28	29	13	13	28
RCA4 (r1i1p1)-NCC-NorESM1-M	0.1	0.0	0.1	0.1	0.3	-0.2	0.0	0.4	6	15	7	5	5	22	23	4
RCA4 (r1i1p1)-MPI-M-MPI-ESM-LR	-0.1	0.1	-0.1	0.0	0.5	0.1	0.3	0.5	14	10	20	9	1	6	2	1
RCA4 (r1i1p1)-IPSL-IPSL-CM5A-MR	0.3	0.2	0.2	0.3	0.3	-0.2	0.0	0.3	1	8	4	1	6	21	19	7
RCA4 (r1i1p1)-NOAA-GFDL-GFDL-ESM2M	-0.1	0.2	-0.1	-0.1	-0.2	0.2	0.1	-0.1	13	5	19	13	25	2	12	23
RCA4 (r1i1p1)-CCCma-CanESM2	0.0	-0.1	0.1	0.0	0.0	-0.1	0.0	0.1	10	24	5	6	14	15	22	13
RCA4 (r1i1p1)-CNRM-CERFACS-CNRM-CM5	0.1	0.1	0.1	0.1	0.2	0.0	0.1	0.2	7	13	9	4	9	11	9	8
RCA4 (r1i1p1)-ICHEC-EC-EARTH	0.0	0.0	0.0	-0.1	-0.1	0.1	-0.1	-0.2	12	17	14	14	20	5	25	24
RCA4 (r12i1p1)-ICHEC-EC-EARTH	-0.1	0.5	-0.2	0.0	-0.1	-0.1	-0.2	-0.1	16	1	27	8	19	12	27	21
RCA4 (r2i1p1)-MPI-M-MPI-ESM-LR	-0.1	0.1	-0.1	0.0	0.5	0.1	0.3	0.5	15	11	21	10	2	7	3	2
RCA4 (r3i1p1)-ICHEC-EC-EARTH	-0.1	0.0	0.0	-0.1	-0.2	0.0	0.1	-0.3	21	19	16	15	24	9	11	27
RCA4 (r3i1p1)-MPI-M-MPI-ESM-LR	0.2	0.0	0.1	0.2	0.2	-0.1	0.0	0.2	2	18	8	2	7	14	15	9
RACMO22T (r1i1p1) - MOHC-HadGEM2-ES	-0.2	-0.3	-0.1	-0.1	-0.1	-0.4	0.2	0.1	24	30	18	19	21	28	4	15
RACMO22T (r1i1p1)-ICHEC-EC-EARTH	-0.1	0.0	0.0	-0.1	0.0	0.3	-0.2	0.0	22	22	12	21	13	1	28	19
HIRHAM5 (r3i1p1)-ICHEC-EC-EARTH	-0.1	0.2	-0.2	0.0	0.0	0.0	0.2	0.0	19	4	25	7	15	8	5	20
HIRHAM5 (r1i1p1)-NCC-NorESM1-M	-0.1	-0.1	0.0	-0.1	0.0	-0.2	-0.1	0.1	18	25	13	20	17	25	26	16
Ensemble mean (24 runs)	0.0	0.1	-0.2	-0.1	0.1	-0.2	0.2	0.2	9	9	23	18	11	26	8	10
CCLM4 (mean)	-0.2	0.0	-0.2	-0.3	-0.1	-0.3	0.0	-0.2	26	20	24	29	22	27	24	25
MPI-REMO2009 (mean)	-0.1	0.2	-0.2	-0.1	0.2	0.1	0.1	0.2	17	7	26	17	8	4	10	11
RCA4 (mean)	0.2	0.2	0.0	0.0	0.1	-0.1	0.2	0.3	5	6	11	11	12	18	7	6
RACMO22T (mean)	-0.2	-0.2	0.0	-0.2	0.0	-0.2	0.0	0.0	25	29	17	23	18	20	17	17
HIRHAM5 (mean)	-0.1	0.1	-0.1	-0.1	0.0	-0.1	0.0	0.0	23	14	22	16	16	17	16	18

7.7 GCM-driven Model Ranking Based on IVS, for CHIRPS Data (Including Top Four Models)

RCM	IVS								Ranking based on IVS							
	PR					CDD	CWD	SDII	PR					CDD	CWD	SDII
	ANN	MAM	OND	90p	99p				ANN	MAM	OND	90p	99p			
CCLM4 (r1i1p1)-MOHC-HadGEM2-ES-HadGEM2-ES	0.3	0.1	0.1	0.9	0.2	12.1	1.0	0.4	20	9	9	22	11	30	21	14
CCLM4 (r1i1p1)-MPI-M-MPI-ESM-LR	0.1	0.7	0.0	0.9	1.6	9.2	0.4	0.0	9	24	3	23	23	29	14	2
CCLM4 (r1i1p1)-CNRM-CERFACS-CNRM-CM5	0.4	0.5	0.0	0.0	1.7	7.0	0.7	0.1	22	22	4	5	24	25	18	10
CCLM4 (r1i1p1)-ICHEC-EC-EARTH-EC-EARTH	0.3	0.3	0.1	0.0	2.0	4.3	1.0	0.0	21	20	7	6	25	16	22	1
MPI-REMO2009 (r1i1p1)-MPI-M-MPI-ESM-LR	0.2	0.0	0.2	0.5	0.6	2.5	5.0	0.0	14	3	11	17	18	8	28	2
MPI-REMO2009 (r12i1p1)-ICHEC-EC-EARTH-EC-EARTH	0.7	0.1	0.3	1.2	0.0	3.0	4.2	0.7	23	6	14	24	1	10	26	19
RCA4 (r1i1p1)-CSIRO-QCCCE-CSIRO-Mk3-6-0	0.2	0.1	0.8	0.6	0.2	3.4	0.1	0.6	15	13	19	20	16	12	10	16
RCA4 (r1i1p1)-MIROC-MIROC5	0.0	1.1	0.6	0.1	0.0	5.9	0.5	0.4	2	26	17	8	2	20	15	15
RCA4 (r1i1p1)-MOHC-HadGEM2-ES	0.1	0.0	0.6	0.3	0.1	3.8	0.0	0.8	11	25	18	13	9	13	3	20
RCA4 (r1i1p1)-NCC-NorESM1-M	0.3	0.1	0.5	0.4	0.1	4.4	0.1	0.1	19	10	16	15	5	17	12	9
RCA4 (r1i1p1)-MPI-M-MPI-ESM-LR	0.0	0.2	0.0	0.0	0.1	6.8	0.0	0.1	3	15	5	1	6	23	6	6
RCA4 (r1i1p1)-IPSL-IPSL-CM5A-MR	0.1	0.1	2.6	0.9	10.2	4.2	0.5	0.6	12	12	25	21	29	15	16	17
RCA4 (r1i1p1)-NOAA-GFDL-GFDL-ESM2M	0.0	1.1	0.3	0.1	0.8	25.2	0.6	0.1	1	27	15	7	21	31	17	8
RCA4 (r1i1p1)-CCCma-CanESM2	0.2	0.0	1.8	0.3	0.3	4.2	0.0	1.3	13	1	22	14	17	14	5	24
RCA4 (r1i1p1)-CNRM-CERFACS-CNRM-CM5	0.0	0.1	0.0	0.0	0.1	3.1	0.9	0.2	5	7	1	4	3	11	20	12
RCA4 (r1i1p1)-ICHEC-EC-EARTH	1.0	0.3	6.0	1.7	1.6	6.2	0.1	1.8	25	17	28	25	22	21	9	25
RCA4 (r12i1p1)-ICHEC-EC-EARTH	0.3	0.1	0.2	0.5	0.6	5.1	0.1	0.3	18	6	10	19	20	18	8	13
RCA4 (r12i1p1)-MPI-M-MPI-ESM-LR	0.0	0.2	0.0	0.0	0.1	6.8	0.0	0.1	4	16	6	2	7	24	7	7
RCA4 (r3i1p1)-ICHEC-EC-EARTH	0.1	0.3	0.0	0.2	0.1	8.5	0.0	0.6	7	18	2	12	10	28	2	18
RCA4 (r3i1p1)-MPI-M-MPI-ESM-LR	46.4	0.2	0.2	0.2	0.1	2.6	0.0	0.2	31	14	12	11	4	9	4	11
RACMO22T (r1i1p1) - MOHC-HadGEM2-ES	0.9	0.7	1.8	3.3	15.4	7.1	4.9	12.5	24	25	21	26	30	26	27	28
RACMO22T (r1i1p1)-ICHEC-EC-EARTH	1.6	0.7	2.0	7.7	9.5	2.1	3.6	10.7	26	23	23	28	28	6	25	27
HIRHAM5 (r3i1p1)-ICHEC-EC-EARTH	0.2	0.3	0.2	0.1	0.6	6.4	0.2	1.2	16	19	13	10	19	22	13	23
HIRHAM5 (r1i1p1)-NCC-NorESM1-M	0.1	0.1	1.5	0.0	0.2	7.4	0.0	0.0	8	8	20	3	13	27	1	4
Ensemble mean (24 runs)	4.2	5.8	13.7	14.9	8.6	0.3	9.4	16.5	30	31	31	31	26	2	30	29
CCLM4 (mean)	0.2	1.2	3.8	0.5	0.2	2.0	0.1	3.9	17	28	27	16	14	5	11	26
MPI-REMO2009 (mean)	2.8	0.4	2.3	4.7	0.1	0.5	15.4	0.9	28	21	24	27	8	3	31	21
RCA4 (mean)	1.7	4.5	13.2	13.5	9.1	0.0	8.0	17.6	27	30	30	30	27	1	29	30
RACMO22T (mean)	3.4	2.4	6.6	9.9	19.1	0.7	1.6	18.9	29	29	29	29	31	4	24	31
HIRHAM5 (mean)	0.1	0.0	2.8	0.5	0.2	2.5	0.8	1.0	10	4	26	18	12	7	19	22
Ensemble mean (best 4)*	0.0	0.1	0.1	0.1	0.2	4.8	1.5	0.1	6	11	8	8	15	18	23	5

7.8 GCM-driven Model Ranking Based on PCCs, for CHIRPS Data (Including Top Four Models)

RCM	Pearson Correlation Coefficient (PCC)								Ranking based on PCC							
	PR					CDD	CWD	SDII	PR					CDD	CWD	SDII
	ANN	MAM	OND	90p	99p				ANN	MAM	OND	90p	99p			
CCLM4 (r1i1p1)-MOHC-HadGEM2-ES-HadGEM2-ES	-0.1	-0.1	-0.1	0.1	0.0	0.1	-0.2	0.0	25	28	26	15	24	7	30	18
CCLM4 (r1i1p1)-MPI-M-MPI-ESM-LR	0.3	0.0	0.3	0.1	0.5	-0.2	0.3	0.4	1	25	3	16	2	28	4	1
CCLM4 (r1i1p1)-CNRM-CERFACS-CNRM-CM5	0.1	0.1	0.2	0.0	0.2	0.0	0.0	0.2	14	13	7	22	13	21	22	10
CCLM4 (r1i1p1)-ICHEC-EC-EARTH-EC-EARTH	-0.1	0.0	-0.1	0.0	-0.1	-0.1	-0.2	-0.1	26	17	29	23	28	25	31	24
MPI-REMO2009 (r1i1p1)-MPI-M-MPI-ESM-LR	0.3	0.2	0.2	0.3	0.5	-0.2	0.2	0.4	2	8	8	1	1	27	1-	2
MPI-REMO2009 (r12i1p1)-ICHEC-EC-EARTH-EC-EARTH	-0.3	-0.2	-0.2	-0.3	-0.2	0.2	-0.2	-0.2	31	30	31	31	31	3	27	28
RCA4 (r1i1p1)-CSIRO-QCCCE-CSIRO-Mk3-6-0	0.0	0.0	0.3	0.0	-0.1	0.1	0.0	-0.2	19	26	2	21	26	9	21	29
RCA4 (r1i1p1)-MIROC-MIROC5	-0.2	0.1	0.2	-0.3	-0.2	0.0	0.0	-0.2	30	11	11	30	29	23	18	31
RCA4 (r1i1p1)-MOHC-HadGEM2-ES	-0.2	0.1	0.2	-0.1	-0.1	-0.1	0.2	-0.1	29	10	12	28	27	26	11	27
RCA4 (r1i1p1)-NCC-NorESM1-M	0.0	-0.1	0.0	-0.1	0.2	0.2	-0.2	0.0	22	27	23	27	11	6	29	16
RCA4 (r1i1p1)-MPI-M-MPI-ESM-LR	0.3	0.0	0.0	0.3	0.4	0.0	0.4	0.3	7	18	20	3	3	16	2	4
RCA4 (r1i1p1)-IPSL-IPSL-CM5A-MR	0.1	0.0	0.1	0.1	0.1	0.2	0.0	-0.1	10	23	17	13	19	5	19	26
RCA4 (r1i1p1)-NOAA-GFDL-GFDL-ESM2M	-0.1	0.3	-0.1	0.0	-0.2	-0.3	0.0	-0.2	24	6	27	26	30	29	23	30
RCA4 (r1i1p1)-CCCma-CanESM2	0.3	0.0	0.3	0.3	0.0	0.3	0.1	0.1	4	21	4	2	22	2	14	13
RCA4 (r1i1p1)-CNRM-CERFACS-CNRM-CM5	0.3	0.1	0.2	0.2	0.1	0.3	0.2	0.1	5	16	5	6	17	1	9	12
RCA4 (r1i1p1)-ICHEC-EC-EARTH	0.3	0.3	0.3	0.2	0.2	0.1	0.1	0.1	6	4	1	9	14	10	17	14
RCA4 (r12i1p1)-ICHEC-EC-EARTH	0.0	0.4	-0.1	0.0	-0.1	0.0	-0.2	-0.1	21	1	28	24	25	19	27	25
RCA4 (r12i1p1)-MPI-M-MPI-ESM-LR	0.3	0.0	0.0	0.3	0.4	0.0	0.4	0.3	8	19	21	4	4	17	3	5
RCA4 (r3i1p1)-ICHEC-EC-EARTH	0.0	0.1	0.1	0.1	0.0	0.0	0.1	0.0	20	12	16	14	21	15	13	17
RCA4 (r3i1p1)-MPI-M-MPI-ESM-LR	0.0	0.1	0.0	0.0	0.0	0.2	0.1	-0.1	18	9	22	25	23	4	15	23
RACMO22T (r1i1p1) - MOHC-HadGEM2-ES	0.1	-0.3	0.2	0.1	0.2	0.0	0.5	0.4	12	31	10	10	10	18	1	3
RACMO22T (r1i1p1)-ICHEC-EC-EARTH	0.1	0.3	0.0	0.0	0.2	0.1	-0.1	0.1	17	3	19	18	12	11	26	15
HIRHAM5 (r3i1p1)-ICHEC-EC-EARTH	-0.1	0.3	0.1	0.1	0.1	-0.1	0.2	0.0	27	5	18	11	15	24	12	19
HIRHAM5 (r1i1p1)-NCC-NorESM1-M	-0.1	-0.2	-0.2	-0.1	0.0	-0.4	0.0	0.0	23	29	30	29	20	31	24	22
Ensemble mean (24 runs)	0.2	0.2	0.1	0.2	0.3	0.0	0.3	0.2	9	7	13	8	6	20	6	11
CCLM4 (mean)	0.1	0.0	0.1	0.0	0.3	0.0	-0.1	0.3	15	22	15	19	8	22	25	6
MPI-REMO2009 (mean)	0.1	0.0	0.0	0.1	0.3	0.1	0.0	0.3	16	24	24	17	7	13	20	9
RCA4 (mean)	0.1	0.3	0.2	0.2	0.1	0.1	0.3	0.0	11	2	6	7	16	8	7	20
RACMO22T (mean)	0.1	0.0	0.2	0.1	0.2	0.1	0.3	0.3	13	20	9	12	9	12	8	8
HIRHAM5 (mean)	-0.1	0.1	-0.1	0.0	0.1	-0.3	0.1	0.0	28	14	25	20	18	30	15	21
Ensemble mean (best 4)*	0.3	0.1	0.1	0.3	0.4	0.0	0.3	0.3	3	15	14	5	5	14	5	7

7.9 Published journal article on model performance assessment and future climate changes for East Africa

Ogega OM, Koske J, Kung'u JB *et al.* Heavy precipitation events over East Africa in a changing climate: results from CORDEX RCMs. *Clim Dyn*. 2020; 55: 993–1009. https://doi.org/10.1007/s00382-020-05309-z

7.10 Published journal article on the impact of future precipitation changes on health in East Africa

Ogega OM and Alobo M. Impact of 1.5 ^{o}C and 2 ^{o}C global warming scenarios on malaria transmission in East Africa [version 3; peer review: 2 approved]. AAS Open Res 2021, 3:22. https://doi.org/10.12688/aasopenres.13074.3

7.11 Published journal article on the impact of climate change on tourism

Ogega OM, Wanjohi HN, Mbugua J. Exploring the Future of Nairobi National Park in a Changing Climate and Urban Growth. In: *Cobbinah P., Addaney M. (eds) The Geography of Climate Change Adaptation in Urban Africa*. Palgrave Macmillan, Cham (2019). http://doi-org-443.webvpn.fjmu.edu.cn/10.1007/978-3-030-04873-0_9

7.12 Published journal article on Building on foundations for climate services for sustainable development: a case of coastal smallholder farmers in Kilifi County, Kenya

Ogega OM, Gyampoh BA, Oludhe C *et al*. Building on foundations for climate services for sustainable development: A case of coastal smallholder farmers in Kilifi County, Kenya. *Climate Services*. 2020; 20:100200. https://doi.org/10.1016/j.cliser.2020.100200

7.13 Approval to conduct research from Graduate School, Kenyatta University

KENYATTA UNIVERSITY
GRADUATE SCHOOL

E-mail: kubps@yahoo.com
dean-graduate@ku.ac.ke
Website: www.ku.ac.ke

P.O. Box 43844, 00100
NAIROBI, KENYA
Tel. 810901 Ext. 57530

Internal Memo

FROM: Dean, Graduate School

DATE: 5th February, 2020

TO: Mr. Obed M. Ogega
C/o Department of Environmental Science & Education
KENYATTA UNIVERSITY

REF: N85/38113/17

SUBJECT: APPROVAL OF RESEARCH PROPOSAL

This is to inform you that the Graduate School Board at its meeting 29th January, 2020 approved your Ph.D. Research Proposal entitled "Intraseasonal Rainfall Variability and Climate Adaption in East Africa"

You may now proceed with your Data collection, subject to clearance with the Director General, National Commission for Science, Technology & Innovation.

As you embark on your data collection, please note that you will be required to submit to Graduate School completed supervision Tracking and Progress Report Forms. The Forms are available at the University's Website under Graduate School webpage downloads.

By copy of this letter, the Registrar (Academic) is hereby requested to grant you substantive registration for your Ph.D. studies.

Thank you.

REUBEN MURIUKI
FOR: DEAN, GRADUATE SCHOOL

c.c. Chairman, Department of Environmental Science & Education
Registrar (Academic) Att; Mrs. Lucy Njenga

Supervisors:

1. Dr. James Koske
   C/o Department of Environmental Science & Education
   KENYATTA UNIVERSITY

2. Prof. James Kung'u
   C/o Department of Environmental Science & Education
   KENYATTA UNIVERSITY

RM/cao